Therapeutic anti-TNFα antibodies differentially affect *Leishmania* infection of primary human macrophages

Dissertation

zur Erlangung des Grades

Doktor der Naturwissenschaften

am Fachbereich Biologie

der Johannes Gutenberg-Universität Mainz

Katharina Arens

geb. am 25.05.1988 in Trier

Mainz, 2018

Dekan:

1. Berichterstatter:

2. Berichterstatter:

Tag der mündlichen Prüfung:

The obtained research data during this work and collaborative studies led to the following publications:

Arens K, Filippis C, Kleinfelder H, Goetzee A, Reichmann G, Waibler Z, Crauwels P, Bagola K and van Zandbergen G. Anti-TNFα therapeutics differentially affect *Leishmania* infection of human macrophages. 2018, submitted to Blood

K.A. and C.F. contributed equally to this work.

Filippis C, **Arens K**, Noubissi Nzeteu GA, Reichmann G, Waibler Z, Crauwels P and van Zandbergen G. Nivolumab enhances *in vitro* effector functions of PD-1^{+} T-lymphocytes and *Leishmania*-infected human myeloid cells in a host cell-dependent manner. Front Immunol. 2017; 8:1880. PMID: 29312350

K.A. and C.F. contributed equally to this work.

Summary

Excessive production of the pro-inflammatory cytokine tumor necrosis factor α (TNFα) is associated with the pathophysiology of human autoimmune diseases. As a consequence, neutralizing antibodies or antibody-derived molecules directed against TNFα have emerged as important therapeutics. Despite the great success of anti-TNFα treatment, serious adverse effects remain and complications include a higher risk for infectious diseases such as leishmaniasis. In this study, we developed an *in vitro* model based on *Leishmania*-infected human macrophages, co-cultured with autologous T-cells, for the analysis and comparison of currently marketed anti-TNFα agents and their potential to contribute to the onset of leishmaniasis. Using our *in vitro* model, we identified that neutralization of soluble TNFα (sTNFα) by the anti-TNFα antibodies Remicade®, Remsima® and Humira® negatively affected infection as treatment with these agents significantly reduced *Leishmania*-induced $CD4^+$ T-cell proliferation and increased the number of infected macrophages. In contrast, we showed that blockade of sTNFα by Cimzia® did not affect T-cell proliferation and infection rates. Moreover, compared to Remicade®, the application of Cimzia® did not impair the phenotype and effector functions of T-cells as shown by the expression levels of PD-1, CD45RO and cytolytic effector proteins. The latter are potentially implicated in intracellular killing of parasites.

We confirmed that the diverging effects of Remicade® or Cimzia® treatment were independent of Fc-Fcγ receptor interaction. However, our data indicate that Cimzia® supports parasite control through its conjugated PEG moiety as PEGylation of Remicade® enhanced T-cell proliferation and thus improved the clearance of intracellular *Leishmania*. This effect was associated with complement activation, showing increased C5a expression upon treatment with PEGylated TNFα inhibitors.

Altogether, our results enhance the understanding of the effectiveness and adverse effects of anti-TNFα treatment. Considering the emergence of leishmaniasis as complication of anti-TNFα therapy, our findings contribute to evaluate different anti-TNFα agents. Based on our results, we propose that the application of Cimzia® may be beneficial for patients living in countries with a high prevalence of leishmaniasis.

Zusammenfassung

Mit der Pathophysiologie von Autoimmunerkrankungen ist eine übermäßige Produktion des pro-inflammatorischen Zytokins Tumornekrosefaktor α (TNFα) assoziiert. Folglich stellen neutralisierende Antikörper oder von Antikörpern abgeleitete Moleküle, die gegen TNFα gerichtet sind, eine wichtige Therapiemöglichkeit dar. Trotz ihres großen Erfolges, kann die anti-TNFα Therapie ernsthafte Nebenwirkungen mit sich bringen. Insbesondere besteht ein deutlich erhöhtes Risiko für das Auftreten von Infektionserkrankungen wie beispielsweise Leishmaniose. In dieser Arbeit entwickelten wir ein *in vitro* Modell basierend auf Leishmanien-infizierten humanen Makrophagen, die mit autologen T-Zellen co-kultiviert wurden. Mit Hilfe dessen wurden zugelassene TNFα Inhibitoren analysiert und deren Einfluss auf die Entstehung von Leishmaniose verglichen. Es konnte gezeigt werden, dass die Neutralisation von sekretiertem TNFα (sTNFα) durch die anti-TNFα Antikörper Remicade®, Remsima® und Humira® die Infektion negativ beeinflusste, da die Leishmanien-induzierte $CD4^+$ T-Zellproliferation reduziert wurde und der Prozentsatz infizierter Makrophagen signifikant anstieg. Im Gegensatz dazu zeigte sich, dass die sTNFα Blockade durch Cimzia® keinen Einfluss auf die T-Zellproliferation und die Infektionsraten ausübte. Zudem beeinträchtigte die Behandlung mit Cimzia®, im Vergleich zu Remicade®, nicht den Phänotyp und die Effektorfunktionen der T-Zellen, was durch die Expressionsstärke von PD-1, CD45RO und zytolytischen Effektormolekülen verdeutlicht wurde. Letztere konnten mit der Abtötung intrazellulärer Parasiten in Zusammenhang gebracht werden.
Unsere Daten bestätigen, dass die voneinander abweichenden Effekte der Remicade® und Cimzia® Behandlung unabhängig von Fc-Fcγ Rezeptorinteraktionen entstanden. Allerdings deuten unsere Ergebnisse daraufhin, dass Cimzia® mit Hilfe seiner PEGylierung zur Kontrolle über die Parasiten beiträgt, da eine PEGylierung von Remicade® die T-Zellproliferation und folglich die intrazelluläre Beseitigung der Leishmanien begünstigte. Dieser Effekt stand im Zusammenhang mit einer Komplementaktivierung, was durch eine verstärkte C5a Expression nach Behandlung mit PEGylierten TNFα Blockern verdeutlicht wurde.

Die in dieser Arbeit gewonnenen Erkenntnisse tragen maßgeblich zum Verständnis der Wirkungsweise der anti-TNFα Therapeutika und ihrer schwerwiegenden Nebenwirkungen bei. In Anbetracht der auftretenden Komplikation Leishmaniose, helfen unsere Ergebnisse

verschiedene TNFα Inhibitoren zu bewerten. Folglich scheint die Behandlung mit Cimzia® für Patienten in Leishmaniose-endemischen Regionen vorteilhaft gegenüber den anderen untersuchten TNFα Blockern.

Table of content

1 Introduction

1.1 Leishmaniasis

1.1.1 *Leishmania* parasites

The infectious disease leishmaniasis is caused by the protozoan parasite *Leishmania* that belongs to the class of Kinetoplastea and the family of Trypanosomatidae (Rioux et al., 1990). In 1903, the British medical doctor Ronald Ross defined the new species *Leishmania* (*L.*) according to its discoverer William Boog Leishman (Steverding, 2017). *Leishmania* are obligate intracellular parasites, which are endemic in tropical and subtropical regions (**Figure 1**). More than 1 million new cases of leishmaniasis are estimated to occur annually, with increased spreading of parasites to previously non-endemic countries (Bogdan, 2012; WHO, 2017). Disease manifestations include cutaneous, mucosal and visceral syndromes, depending on the parasite species and the host's immune response (Kaye and Scott, 2011). Skin lesions of cutaneous leishmaniasis (CL), caused by *L. major* (*Lm*), *L. tropica*, *L. braziliensis* and *L. aethiopica*, are usually self-healing, but often result in disfiguring scars. Mucocutaneous leishmaniasis (ML) is associated with *L. braziliensis*, *L. guyanensis* and *L. donovani*. This manifestation extensively damages oral-nasal and pharyngeal cavities. Visceral leishmaniasis (VL), also known as "kala azar", is the most serious and usually fatal form of leishmaniasis if untreated. VL affects visceral organs and is characterized by fever, weight loss, anemia and a severe damage to the liver as well as the spleen. *L. donovani* and *L. infantum* induce this form of leishmaniasis (Desjeux, 2004; Kaye and Scott, 2011).

Therapy of leishmaniasis depends on the causative *Leishmania* subspecies, the severity of the disease and the immune status of the patient. Thus, careful diagnosis is always crucial. As indicated above, skin lesions of CL are usually self-healing and local treatment with heat therapy or cryotherapy is sufficient. In contrast, the more severe forms ML or VL require systemic medical treatment with intravenous amphotericin B or oral miltefosine to prevent morbidity and mortality. To date, no vaccine or chemoprophylaxis is available (Aronson et al., 2017).

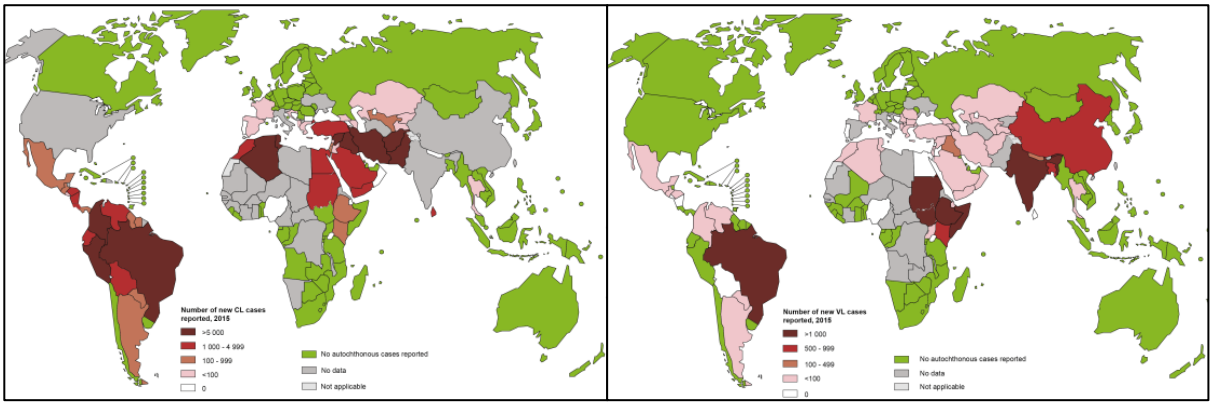

Figure 1: Global distribution of cutaneous (left) and visceral (right) leishmaniasis in 2015 (WHO, 2017).

1.1.2 Life cycle of *Leishmania* parasites

During their life cycle (**Figure 2**), *Leishmania* alternate between female sandflies (*Phlebotomus*, *Lutzomyia*) and mammalians as hosts. Parasites reside in the midgut of sandflies in an alkaline pH environment with temperatures between 22-28°C (Zilberstein and Shapira, 1994). Flagellated, non-infective procyclic promastigotes divide in a process called metacyclogenesis and differentiate into the virulent metacyclic form that migrates to the front part of the intestinal tract (Sacks, 1989; McConville et al., 1992). During the blood meal of a sandfly, these metacyclic promastigotes, accompanied by immunomodulatory parasite-derived proteophosphoglycans and various salivary components, are transmitted to a mammalian host. Inside the mammalian host, the majority of parasites is efficiently cleared by complement components of the innate immune system (**1.1.3**). Parasites that manage to evade this elimination are engulfed by macrophages, monocytes, dendritic cells (DCs), stromal cells and neutrophils.

Of note, the virulent inoculum of *Leishmania* consists of viable and apoptotic promastigotes. Apoptotic parasites exposing phosphatidylserine are recognized as harmless, which supports the production of anti-inflammatory cytokines such as transforming growth factor β (TGF-β) and thus suppresses the activation of antimicrobial effector functions of immune cells. This, in turn, allows for a better survival of the viable *Leishmania* (van Zandbergen et al., 2006).

Inside macrophages, promastigotes reside in phagosomes, called parasitophorous vacuoles, where they delay the phagolysosomal biogenesis to evade microbicidal mechanisms. Acidic pH conditions (pH <5.5) and higher temperatures (33-37°C) in host phagosomes promote

differentiation of flagellated promastigotes into aflagellated, immotile amastigotes (Tsigankov et al., 2014). Differentiation starts within the first hours after phagocytosis and takes up to 5 days (Courret et al., 2002). Amastigotes then replicate, even in the compartments that fuse with lysosomes, and rupture host cells to spread to other immune cells. The life cycle of *Leishmania* is completed when a sandfly takes up amastigote-infected phagocytes during another blood meal. These amastigotes then redifferentiate into promastigotes in the digestive tract of the sandfly (Kaye and Scott, 2011).

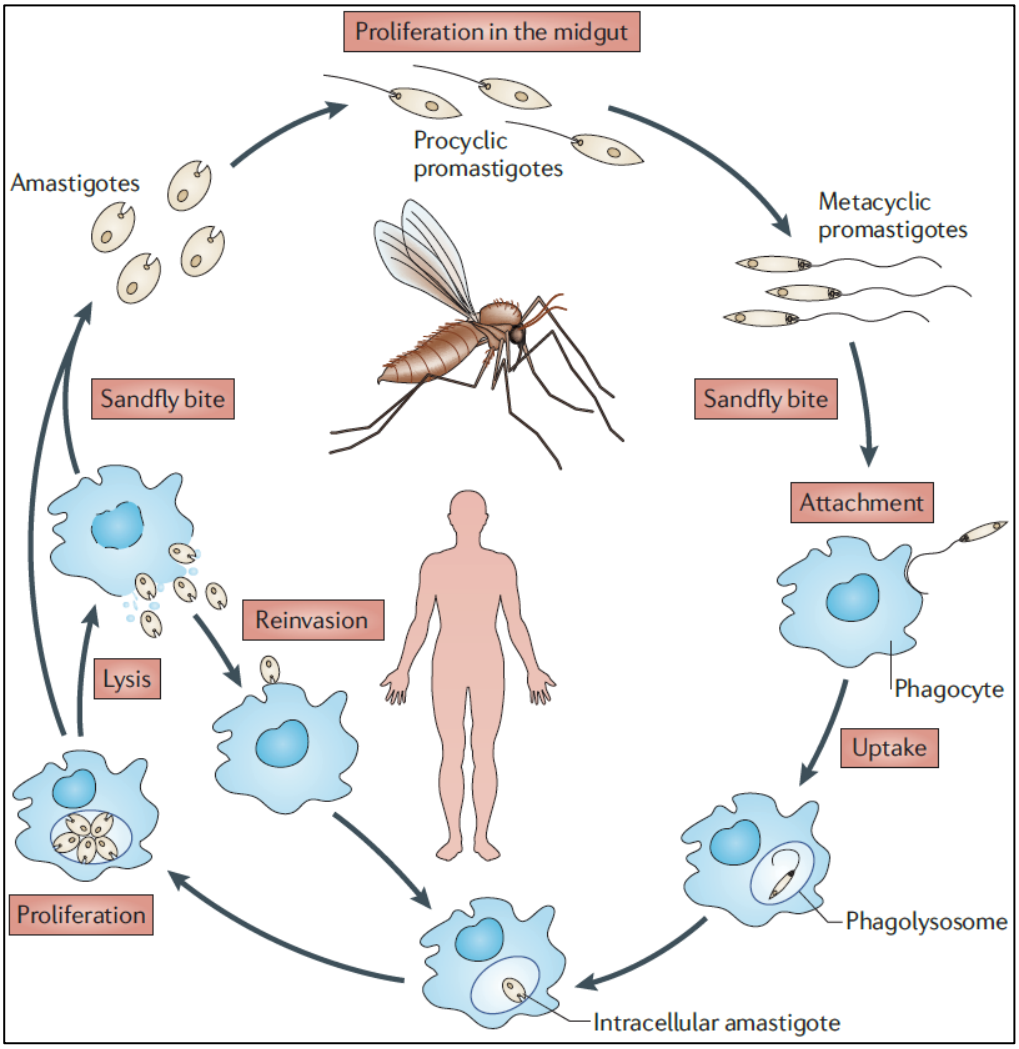

Figure 2: Life cycle of *Leishmania* parasites. During metacyclogenesis in the midgut of sandflies, non-infective procyclic *Leishmania* promastigotes divide and differentiate into the virulent metacyclic form. These parasites are transmitted to a mammalian host by the bite of a sandfly. Within the skin, *Leishmania* are engulfed by phagocytes such as neutrophils, macrophages or dendritic cells. Inside macrophages, promastigotes reside in phagolysosomal compartments, where they transform into aflagellated amastigotes dependent on pH and temperature changes. These amastigotes replicate and spread to other cells upon cell rupture or are taken up during a blood meal of another sandfly (Kaye and Scott, 2011).

1.1.3 Innate immunity in response to *Leishmania* infection

Inside the mammalian host, the complement system detects and eliminates the vast majority of invading *Leishmania* parasites (Stebut and Tenzer, 2017). Complement was discovered by Jules Bordet in the 19th century. The system is composed of more than 30 soluble or membrane-bound proteins, which represent a first line of innate defense against invading pathogens (Sarma and Ward, 2011). Three different cascades are known to be involved in complement activation: the classical, the lectin and the alternative pathway (**Figure 3**). In all three pathways, inactive zymogens are sequentially cleaved leading to the formation of C3 and C5 convertase. C3 convertase processes complement component C3 into C3a and C3b, whereas C5 convertase processes C5 into C5a and C5b. C3a and C5a are anaphylatoxins, potent inflammatory mediators that activate immune cells *via* the complement receptors C3aR and C5aR. C3b is an opsonin supporting phagocytosis and C5b recruits C6, C7, C8 and C9 that contribute to the assembly of the membrane attack complex (MAC). The MAC inserts into the membrane and causes osmotic lysis of pathogens. Dependent on the complement pathway, initiating factors and the composition of convertases differs. The classical pathway is induced upon binding of C1 to the fragment crystallizable (Fc) portion of antibody-antigen complexes. The lectin pathway is activated by mannose-binding lectin (MBL) or Ficolin that bind to carbohydrate structures on pathogen surfaces and activation of the alternative pathway results from spontaneous hydrolysis ("tick over") of complement component C3 (reviewed by Merle et al., 2015). The different complement cascades and involved proteins are depicted in **Figure 3**.

Some parasites manage to evade destruction by the complement system through defense mechanisms. Metacyclic promastigotes highly express lipophosphoglycan (LPG), which interferes with the insertion of the MAC. Glycoprotein 63 (GP63), a metalloproteinase expressed by *Leishmania*, inactivates surface-attached C3b (iC3b) and thus hinders the formation of C5 convertase. In addition, kinases deactivate the classical and alternative complement pathway by phosphorylating complement proteins (Bogdan and Röllinghoff, 1998).

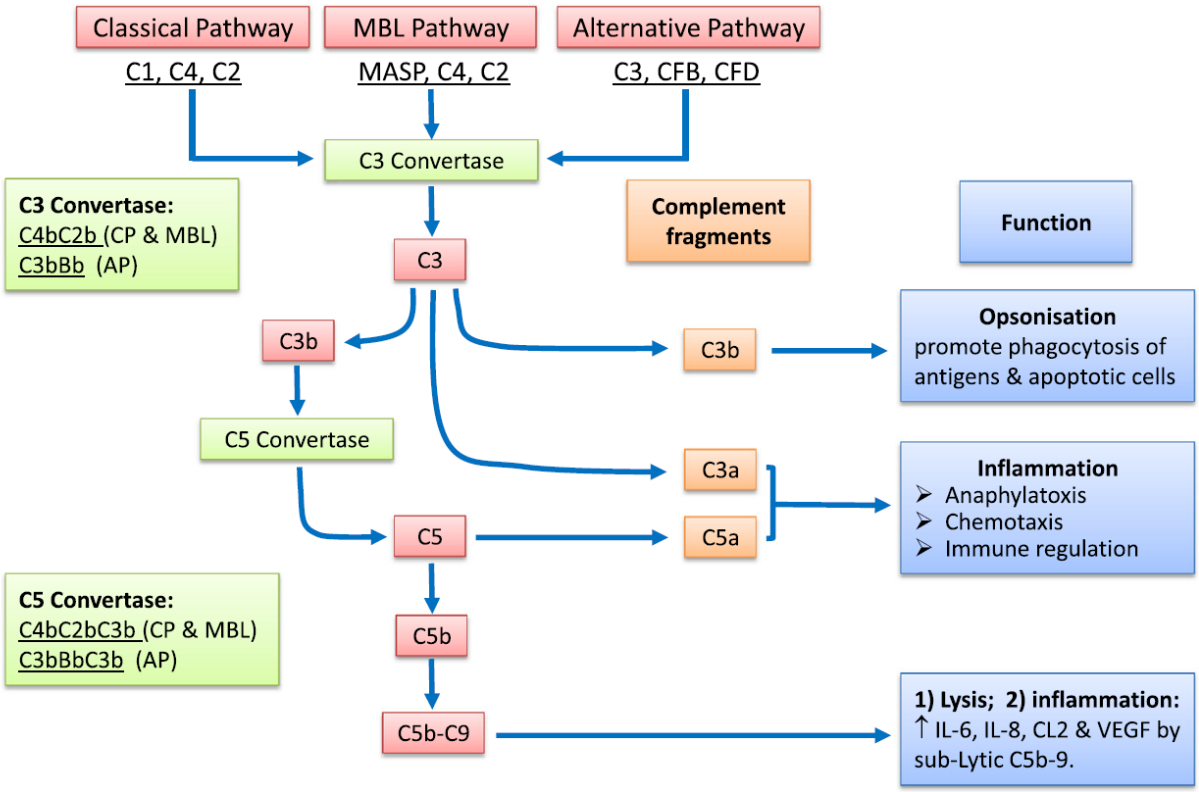

Figure 3: Pathways and components of the complement system. *Classical pathway*: Complement component C1 binds to the Fc portion of antibody-antigen complexes, resulting in the cleavage of C4 and C2 and the formation of C3 convertase (C4bC2b). *MBL pathway*: Mannose-binding lectin (MBL) or Ficolin bind to carbohydrate structures on the pathogen surface. Conformational changes of MBL-associated proteins (MASPs) lead to the cleavage of C4 and C2 and the assembly of the C3 convertase (C4bC2b). *Alternative pathway:* Spontaneous hydrolysis of C3 and the recruitment of factor B and factor D lead to the formation of a different C3 convertase (C3bBb). All of the 3 pathways converge upon the formation of C3 convertase, which further cleaves C3 into C3a and C3b. C3b is required for the assembly of the C5 convertase cleaving C5 into C5a and C5b. Finally, the membrane attack complex (MAC) consisting of C5b-C9 is inserted into the pathogen membrane, forming a pore and resulting in cell lysis (Xu and Chen, 2016).

Inside the mammalian host, parasites release *Leishmania* chemotactic factor (LCF), which supports neutrophil recruitment to the site of infection within minutes (van Zandbergen et al., 2002). These immune cells ingest both viable and apoptotic *Leishmania*, the apoptotic parasites inhibit anti-leishmanial activity of neutrophils so that viable parasites can survive (van Zandbergen et al., 2006). Infected neutrophils eventually undergo apoptosis and are ingested by macrophages through receptor-mediated phagocytosis (van Zandbergen et al., 2004; Peters et al., 2008). Thus, parasites are silently transferred to macrophages *via* neutrophils as "Trojan Horses" (Ritter et al., 2009). Macrophages are the primary host cells of *Leishmania*, allowing their replication, but they are also responsible for parasite elimination through reactive oxygen species (ROS) or nitric oxide (NO) (**1.1.4**). DCs are

permissive host cells, supporting manifestation of the disease. However, upon infection, they upregulate expression of major histocompatibility complex class II (MHC-II) molecules, which is important for priming and activating *Leishmania*-specific T-cells in adaptive immunity (Kaye and Scott, 2011).

1.1.4 Macrophages as host cells of *Leishmania* parasites

Macrophages, originally discovered by the Russian zoologist Elie Metchnikoff in 1882, are myeloid immune cells that are present in all vertebrates (Tauber, 2003). They reside in various tissues such as the skin, gut, brain or lung, where they phagocytose large particles (>0.5 µm) including prokaryotic and eukaryotic cells. According to their main function, they are classified as professional phagocytes, a group also comprising neutrophils, monocytes and immature DCs (Silva and Correia-Neves, 2012). Macrophages contribute to innate and adaptive defense mechanisms as well as tissue homeostasis. In the case of cell homoeostasis, macrophages mainly originate from embryonic progenitors that seed developing tissues before birth. During pathological inflammation, they predominantly differentiate from monocytes that circulate in blood and rapidly infiltrate infected tissues. These monocytes continuously develop from hematopoietic stem cells, located in the bone marrow (Ginhoux and Jung, 2014; Varol et al., 2015). Macrophages engulf invading pathogens, which triggers the expression of costimulatory molecules such as CD40, CD54 and CD80/CD86 and the production of pro-inflammatory cytokines or chemokines such as TNFα, IL-6, TIMP-1, IL-1RA, MIP-1α, MIP-1β and MCP-1 (Stebut and Tenzer, 2017).

Although *Leishmania* parasites infect various cell types, macrophages belong to the most important host cells as non-multiplying promastigotes convert into replicative amastigotes (**1.1.2**). Parasites are taken up by receptor-mediated phagocytosis through several mechanisms. The complement component C3b opsonizes promastigotes, which then bind to complement receptor 1 (CR1) on macrophages. Due to the factor 1 cofactor and GP63, C3b is rapidly cleaved leading to iC3b, which preferentially binds to CR3. This makes CR3 the most important complement receptor for parasite adhesion. In addition, parasite GP63 is capable of directly binding to fibronectin receptor and LPG interacts with mannose-fucose receptor on the surface of macrophages (Kane and Mosser, 2000). Of note, engagement of

different receptors can have a different outcome. Hence, virulent metacyclic promastigotes preferentially use CR3 ligation, which does not trigger nicotinamide adenine dinucleotide phosphate (NADPH) oxidase activation (Sehgal et al., 1993), whereas avirulant procyclic promastigotes mainly interact with mannose-fucose receptor, leading to an inflammatory response (Linehan et al., 2000). As previously described (**1.1.3**), *Leishmania* can additionally enter macrophages by the "Trojan Horse" strategy *via* apoptotic neutrophils.

Inside the macrophage, parasites delay acidification of parasitophorous vacuoles through insertion of LPG into the phagosomal membrane, which alters intracellular trafficking and compartment maturation (McConville et al., 1992; Moradin and Descoteaux, 2012). This allows promastigotes to differentiate into amastigotes. During the transformation process parasitophorous vacuoles become more acidic (pH 4.7–5.2) and lysosomal hydrolases and late endosomal/lysosomal proteins such as Rab7 and LAMP-1 are associated (Stebut and Tenzer, 2017).

In mice, intracellular parasites are eliminated through ROS, activated by the NADPH oxidase complex, or NO, produced by inducible NO synthase (iNOS). Effective parasite elimination requires activation of macrophages by IFNγ and TNFα (Horta et al., 2012). The relevance of ROS and NO for parasite elimination in humans is not well understood and may be specific to certain *Leishmania* species (Scott and Novais, 2016). However, iNOS expression was demonstrated in skin lesions of CL patients infected with *L. mexicana*. Levels of iNOS were higher in localized CL (low amount of parasites), compared to diffuse CL (high parasite burden) (Qadoumi et al., 2002). Carneiro et al. detected NO and ROS expression in monocytes from CL patients after *in vitro* infection with *L. braziliensis* (Carneiro et al., 2016).

Inside the phagolysosomal compartment, proteins of killed parasites are processed and presented as antigens *via* MHC-II or MHC-I to orchestrate the adaptive immune response (Neefjes et al., 2011). Interestingly, some *Leishmania* species are able to interfere with T-cell responses as they downregulate antigen presentation by macrophages (Gupta et al., 2013). It is yet unclear whether dermal DCs or macrophages transport antigens from the initial site of infection to lymph nodes to initiate an adaptive immunity (Kaye and Scott, 2011). Though, recent data from murine models support an important role of DCs in this process (Stebut and Tenzer, 2017).

In contrast to promastigotes, *Leishmania* amastigotes harbor several defense mechanisms to survive within phagolysosomes. They are adapted to acidic pH and resistant to hydrolytic environments. Amastigotes degrade heme and prevent the formation of the NADPH oxidase complex to circumvent ROS generation (Moradin and Descoteaux, 2012). Upon cell rupture, potentially mediated by pore-forming cytolysin (leishporin), amastigotes enter neighboring macrophages *via* Fcγ receptors (FcγRs) and phosphatidylserine receptors (Horta et al., 2012; Stebut and Tenzer, 2017). Antibodies such as immunoglobulin G (IgG) directed against parasites cover their surface and promote FcγR-mediated phagocytosis by macrophages (Polando et al., 2013). It has been suggested that PS on the surface of amastigotes mimics apoptotic cells and thus allows non-inflammatory internalization by macrophages (Wanderley et al., 2006).

1.1.5 Adaptive immunity in response to *Leishmania* infection

The activation of T-cells is essential for the adaptive immune response towards *Leishmania* parasites as T-cells contribute to parasite control through the secretion of various cytokines and the activation of infected macrophages (Bogdan and Röllinghoff, 1998; da Silva Santos and Brodskyn, 2014). $CD4^+$ T-helper cells (Th), *via* their T-cell receptor (TCR)/CD3 complex, recognize exogenous antigens that are loaded on MHC-II molecules. The latter are expressed on professional antigen presenting cells (APCs) such as macrophages, DCs and B-cells. Cytotoxic $CD8^+$ T-cells bind to endogenous antigens presented by MHC-I molecules that are expressed on all nucleated cells (Neefjes et al., 2011). Antigen presentation involves co-stimulatory molecules and cytokines such as CD28 and IL-2, which are required to complement T-cell activation (Alexander and Brombacher, 2012). Of note, in a process called cross-presentation, foreign proteins are also loaded on MHC-I molecules (Fehres et al., 2014).

Early studies of adaptive immunity in mice infected with *L. major* demonstrated that IFNγ- and TNFα-producing $CD4^+$ Th1 cells of C57BL/6 mice are associated with disease resolution. In contrast, IL-4- and IL-13-producing Th2 cells lead to disease susceptibility in BALB/c mice. Although in humans Th1 responses are thought to be beneficial for host defense compared to Th2, this dichotomy is very simplified and mechanisms are far more complex and not yet

fully elucidated (Kharazmi et al., 1999; Ruiz and Becker, 2007; Alexander and Brombacher, 2012). However, cytokines that are produced by T-cells seem to be either associated with disease resolution or progression. In this context, development of diffuse CL is characterized by high IL-10 and IL-4 levels and a lack of IFNγ production. In contrast, in patients suffering from localized CL, a mixture of pro- and anti-inflammatory cytokines was found (da Silva Santos and Brodskyn, 2014). In ML, an exacerbated Th1 response was detected with a lack of immunoregulation by anti-inflammatory cytokines such IL-10 (Gaze et al., 2006; Gollob et al., 2014). Patients suffering from active VL are characterized by a compromised T-cell response and high IL-10 plasma levels leading to an ineffective leishmaniacidal immune response (Hailu et al., 2005).

In contrast to $CD4^+$ T-cells, the role of $CD8^+$ T-cells is more controversial. $CD8^+$ T-cells, activated *via* cross-presentation of *Leishmania* antigens, seem to be less relevant for disease resolution and in some cases they even support disease progression (Kaye and Scott, 2011). Cytotoxicity of $CD8^+$ T-cells towards target cells is exerted through the release of pore-forming perforin that allows entry of proteases such as granzyme A and granzyme B. These proteases induce caspase-dependent apoptosis in target cells (Barry and Bleackley, 2002). Expression of granzyme A and granzyme B positively correlated with lesion progression in patients suffering from CL (da Silva Santos and Brodskyn, 2014). By contrast, $CD8^+$ T-cells are also associated with disease amelioration through the production of IFNγ and macrophage activation (Ruiz and Becker, 2007). An increase in *L. braziliensis* reactive $CD8^+$ T-cells was observed during the healing process of CL (Da-Cruz et al., 2002).

In most cases, infection of mice and humans with *Leishmania* parasites induces life-long immunity. Interestingly, after control of a primary infection, some parasites can persist in the host and are shown to contribute to the immunity of healed individuals (Zaph et al., 2004; Gollob et al., 2005). In mice, persistent *L. major* parasites led to the maintenance of a small population of $CD4^+$ effector memory T-cells that responded quickly upon reinfection. In contrast, central memory T-cells protected mice against *L. major*, even in the absence of persistent parasites (Zaph et al., 2004; Keshavarz Valian et al., 2013). In patients with a history of CL, $CD4^+$ memory T-cells expressing the marker CD45RO, were identified in response to stimulation with soluble *Leishmania* antigen (SLA). These memory T-cells

comprised both central memory T-cells and effector memory T-cells (Keshavarz Valian et al., 2013).

Taken together, during the last years, we began to obtain a more comprehensive picture of adaptive immunity towards *Leishmania* parasites, although many questions remain. Differences among *Leishmania* species and hosts lead to complex and diverging immune responses that are difficult to elucidate.

1.2 Anti-TNFα therapy

1.2.1 The pro-inflammatory cytokine TNFα

The term tumor necrosis factor (TNF) was initially introduced 1975 by Carswell et al. for the serum of endotoxin-treated mice that caused necrosis of tumors (Carswell et al., 1975). In the mid-80s, Aggarwalt et al. purified TNFα and the structurally and functionally related TNFβ from supernatants of human cell lines (Aggarwal et al., 1985a; Aggarwal et al., 1985b). Nowadays, more than 50 molecules have been identified to belong to the TNF superfamily. However, the pleiotropic pro-inflammatory cytokine TNFα is one of the most intensively studied molecules due to its versatile biologic effects in physiology and pathology (Aggarwal et al., 2012).

Homotrimeric TNFα is initially expressed as 26 kDa membrane-integrated form (mTNFα) on monocytes, macrophages, activated NK-cells, T-cells and B-cells, but also on non-immune cells such as endothelial cells and fibroblasts. Upon cleavage by metalloproteases such as TNFα-converting enzyme (TACE), the 17 kDa soluble TNFα (sTNFα) is released. It allows for endocrine functions and signaling to distant sites (Horiuchi et al., 2010; Sedger and McDermott, 2014). TNFα signals through two receptors, membrane TNF receptor 1 (mTNFR1) and 2 (mTNFR2) (**Figure 4**). In contrast to mTNFR1, which is expressed on virtually all nucleated cells, mTNFR2 expression is limited to immune and endothelial cells. Both sTNFα and mTNFα bind to mTNFR1, whereas mTNFR2 is proposed to be mainly activated by mTNFα (Mitoma et al., 2016).

Signaling through mTNFR1 leads to the recruitment of TNFR1-associated death domain protein (TRADD), which builds a platform for the formation of different signaling complexes (I, IIa, IIb and IIc). Signaling through complex I promotes the activation of nuclear factor κB

(NFκB) as well as mitogen-activated protein kinases (MAPKs) and thus, results in inflammation, tissue degeneration, cell survival, proliferation or defense mechanism against pathogens. The assembly of complex IIa and IIb activates caspases that subsequently initiate apoptosis, which is important during homeostasis, inflammation, immunity and disease pathogenesis. Intact apoptotic cells are silently cleared by macrophages, without initiation of inflammation. Complex IIc leads to necroptosis in target cells through the activation of mixed lineage kinase domain-like protein (MLKL). Necroptosis is characterized by plasma-membrane rupture and a release of intracellular contents, leading to local inflammation. Thus, cell damage by TNFα-induced necroptosis can contribute to inflammatory processes in the skin or mucosal surfaces. Engagement of mTNFR2 activates TNFR-associated factor 2 (TRAF2), leading to the assembly of complex I and activation of NFκB, MAPKs and protein kinase B (AKT). This pathway mainly results in tissue regeneration, inflammation, proliferation, survival or host defense against pathogens (reviewed by Kalliolias and Ivashkiv, 2016).

Besides TNFα, both TNFRs can be released from the surface by proteolytic cleavage, resulting in sTNFR1 and sTNFR2. Receptor shedding is thought have regulatory functions through sequestering extracellular TNFα and inhibiting signal transduction (van Zee et al., 1992). Interestingly, in a process called reverse signaling, signals are transmitted to the cell displaying mTNFα. Harashima et al. demonstrated that treatment with polyclonal antibodies, directed against TNFα, induced E-selectin expression on human $CD4^+$ T-cells expressing mTNFα *via* an outside-to-inside signal (Harashima et al., 2001).

Despite progress, many open questions persist in the understanding of TNFα signal transduction and its biological functions. The presence of soluble and membrane-integrated receptors and ligands, the different cell types that are involved and the cellular contexts make it difficult to investigate TNFα-mediated signaling and thus, detailed mechanisms remain to be entirely clarified.

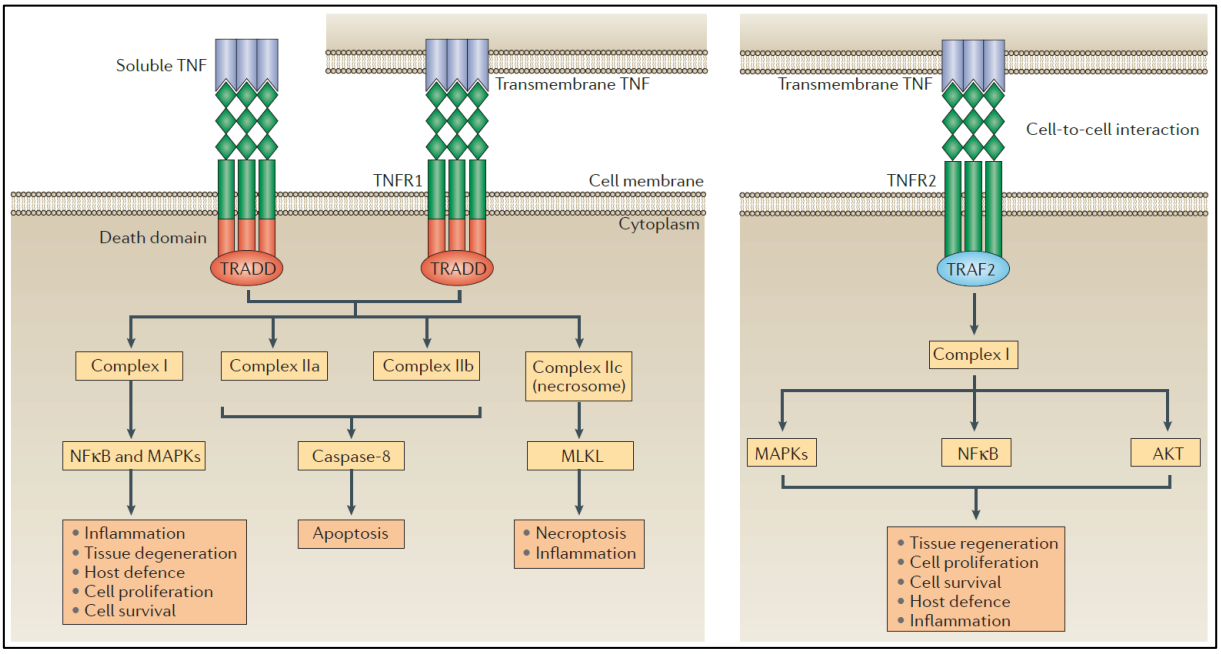

Figure 4: TNFα signaling pathways *via* mTNFR1 and mTNFR2. Activation of mTNFR1 by sTNFα or mTNFα recruits the adapter protein TRADD and triggers the formation of complex I. NFκB and MAPKs activation mediates inflammation, tissue degeneration, cell survival and proliferation as well as host defense against pathogens. Alternatively, complex IIa and IIb assembly induces apoptosis *via* caspase-8 and complex IIc initiates necroptosis as well as inflammation *via* MLKL. In contrast to mTNFR1, mTNFR2 is thought to be predominantly activated by mTNFα. Activation recruits TRAF2 and leads to the formation of complex I. Activation of NFκB, MAPKs and AKT induces tissue regeneration, cell proliferation and cell survival as well as inflammation and host defense against pathogens. Abbreviations: AKT, protein kinase B; MAPK, mitogen-activated protein kinase; MLKL, mixed lineage kinase domain-like protein; mTNFα, membrane TNFα; mTNFR, membrane TNFα receptor; NFκB, nuclear factor κB; sTNFα, soluble TNFα; TRADD, TNFR1-associated death domain protein; TRAF2, TNFR-associated factor 2; TNFα, tumor necrosis factor α (Kalliolias and Ivashkiv, 2016).

1.2.2 Pathogenic effects of TNFα: inflammatory and autoimmune diseases

TNFα exerts a wide range of biological functions contributing to inflammation, tissue destruction or host defense (**1.2.1**). A prerequisite for these processes is regulation of TNFα activity as effects might otherwise be pathogenic. Uncontrolled production of TNFα is implicated in the pathogenesis of severe inflammatory/autoimmune diseases such as rheumatoid arthritis, inflammatory bowel disease, psoriasis, psoriatic arthritis, ankylosing spondylitis and juvenile idiopathic arthritis (Bradley, 2008; Kalliolias and Ivashkiv, 2016). Prevalence and symptoms of these diseases are listed in **Table 1**.

Table 1: Prevalence and symptoms of TNFα-associated autoimmune diseases.

Disease	Prevalence	Symptoms
Rheumatoid arthritis[1]	0.3-1.0% worldwide	Synovial inflammation, joint destruction, impaired movement, pain, swelling, depression, fatigue
Inflammatory bowel disease[2,3]	1.5% US adults	Inflammation of small and large intestine, diarrhea, abdominal pain, bloody stools and vomiting
Psoriasis[4]	0.9-8.5 % worldwide	Epidermal hyperplasia, skin lesions (knee, elbow, scalp)
Psoriatic arthritis[4] (often associated with psoriasis)	0.16-0.25% worldwide	Synovial hyperplasia, immune cell infiltration in skin and synovium, pain, swelling, joint tenderness
Ankylosing spondylitis[5]	0.5% worldwide	Rheumatic disease involving sacroiliac joints and axial skeleton, inflammatory back pain, stiffness, loss of mobility, increased bone formation in the spine
Juvenile idiopathic arthritis[6]	0.1% worldwide	Inflammatory joint disease, chronic synovitis, lymphadenopathy, pericarditis, uveitis, fever, anorexia, weight loss, anemia

[1]Chaudhari et al., 2016; [2]Fakhoury et al., 2014; [3]CDC, 2017; [4]Coates et al., 2016; [5]Shaikh, 2007; [6]Arthritis Foundation, 2017

Numerous studies demonstrated the relevance of TNFα for autoimmune diseases. Plasma levels and intracellular expression of TNFα in circulating $CD4^+$ T-cells were found to be increased in patients suffering from psoriasis compared to healthy controls (Kagami et al., 2010). Similarly, plasma levels were elevated in patients with ankylosing spondylitis, inflammatory bowel disease and juvenile idiopathic arthritis (Maeda et al., 1992; Bal et al., 2007). In the synovium of rheumatoid arthritis and psoriatic arthritis patients as well as the lamina propria of inflammatory bowel disease patients, TNFα expression was also increased

(Murch et al., 1993; van Kuijk et al., 2006). Moreover, levels of mTNFR2 on mucosal $CD4^+$ T-cells from inflammatory bowel disease patients were increased compared to healthy controls (Atreya et al., 2011). Detailed mechanisms underlying excessive TNFα or mTNFR production remain unclear. However, TNFα gene promoter polymorphisms have been shown to contribute to the development of TNFα-associated autoimmune diseases (El-Tahan et al., 2016). Besides excessive production of TNFα, these inflammatory diseases are characterized by increased levels of other cytokines (*e.g.* IFNγ) as well as an accumulation of immune cells (*e.g.* macrophages, T-cells, B-cells).

Genetic predisposition, environmental factors and, in the case of IBD, intestinal microbial flora are involved in disease pathogenesis (Rai and Wakeland, 2011; Zhang and Li, 2014). However, precise mechanisms that lead to inflammatory diseases are not fully understood.

1.2.3 Anti-TNFα antibodies and antibody-derived molecules

Given the pleiotropic effects of TNFα and its implication in the development of various autoimmune diseases (**1.2.2**), this cytokine is a promising target for therapy. Advances in biotechnology during the last decades enabled the development of monoclonal antibodies (mAbs) that bind target molecules with high specificity (Singh et al., 2017). To date, 15 antibody-based therapies directed against TNFα are approved for clinical use, which revolutionized therapy of autoimmune diseases (European Medicines Agency, 2017). Anti-TNFα mAbs or antibody-derived molecules that are currently authorized by the European Medicine Agency (EMA) are listed in **Table 2**.

Remicade®, a chimeric murine-human IgG1 mAb, was the first anti-TNFα mAb. It was approved by the EMA in 1999. Further TNFα blockers like the fully human mAbs Humira® and Simponi®, the TNFR2-Fc fusion protein Enbrel® and the PEGylated humanized Fab-derived inhibitor Cimzia® followed in subsequent years (European Medicines Agency, 2017).

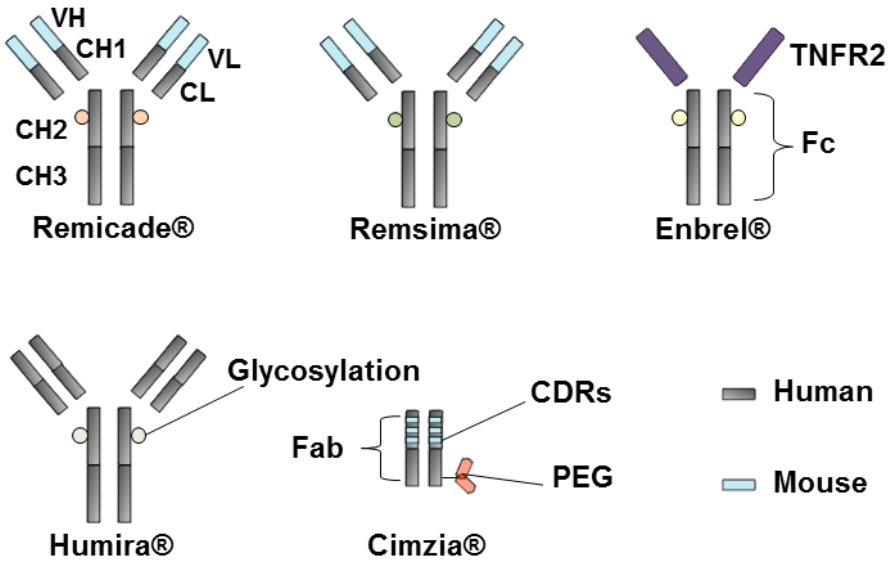

Figure 5: Structures of therapeutic anti-TNFα agents. Remicade® and its biosimilar Remsima® are chimeric murine-human IgG1 antibodies. They share an identical amino acid sequence. Enbrel® is a fusion protein of the extracellular domain of human TNFR2 and the Fc region of human IgG1. Humira® is a fully human IgG1 antibody and Cimzia® is a PEGylated Fab fragment of a humanized anti-TNFα antibody. Abbreviations: CDRs, complementarity determining regions; CH, heavy-chain constant region; CL, light-chain constant region; Fab, fragment antigen-binding; Fc, fragment crystallizable; PEG, polyethylene glycol; VH, heavy-chain variable region; VL, light-chain variable region.

The structures of Enbrel® and Cimzia® significantly differ from other TNFα inhibitors (**Figure 5**). Enbrel® consists of the Fc region of human IgG1, which is fused to two molecules of TNFR2 (Goffe and Cather, 2003). Cimzia® is an antigen-binding fragment (Fab) of a humanized anti-TNFα mAb (Goel and Stephens, 2010). Furthermore, Cimzia® is the only anti-TNFα agent with a site-specific attachment of a 40 kDa polyethylene glycol (PEG) moiety.

Due to reduced size, Fab molecules have only short circulation half-lives and are rapidly degraded in patients (Nelson, 2010). In order to improve half-life and bioavailability as well as chemical and biological properties, these molecules are modified with a PEG moiety. PEG reduces renal clearance by increasing the molecule size. It is highly soluble in water and thus, improves solubility of the conjugated molecule, which allows high concentrations of PEGylated molecules without aggregation. This enables subcutaneous administration of pharmaceuticals, which improves tolerability. Moreover, the PEG moiety is described to decrease immunogenicity and proteolytic degradation of the conjugated substances (Pasut, 2014).

Antibodies are large and complex molecules. Structural disparities such as differences in the amino acid sequence, glycosylation or antibody format result in various modes of action

(Mitoma et al., 2016). Hence, indications of approved anti-TNFα agents differ (European Medicines Agency, 2017). The TNFα blockers Remicade®, Humira®, Enbrel® and Cimzia® demonstrated similar binding affinities towards sTNFα and mTNFα (Mitoma et al., 2016). However, Enbrel® binds homotrimeric TNFα in a 1:1 ratio, whereas three molecules of Remicade® can bind one molecule of TNFα. As a consequence, Remicade® is capable of forming large protein complexes (Scallon et al., 2002; Mitoma et al., 2016). In contrast to the other full-length anti-TNFα antibodies, Enbrel® and Cimzia® showed reduced or no antibody-dependent cell-mediated cytotoxicity (ADCC) and complement-dependent cytotoxicity (CDC) towards mTNFα expressing cells, respectively (Nesbitt et al., 2007; Mitoma et al., 2008).

ADCC is an effector function of antibodies, bound to target molecules on cell surfaces. The IgG Fc region of the antibody is recognized by immune cells such as NK-cells and macrophages, bearing FcγRs. Stimulated NK-cells release perforin, granulysin and granzymes, which induces apoptosis of target cells. Activated macrophages secrete proteases, ROS as well as cytokines and they are able to phagocytose antibody-coated cells to tackle infections (Strome et al., 2007; Ochoa et al., 2017). In CDC, complement component C1 binds to the Fc part of target-bound antibodies. This activates the complement cascade (**1.1.3**), leads to MAC formation and consequently to target cell death (Strome et al., 2007).

The lack of ADCC and CDC activity upon Cimzia® treatment is caused by the absence of an Fc region in this drug. In respect of Enbrel®, the absence of the first constant region of the heavy chain (CH1) might explain its only weak induction of CDC. The reason why Enbrel® only exerts low ADCC activity remains unclear (Mitoma et al., 2016). In contrast to Remicade®, Enbrel® and Cimzia® are not licensed for the treatment of IBD by the EMA (European Medicines Agency, 2017). One possible explanation may be that Remicade®, in contrast to Enbrel® and Cimzia®, is capable to promote lysis of mTNFα expressing cells. This mechanism of action is potentially relevant for the treatment of IBD (Mpofu et al., 2005).

Table 2: Approved anti-TNFα monoclonal antibodies or antibody-based molecules for the treatment of autoimmune diseases (European Medicines Agency, 2017).

Tradename	Active substance	Indication	Date of Authorization
Remicade®	Infliximab	RA, PsA, Ps, AS, CD, UC	1999
Enbrel®	Etanercept	RA, PsA, Ps, AS, JIA	2000
Humira®	Adalimumab	RA, PsA, Ps, AS, CD, UC, JIA	2003
Cimzia®	Certolizumab pegol	RA	2009
Simponi®	Golimumab	RA, PsA, AS, UC	2009
Remsima®	Infliximab	RA, PsA, Ps, AS, CD, UC	2013
Inflectra®	Infliximab	RA, PsA, Ps, AS, CD, UC	2013
Benepali®	Etanercept	RA, PsA, Ps	2016
Flixabi®	Infliximab	RA, PsA, Ps, AS, CD, UC	2016
Lifmior®	Etanercept	PsA, Ps, AS	2017
Solymbic®	Adalimumab	RA, PsA, Ps, AS, CD, UC	2017
Amgevita®	Adalimumab	RA, PsA, Ps, AS, CD, UC, JIA	2017
Erelzi®	Etanercept	RA, PsA, Ps, AS, JIA	2017
Imraldi®	Adalimumab	RA, PsA, Ps, AS, CD, UC	2017
Cyltezo®	Adalimumab	RA, PsA, Ps, AS, CD, UC, JIA	2017

Abbreviations: AS, ankylosing spondylitis; CD, Crohn's disease; JIA, juvenile idiopathic arthritis; Ps, psoriasis; PsA, psoriatic arthritis; RA, rheumatoid arthritis; UC, ulcerative colitis.

Patent expiration of anti-TNFα agents enabled the development of biosimilars by competitor companies. These are highly similar copy versions of first generation biologics (originators) (Mantzaris, 2016). Driving forces that promote marketing of biosimilars are the reduction of medication costs and the increase of market competition, providing new treatment options for patients (Konara et al., 2016). Competitor companies need to set up new production lines without knowing detailed manufacturing processes of the originator. This can lead to

minor or major variations between the biosimilar and its reference product, despite their identical amino acid sequence. Potential post-translational modifications such as glycosylation, acetylation and phosphorylation are cell-type specific and pH- as well as temperature-dependent and could therefore influence the final properties of generated drugs (Theillet et al., 2012; Kannicht et al., 2013).

Marketing authorization of a biosimilar medicine requires demonstration of similarity in terms of structure, safety, efficacy and immunogenicity in comparison with the originator (EMA, 2017). Remsima® was the first infliximab-based biosimilar antibody that successfully demonstrated similarity to Remicade®, albeit minor differences were detected regarding fucosylation of glycans. This led to different binding affinities towards FcγRs and consequently, ADCC activity of Remsima® was lower compared to Remicade® in the most sensitive *in vitro* assay. However, these minor variations were not considered clinically relevant as aberrant effects were absent in experiments that were more representative of pathophysiological conditions. Thus, Remsima® received marketing authorization by the EMA in 2013 (EMA, 2013). Further biosimilars that hitherto gained approval for the treatment of TNFα-associated autoimmune diseases are listed in **Table 2**.

1.2.4 Anti-TNFα therapy and leishmaniasis

One major risk of anti-TNFα therapy is a higher susceptibility to serious bacterial, viral and parasitic infections (Bongartz et al., 2006; Minozzi et al., 2016). Several immunosuppressive mechanisms caused by TNFα inhibition are thought to contribute to these adverse effects. TNFα is required for host defense against viral pathogens (*e.g.* hepatitis B) and the formation of granulomas, which is important to control tuberculosis. Neutropenia is also associated with anti-TNFα treatment and supports fungal infections caused by *Candida* or *Aspergillus*. Moreover, TNFα is essential for macrophage activation and the clearance of intracellular pathogens such as *Salmonella* or *Listeria* (Ali et al., 2013).

Leishmania parasites reside and multiply within macrophages (**1.1.4**). Several murine studies demonstrated the importance of TNFα for parasite control and elimination by macrophages. Local treatment of *L. major*-infected mice with recombinant TNFα decelerated lesion growth (F Y Liew, C Parkinson, S Millott, A Severn, and M Carrier, 1990), whereas neutralization of

TNFα by antibodies promoted disease development (Liew et al., 1990a; Theodos et al., 1991). Anti-TNFα treatment of *L. major*-infected C57BL/6 mice resulted in an increased parasite number and lesion size. Furthermore, iNOS expression was reduced in macrophages upon TNFα blockade (Fonseca et al., 2003). Knock-out of TNFα in resistant C57BL/6 mice delayed T-cell proliferation and resulted in fatal VL after infection with *L. major* (Wilhelm et al., 2001; Wilhelm et al., 2005).

Besides the data obtained in mice, also studies with human cells or subjects revealed a correlation of TNFα with *Leishmania* infection. *In vitro* infection of human neutrophils with *L. major* promastigotes induced TNFα secretion into cell supernatants (van Zandbergen et al., 2006). Serum levels of TNFα were highly elevated in patients with CL or VL during active disease and TNFα concentrations declined upon effective therapy (Barral-Netto et al., 1991; Nateghi Rostami et al., 2015). Similarly, Ribeiro-de-Jesus et al. demonstrated that TNFα levels in supernatants of *L. amazonensis*-stimulated PBMCs obtained from CL and ML patients were significantly reduced after successful therapy (Ribeiro-de-Jesus et al., 1998). Furthermore, increased expression of TNFα was found in lesions of CL and ML patients compared to healthy controls (Galdino et al., 2014).

In addition to its protective effects, TNFα has also been linked to tissue destruction and lesion development in leishmaniasis (Oliveira et al., 2011; Oliveira et al., 2014). These somehow contradictory findings indicate that TNFα participates in the inflammatory response in order to eliminate parasites, but continued and excessive production potentially contributes to disease pathology. The reduction of TNFα levels in patients after healing, supports this assumption (Castellano et al., 2009).

Immunosuppressive anti-TNFα therapy of patients suffering from autoimmune diseases is linked to leishmaniasis. Several case reports indicate the onset of leishmaniasis after treatment with anti-TNFα agents (Catala et al., 2015; Guarneri et al., 2017). Guarneri et al. reported that ML and VL developed in a psoriatic arthritis patient treated with Simponi® (Guarneri et al., 2017). A patient suffering from rheumatoid arthritis developed VL and CL was detected in an ankylosing spondylitis patient. In both cases, leishmaniasis was caused by *L. infantum* and developed after 9 infusions of Remicade® (Fabre et al., 2005; Hakimi et al., 2010). Humira® treatment provoked ML in a psoriatic arthritis and CL in a rheumatoid arthritis patient (Guedes-Barbosa et al., 2013; Micallef and Azzopardi, 2014). Bagala et al.

reported the onset of VL after the treatment with Enbrel® for rheumatoid arthritis and Jeziorski et al. described a mucosal relapse of VL after Remicade® and Enbrel® treatment of a child infected with *L. infantum* and suffering from juvenile idiopathic arthritis (Bagalas et al., 2007; Jeziorski et al., 2015).

It is difficult to discriminate recent *Leishmania* infection from reactivation of a latent infection as patients were not tested for *Leishmania* prior to initiating anti-TNFα therapy (Leonardis et al., 2009). However, Franklin et al. reported reactivation of latent CL in a rheumatoid arthritis patient treated with Humira®. This patient lived in a non-endemic area during anti-TNFα therapy, but had immigrated from endemic areas years ago (Franklin et al., 2009). Tektonidou et al. described a possible reactivation of a latent *Leishmania* infection in a Remicade®-treated psoriatic arthritis patient, who had been exposed to the parasite 5 years ago (Tektonidou and Skopouli, 2008).

Interestingly, differences have been observed regarding the risk of infection. An increased incidence of leishmaniasis is indicated for the treatment of patients with Remicade® or Humira® compared to Enbrel® (Salmon-Ceron et al., 2011; Zanger et al., 2012). Similarly, a higher risk of tuberculosis has been reported in Remicade®- or Humira®-treated patients in comparison with Enbrel® (Mitoma et al., 2016).

Despite these adverse effects, TNFα blockers have emerged as powerful tool for the treatment of inflammatory diseases. They significantly contribute to disease control and improve patients' quality of life. In order to minimize adverse effects, patients must be informed about the potential risk of infections and screening for latent tuberculosis or leishmaniasis prior to initiation of anti-TNFα therapy is recommended in endemic areas (Ali et al., 2013).

1.3 Hypothesis and aims

Excessive production of the pro-inflammatory cytokine TNFα has been implicated in the pathophysiology of several inflammatory/autoimmune diseases. Over the last 20 years, the development of anti-TNFα agents, which inhibit TNFα activity, has revolutionized therapy. However, immunosuppressive anti-TNFα treatment is associated with an increased risk of developing infectious diseases such as leishmaniasis. TNFα inhibitors that have been approved by the EMA strongly differ in their structure and they exert different effector functions. With the aim to elucidate the mechanisms of action of different anti-TNFα agents in the context of leishmaniasis and to compare their impact on parasite control in humans, we investigated the following hypothesis in the present study:

"*Therapeutic TNFα inhibitors differentially affect host defense against Leishmania parasites.*"

We tested this hypothesis including the following objectives:

1. Establishment and characterization of an *in vitro* model, representative for human cutaneous leishmaniasis. This model is based on *L. major*-infected primary human macrophages as host cells in co-culture with autologous T-cells as effector cells.

2. Comparison of Remicade®, Remsima®, Humira® and Cimzia® in the *in vitro* model by analyzing their effects on *L. major*-induced T-cells and *L. major* infection rates in macrophages. Selected agents represent different structures: Remicade® is a chimeric murine-human and Humira® a fully human IgG1 anti-TNFα antibody. Cimzia® is a PEGylated Fab fragment of a humanized anti-TNFα antibody and the biosimilar Remsima® shares an identical amino acid sequence with its originator Remicade®, but demonstrated differences in posttranslational modifications.

3. Analyzing the neutralizing capacity of anti-TNFα agents towards sTNFα and mTNFα as well as the induction of ADCC and CDC towards mTNFα expressing cells

4. Investigating the structural differences of tested anti-TNFα agents that potentially lead to diverging effects on parasite control.

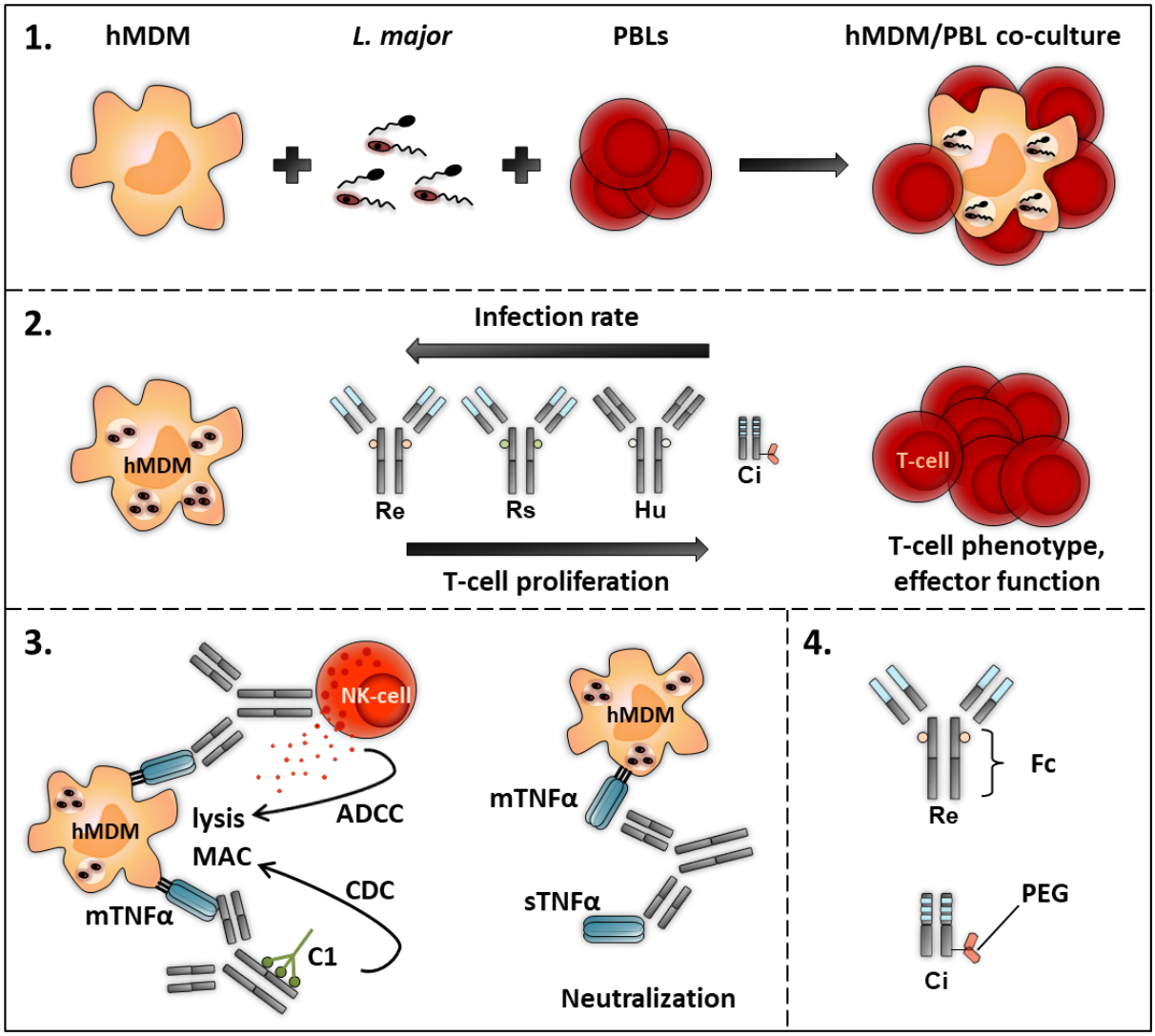

Figure 6: Schematic representation of the aims of this work. (1) Establishment of an *in vitro* model based on primary human macrophages that were infected with fluorescent *L. major* and co-cultured with autologous T-cells. (2) Comparison of the anti-TNFα agents Remicade® (Re), Remsima® (Rs), Humira® (Hu) and Cimzia® (Ci) in the *in vitro* model by analyzing their effects on *L. major*-induced T-cells and *L. major* infection rates in macrophages. (3) Investigating the ADCC and CDC activity towards mTNFα expressing cells as well as the neutralizing capacity of anti-TNFα agents towards sTNFα and mTNFα. (4) Examination of the structural differences of studied TNFα blockers that potentially result in diverging effects on parasite control.

2 Material and methods

2.1 Materials

2.1.1 Chemicals

β-Mercaptoethanol	Sigma-Aldrich, Taufkirchen, GER
Ammonium chloride	In-house facility PEI, Langen, GER
Aqua bidest.	In-house facility PEI, Langen, GER
Bovine Serum Albumin (BSA)	Applichem, Darmstadt, GER
CASYton	OLS-OMNI, Bremen, GER
Difco™ Brain Heart Infusion Agar	Becton Dickenson, Sparks, USA
Dimethyl sulfoxide (DMSO)	Sigma Aldrich, Taufkirchen, GER
Ethanol (EtOH), absolut	Applichem, Darmstadt, GER
FACS Clean	In-house facility PEI, Langen, GER
FACS Flow (Sheath Solution)	In-house facility PEI, Langen, GER
FACS Rinse	In-house facility PEI, Langen, GER
Fetal calf serum (FCS)	Sigma-Aldrich, Taufkirchen, GER
Glutamine (L-Glutamine)	Biochrom AG, Berlin, GER
HEPES	Biochrom AG, Berlin, GER
High purity water	In-house facility PEI, Langen, GER
Histopaque 1077	Sigma-Aldrich, Taufkirchen, GER
Human recombinant GM-CSF	Bayer, Leverkusen, GER
Human serum Type AB	Sigma-Aldrich, Taufkirchen, GER
Hygromycin B, solution	Invitrogen, San Diego, USA
Immersion oil (Immersol™ 518F)	Carl Zeiss, Jena, GER
Methanol	Merck, Darmstadt, GER
MS-PEG Methyl-PEG_{24}-N-Hydroxysuccinimid-Ester	Thermo Scientific, Dreieich, GER

Paraformaldehyde (PFA)	Sigma-Aldrich, Taufkirchen, GER
Penicillin/Streptomycin	Biochrom AG, Berlin, GER
Phosphate buffered saline (1x PBS) w/o Ca^{2+}, Mg^{2+}; pH 7.1; cell culture, FC, IF	In-house facility PEI, Langen, GER
Phosphate buffered saline (1x PBS) w/o Ca^{2+}, Mg^{2+}; pH 7.4; ELISA	In-house facility PEI, Langen, GER
Polyglobin®	Bayer, Leverkusen, GER
ProLong® Gold antifade reagent	Invitrogen, Darmstadt, GER
Propidium iodide (PI)	Sigma-Aldrich, Taufkirchen, GER
Rabbit Blood, defibrinated	Elocin-Lab GmbH, Gladbeck, GER
Roswell Park Memorial Institute (RPMI) 1640 Medium	Sigma-Aldrich, Deisenhof, GER Biowest (VWR), Darmstadt, GER
Saponin from Quillaja bark	Sigma-Aldrich, Taufkirchen, GER
TAPI-1 (TACE inhibitor)	Enzo Life Sciences, Lausen, CHE
Tween20	Sigma-Aldrich, Steinheim, GER

2.1.2 Cell culture media

Leishmania promastigotes (*Lm*-medium)	500 ml	RPMI-1640 Medium
	5%	FCS (v/v)
	2 mM	L-Glutamine
	50 µM	β-Mercaptoethanol
	100 U/ml	Penicillin
	100 µg/ml	Streptomycin
	10 mM	HEPES
Primary human cells (complete-medium)	500 ml	RPMI-1640 Medium
	10%	FCS (v/v)
	2 mM	L-Glutamine
	50 µM	β-Mercaptoethanol
	100 U/ml	Penicillin
	100 µg/ml	Streptomycin
	10 mM	HEPES

Novy-McNeal-Nicolle (NNN) Blood Agar	100 ml	defibrinated rabbit blood
	20.8 g	Difco™ Brain Heart Infusion agar
	400 ml	high-purity water
	100 ml	PBS w/o Ca^{2+} and Mg^{2+}, pH 7.1
	66.2 U/ml	Penicillin
	66.2 µg/ml	Streptomycin

2.1.3 Buffer and solutions

Ammonium chloride solution	0.15 M	Ammonium chloride
		Aqua bidest.
AutoMACS buffer pH 7.2		1x PBS
	2 mM	EDTA
	0.5%	BSA (w/v)
FC blocking buffer		1x PBS
	10%	FCS (v/v)
	10%	Human serum (v/v)
FC staining buffer		1x PBS
	1%	FCS (v/v)
	1%	Human serum (v/v)
IF permeabilization solution		1x PBS
	0.5%	triton
Intracellular FC / IF fixation solution		1x PBS
	4%	PFA
Intracellular FC / IF blocking buffer		1x PBS
	10%	FCS (v/v)
	10%	Human serum (v/v)
	0.5%	Saponin (w/v)

Intracellular FC / IF staining buffer		1x PBS
	1%	FCS (v/v)
	1%	human serum (v/v)
	0.5%	saponin (w/v)
1x PBS w/o Ca^{2+} and Mg^{2+} pH 7.1 / pH 7.4	136.9 mM	sodium chloride
	2.68 mM	potassium chloride
	1.47 mM	potassium dihydrogen orthophosphate
	8.1 mM	sodium dihydrogen phosphate
		Aqua bidest
Washing buffer (PBMC isolation)		1x PBS
	5%	complete-medium (v/v)

2.1.4 *Leishmania* strains

Leishmania major isolate MHOM/IL/81/FEBNI:

Originally isolated from a skin biopsy of an Israeli patient and kindly provided by Dr. Frank Ebert (Bernhard Nocht Institute for Tropical Medicine, Hamburg, Germany)

Leishmania major DsRed / EGFP:

MHOM/IL/81/FEBNI isolates were genetically transfected with the red fluorescent DsRed (from Discosoma) or green fluorescent EGFP (from Aequoria victoria) gene. Hygromycin phosphotransferase was used as selection marker (Misslitz et al., 2000).

2.1.5 Primary human cells

Buffy coats were obtained from the blood donation service in Frankfurt (DRK-Blutspendedienst) and human peripheral blood mononuclear cells (PBMCs) were isolated as described in **2.2.2.1**. Blood donors were healthy individuals, which have not been exposed to *Leishmania* before.

2.1.6 Antibodies

Neutralizing antibodies

Remicade®, infliximab, approx. 149 kDa	Janssen Biologics, Leiden, NL
Remsima®, infliximab, approx. 149 kDa	Celltrion Healthcare, Incheon, KOR
Humira®, adalimumab, approx. 148 kDa	AbbVie, Chicago, USA
Cimzia®, certolizumab pegol, approx. 91 kDa including 2x20 kDa PEG	UCB, Brussels, BEL
Mouse anti-human IFNγ, clone B27 (purified)	BioLegend, San Diego, USA
Mouse anti-human mTNFR1, clone H398 (purified)	eBioscience, Waltham, USA
Mouse anti-human mTNFR2, clone utr1 (purified)	BMA Biomedicals, Augst, CHE

Fluorescent antibodies

Goat F(ab')2 anti-human IgG Fc RPE, polyclonal	Dianova, Hamburg, GER
Mouse anti-human CD3 PB, clone UCHT1	BD Pharmingen, Heidelberg, GER
Mouse anti-human CD4 APC-Cy7, clone OKT4	BioLegend, San Diego, USA
Mouse anti-human CD8 APC-Cy7, clone SK1	BioLegend, San Diego, USA
Mouse anti-human CD16 APC, clone 3G8	BioLegend, San Diego, USA
Mouse anti-human CD25 APC, clone M-A251	BioLegend, San Diego, USA
Mouse anti-human CD32 FITC, clone 3D3	BD Pharmingen, Heidelberg, GER
Mouse anti-human CD45RO PE, clone UCHL1	BD Pharmingen, Heidelberg, GER
Mouse anti-human CD64 APC, clone 10.1	BioLegend, San Diego, USA
Mouse anti-human CD69 APC, clone FN50	BioLegend, San Diego, USA
Mouse anti-human granulysin A647, clone DH2	BioLegend, San Diego, USA
Mouse anti-human granzyme A A647, clone CB9	BioLegend, San Diego, USA
Mouse anti-human granzyme B A647, clone GB11	BioLegend, San Diego, USA

Mouse anti-human mTNFα PE, clone Mab11	BD Pharmingen, Heidelberg, GER
Mouse anti-human mTNFR1 APC, clone 16803	R&D Systems, Minneapolis, USA
Mouse anti-human mTNFR2 APC, clone 22235	R&D Systems, Minneapolis, USA
Mouse anti-human PD-1 PE, clone MIH4	BD Pharmingen, Heidelberg, GER
Mouse anti-human perforin APC, clone dG9	BioLegend, San Diego, USA

Isotype controls

Mouse IgG1 kappa A647, APC, APC-Cy7, FITC, PB, PE, clone MOPC-21	BioLegend, San Diego, USA
Mouse IgG1 kappa APC, clone 11711	R&D Systems, Minneapolis, USA
Mouse IgG2a APC, clone 20102	R&D Systems, Minneapolis, USA
Mouse IgG2a kappa PE, clone MOPC-173	BioLegend, San Diego, USA
Mouse IgG2b kappa APC, APC-Cy7, clone MPC-11	BioLegend, San Diego, USA

2.1.7 Dyes

CFSE (5(6)-Carboxyfluorescein diacetate N-succinimidyl ester)	Sigma Aldrich, Steinheim, GER
Hoechst 34580	BD Pharmingen, Heidelberg, GER
Diff-Quik	Medion Diagnostics, Düdingen, CH

2.1.8 Ready to use kits

CD14 MicroBeads, human	Miltenyi Biotec, Bergisch Gladbach, GER
Pan T Cell Isolation Kit, human	Miltenyi Biotec, Bergisch Gladbach, GER
Naive Pan T Cell Isolation Kit, human	Miltenyi Biotec, Bergisch Gladbach, GER
Human TNFα DuoSet ELISA	R&D systems, Minneapolis, USA

Human IL-10 DuoSet ELISA	R&D systems, Minneapolis, USA
Human IFNγ DuoSet ELISA	R&D systems, Minneapolis, USA
LEGEND MAX™ Human C5a	BioLegend, San Diego, USA

2.1.9 Laboratory supplies

Cell culture flasks with filter ($25\ cm^2$, $75\ cm^2$)	Greiner Bio-One, Frickenhausen, GER
Cell culture petri dish (10 cm diameter)	Sarstedt, Nümbrecht, GER
Cell culture plates (96-well f-/v-/u-bottom)	Sarstedt, Nümbrecht, GER
Cell culture plates (6-well flat)	Sarstedt, Nümbrecht, GER
Cellfunnel (single, double)	Tharmac GmbH, Waldsolms, GER
Cellspin filter cards (one/two hole/s)	Tharmac GmbH, Waldsolms, GER
Cell Scraper, 16 cm	Sarstedt, Nümbrecht, GER
Centrifuge tubes (0.2 ml)	Sarstedt, Nümbrecht, GER
Centrifuge tubes (1.5 ml, 2.0 ml)	Eppendorf, Hamburg, GER
Chamber slide, 12-well, removable	ibidi GmbH, Planegg / Martinsried, GER
Cover Slide (24x50 mm)	VWR, Darmstadt, GER
Cryogenic vial (2 ml)	Greiner Bio-One, Frickenhausen, GER
Cytocentrifuge Slides one circle, uncoated	Tharmac GmbH, Waldsolms, GER
FACS microtubes (2 ml)	Micronic, Lelystad, NL
FACS tubes (5 ml) with snap-cap	Greiner Bio-One, Frickenhausen, GER
Falcons (15 ml, 50 ml)	Greiner Bio-One, Frickenhausen, GER
Filters, polyethersulfone, 0.22 µm; 0.45 µm	Merck Millipore, Billerica, USA
Gloves	B. Braun, Melsungen, GER
Microplate (96-well flat, transparent)	Greiner Bio-One, Frickenhausen, GER
Multichannel pipette (Research® Plus)	Eppendorf, Hamburg, GER

Mr. Frosty Freezing Container	Thermo Scientific, Dreieich, GER
Neubauer improved cell counting chamber (depth 0.1 mm, 0.02 mm)	VWR, Darmstadt, GER
Petri dish (3 cm diameter)	Greiner Bio-One, Kremsmünster, AUT
Pipette controller (accu-jet® pro)	BRAND, Wertheim, GER
Pipette Research® plus (0.5-10 µl, 10-100 µl, 20-200 µl, 100-1000 µl)	Eppendorf, Hamburg, GER
Pipette tips (0.5-10 µl, 2-200 µl, 50-1000 µl)	Eppendorf, Hamburg, GER
Serological pipettes, sterile (2.5 ml, 5 ml, 10 ml, 25 ml)	Greiner Bio-One, Kremsmünster, AUT
Sterile filter (0.22 µm, 0.45 µm)	Sarstedt, Nümbrecht, GER
Transfer pipette (3.5 ml)	Sarstedt, Nümbrecht, GER

2.1.10 Instruments

Centrifuges

BIOLiner Buckets (75003670; 7500368)	Thermo Scientific, Dreieich, GER
Bioshield 1000 A swing-out rotor	Thermo Scientific, Dreieich, GER
Bench top centrifuges 5430 and 5430R	Eppendorf, Hamburg, GER
Cytocentrifuge Cellspin II Universal 320R	Tharmac GmbH, Waldsolms, GER
Heraeus Megafuge 40R	Thermo Scientific, Dreieich, GER
Sprout Mini-Centrifuge	Biozym, Hamburg, GER

Flow cytometer

Flow Cytometer LSR II SORP	Becton Dickinson, Heidelberg, GER

Imaging

Microscope AxioPhot	Carl Zeiss, Jena, GER
Microscope Axio Observer.Z1	Carl Zeiss, Jena, GER
Microscope Primo Star	Carl Zeiss, Jena, GER

Incubators

CO_2-Incubator Forma Series II Water Jacket	Thermo Scientific, Marietta, USA
CO_2 incubator, Heraeus Auto Zero	Thermo Scientific, Dreieich, GER

Lamina air flow

Workbench MSC-Advantage	Thermo Fisher Scientific, Dreieich, GER
Steril Gard III Advance	The Baker Company, Sanford, USA
Steril Gard Hood	The Baker Company, Sanford, USA

Others

Analytical balance KB BA 100	Sartorius, Göttingen, GER
AutoMACS Pro separator	Miltenyi Biotec, Bergisch Gladbach, GER
Autoclave Systec vx-150	Systec, Wettenberg, GER
CASY Modell TT	Roche Innovatis AG, Reutlingen, GER
ELISA Reader Infinite® F50	Tecan Group Ltd, Männedorf, CHE
Freezer (-20°C)	Bosch, Stuttgart, GER
Freezer U725-G (-80°C)	New Brunswick Scientific, Nürtingen, GER
Ice machine AF 1000	Scotsman, Pogliano Milanese, ITA
Magnetic stirrer IKA® C-MaG HS7	IKA®-Werke, Staufen, GER

Nitrogen container “Chronos”	Messer, Bad Soden, GER
pH Meter PB-11	Sartorius, Göttingen, GER
Ultrasonic bath Sonorex Super RK103H	Bandelin, Berlin, GER
Vortex mixer VV3	VWR International, Darmstadt, GER
Water bath	Köttermann, Uetze, GER

2.1.11 Software

Axio Vision Rel. 4.8	Carl Zeiss, Jena, GER
BD Diva Software (v6.1.3)	Becton Dickinson, Heidelberg, GER
Citavi v5	Swiss Academic, Wädenswil, CHE
FlowJo v10	Miltenyi Biotec, Bergisch Gladbach, GER
GraphPad Prism v7	GraphPad Software, La Jolla, USA
Microsoft® Office 2010	Microsoft, Redmont, USA

2.2 Methods

2.2.1 Cell culture of *Leishmania major*

All cell culture procedures were carried out under sterile and endotoxin free conditions in a laminar flow hood.

2.2.1.1 *In vitro* cultivation of *Leishmania major*

Leishmania promastigotes were cultured in biphasic NNN blood agar medium (**2.2.1.3**). After 6-8 days of cultivation, *Leishmania* suspension was diluted in *Lm*-medium (1:10) and counted (**2.2.1.2**). Parasite suspension was adjusted to a concentration of $1x10^6$/ml and 100 µl were distributed to each well of a new blood agar plate using a multi-channel pipette. Parasites were incubated at 27°C and 5% CO_2 and after 8 serial passages new *Leishmania* were thawed (**2.2.1.4**). For transgenic DsRed or EGFP expressing *Leishmania* parasites, culture medium was supplemented with Hygromycin (20 µg/ml).

2.2.1.2 Counting *Leishmania major* promastigotes

Leishmania parasites were counted using a hemocytometer (Neubauer chamber; depth: 0.02 mm). 5 µl of the diluted cell suspension were added to the chamber and 8 small squares were counted at a 40x magnification. Both viable and apoptotic parasites were counted to determine the total amount of *Leishmania*. In order to calculate cell concentrations, the following formula was used:

$$\frac{Leishmania}{\text{ml}} = \frac{\text{total number of } Leishmania \text{ x } 16}{\text{counted squares}}\ 5\text{x}10^4$$

2.2.1.3 Preparation of blood agar plates

For the preparation of blood agar, 20.8 g Brain Heart Infusion (BHI) agar was dissolved in 400 ml water and autoclaved for 15 min at 121°C. BHI agar was cooled down (~55°C) and added to 100 ml pre-warmed PBS (42°C) in a petri dish (Ø25 cm). 4 ml penicillin/streptomycin and 100 ml aseptically collected defibrinated rabbit blood were added. Finally, 60 µl blood agar were distributed to each well of a flat-bottom 96-well plate using a multi-channel pipette. Plates were prepared in a 45° angle for pipetting. They were sealed and stored at 4°C for up to 4 months.

2.2.1.4 Long-time storage of *Leishmania* parasites

100-200x10^6 *Leishmania* promastigotes were pelleted (2400x g, 8 min, RT), resuspended in 1 ml cold *Lm*-medium supplemented with 20% FCS and 10% DMSO and transferred into cryotubes. Cells were cooled down overnight to -80°C using a Mr. Frosty freezing container and transferred to a liquid nitrogen tank for long-time storage.

Parasites were thawed by placing cryotubes in a water bath (37°C) until the last ice crystals were visible. *Leishmania* suspension was slowly diluted using 7 ml *Lm*-medium and centrifuged (2400x g, 8 min, RT). Promastigotes were resuspended in 12 ml *Lm*-medium and 100 µl of the cell suspension were transferred to a new blood agar plate (100 µl/well). Parasites were used for experiments from the second passage.

2.2.2 Cell culture of primary human cells

2.2.2.1 Isolation of peripheral blood mononuclear cells (PBMCs)

Buffy coats (30-50 ml) of healthy donors were diluted with pre-warmed 1x PBS to a final volume of 100 ml. For separation, 25 ml of the diluted blood sample were carefully layered over 15 ml pre-warmed leukocyte separation medium (Histopaque 1077) in a 50 ml tube and centrifuged (573x g, 30 min, RT) with lowest acceleration and deceleration. The interphase, containing PBMCs, was distributed to 6 new 50 ml tubes and washing buffer was added to a final volume of 50 ml. For removal of residual granulocytes, cell debris and platelets multiple washing steps at 1084x g, 573x g and 143x g (8 min, RT) were performed. Erythrocytes were lysed by incubation with 10 ml cold ammonium chloride (10-15 min, 20°C). After 2-3 final washing steps (143x g, 8 min, RT) until the supernatant was clear, cell count of PBMCs was determined using a CASY Cell Counter (**2.2.2.2**). Monocytes were separated from peripheral blood lymphocytes (PBLs) by plastic adherence (**2.2.2.3**) or magnetic-activated cell sorting (MACS) (**2.2.2.4**).

2.2.2.2 Counting PBMCs, monocytes, macrophages, PBLs or T-cells

10 µl cell suspension were diluted in 10 ml CASY ton in a CASY tube and measured using an automatic CASY Cell Counter (150 µm capillary), which specifies cell concentration, viability, size, debris as well as aggregation. Cell concentrations were divided by the aggregation factor to obtain final values.

2.2.2.3 Separation of monocytes by plastic adherence and generation of hMDMs

For the isolation of monocytes by plastic adherence, 40-50x10^6 freshly isolated PBMCs were seeded in 5 ml complete-medium supplemented with 1% human serum in a 25 cm^2 culture flask. Cells were incubated for 1 h (37°C, 5% CO_2) enabling monocytes to adhere to the plastic. Cell supernatants containing non-adherent PBLs were removed by gently washing the flasks 2 times with pre-warmed washing buffer. PBLs were collected in 50 ml tubes and stored frozen (**2.2.2.5**). Monocytes were differentiated into human monocyte-derived macrophages (hMDMs) in complete-medium supplemented with 10 ng/ml granulocyte-macrophage colony-stimulating factor (GM-CSF) over a period of 5-7 days at 37°C and 5% CO_2.

2.2.2.4 Separation of monocytes by MACS and generation of hMDMs

Human monocytes were enriched by $CD14^+$ separation using CD14 Microbeads and the autoMACS Pro Separator. 100x10^6 freshly isolated PBMCs were transferred to a 15 ml tube and washed with 10 ml autoMACS buffer (143x g, 8 min, RT). The pellet was resuspended in 400 µl autoMACS buffer and incubated with 40 µl CD14 MicroBeads for 15 min at 4°C. Excess beads were removed by washing with 10 ml autoMACS buffer (143x g, 8 min, RT) and the pellet was resuspended in 500 µl autoMACS buffer. Labeled cells were separated with the autoMACS Pro Separator (program: “posseld”, positive selection double column). Enriched monocytes were centrifuged (143x g, 8 min, RT), resuspended in complete-medium, counted (**2.2.2.2**) and 4x10^6 cells/well in 2.5 ml complete-medium were seeded (6-well plate). Medium was supplemented with GM-CSF (10 ng/ml) to differentiate monocytes into hMDMs and cells were incubated for 5-7 days at 37°C and 5% CO_2. After 3 days of cultivation, the culture media were exchanged. Cell supernatants were transferred to 15 ml tubes, centrifuged (143x g, 8 min, RT) and pellets were resuspended in fresh complete-medium containing 10 ng/ml GM-CSF. The $CD14^-$ fraction of autoMACS separation comprised PBLs and was stored frozen (**2.2.2.5**).

2.2.2.5 Freezing and thawing of PBLs

Non-adherent PBLs (separation by plastic adherence) or $CD14^-$ PBLs (separation by autoMACS) were resuspended in 2 ml complete-medium supplemented with 40% FCS and

10% DMSO and equally distributed to 2 cryovials. Samples were gradually (1°C/min) frozen in a Mr. Frosty freezing container placed in a -80°C laboratory freezer.

Cryovials were quickly thawed in a water bath (37°C) until the last ice crystals were visible. Cells were carefully transferred to 10 ml pre-warmed complete-medium and DMSO was removed by centrifugation (143x g, 8 min, RT). Cell pellets were resuspended in complete-medium and the cell count of PBLs was determined (**2.2.2.2**).

2.2.2.6 Harvesting adherent macrophages

Morphology of differentiated hMDMs (day 5-7) was examined under the microscope. Prior to harvesting cells, flasks or plates were kept on ice (30 min) to facilitate detachment of hMDMs. Cells were harvested using a cell scraper and flasks/plates were washed once with cold 1x PBS to collect residual hMDMs. Samples were pooled in a 50 ml tube, centrifuged (143x g, 8 min, RT) and the cell pellet was resuspended in 1-2 ml complete-medium. Cell counts were determined as described (**2.2.2.2**).

2.2.2.7 Separation of T-cells by MACS

Stored PBLs were thawed (**2.2.2.5**) and counted (**2.2.2.2**). Untouched $CD3^+$ or naive $CD3^+$ T-cells were obtained using the Pan T-Cell Isolation Kit or the Naive Pan T-Cell Isolation Kit as described by the manufacturer. Separation was carried out with the autoMACS Pro Separator (program: “depletes”).

2.2.3 *Leishmania*-based infection model

2.2.3.1 Infection of macrophages with *Leishmania major*

Harvested hMDMs (**2.2.2.6**) were stained with 4 µM CFSE in complete-medium for 15 min (37°C). Excess CFSE was removed by washing cells once with complete-medium and $0.6x10^6$ hMDMs in 60 µl complete-medium were transferred to 1.5 ml microcentrifuge tubes. For infection, $12x10^6$ *Leishmania* promastigotes in 6 µl complete-medium were added (multiplicity of infection (MOI) = 20) and hMDMs were incubated at 37°C, 5% CO_2. After 3 h, extracellular parasites were removed by washing hMDMs twice with 900 µl complete-medium. Thereafter, pellets were resuspended in a final volume of 1000 µl and samples were incubated for 24 h (37°C, 5% CO_2).

2.2.3.2 Co-incubation of hMDMs with PBLs or T-cells

24 h after infection with *Leishmania*, hMDMs were distributed ($0.1x10^6$ cells/tube in 167 µl complete-medium) to enable longer cultivation. Stored PBLs were thawed (**2.2.2.5**), counted (**2.2.2.2**), separated by MACS if necessary (**2.2.2.7**) and labeled with 4 µM CFSE as described (**2.2.3.1**). For the PBL-based T-cell assay, $0.5x10^6$ PBLs and for the purified T-cell-based T-cell assay, $0.5x10^6$ separated T-cells in 833 µl complete-medium were added to distributed hMDMs. Co-cultures were incubated for a further period of 6 days (37°C, 5% CO_2).

2.2.3.3 Blockade of cytokines and receptors

If not indicated otherwise, anti-TNFα agents were used in equimolar amounts (20 µg/ml Remicade®, 20 µg/ml Remsima®, 20 µg/ml Humira® and 13 µg/ml Cimzia®). IFNγ was neutralized using 10 µg/ml of anti-IFNγ antibody and mTNFRs were blocked with 1 µg/ml of anti-mTNFR1 antibody or anti-mTNFR2 antibody. Neutralizing agents were added to each microcentrifuge tube immediately after the addition of PBLs or T-cells (**2.2.3.2**). FcγRs on hMDMs were saturated by pre-incubation (1 h, 37°C) with 20 µg/ml of the IgG preparation Polyglobin® prior to distribution of hMDMs and the addition of PBLs or T-cells (**2.2.3.2**). All agents remained in culture media over the whole period of incubation (6 days).

2.2.3.4 PEGylation of Remicade®

Primary amino ($-NH_2$) groups of Remicade® were PEGylated with 1.2 kDa MS-PEG. If not indicated otherwise, Remicade® was incubated with 20-fold molar excess of MS-PEG for 30 min (RT) as recommended by the manufacturer. PEG-Remicade® and Remicade® were added in equimolar amounts to infected hMDMs as described (**2.2.3.3**).

2.2.4 Flow cytometry

By flow cytometry, hMDMs (24 h post-infection) or hMDM/PBL co-cultures (7 d post-infection) were analyzed to determine expression of specific markers, T-cell proliferation, *Lm* infection rates or cell viability. For this purpose, cell suspensions of corresponding conditions were pooled in 15 ml tubes and centrifuged (143x g, 8 min, RT). Cell supernatants were collected in 96-well plates (duplicates) and stored frozen at -80°C for ELISA analysis (**2.2.6**). Cell pellets were resuspended in 300 µl ice cold FC blocking buffer, incubated for 10 min

(4°C) and 0.15-0.4x10^6 cells per well were seeded in 96-well plates. Subsequently, cells were washed once with 100 µl FC staining buffer and incubated in 100 µl antibody staining solution for 30 min at 4°C in the dark. Fluorescent-labeled antibodies and the respective isotype controls were diluted in FC staining buffer as defined by the manufacturers. After incubation, cells were washed with FC staining buffer and pellets were resuspended in 100 µl FC staining buffer. Samples were incubated for 5-10 min with PI (5 pg/ml) before measurement to discriminate dead cells (PI^+). For intracellular analysis cells were fixed in 100 µl 4% PFA solution (10 min, 4°C) and permeabilized in intracellular FC blocking solution (10 min, 4°C) prior to staining. Staining was carried out in intracellular FC staining buffer. Samples were recorded using a BD LSR II SORP flow cytometer and analyzed by FlowJo software. Gating strategies are depicted in **Figure 9**. The mean fluorescence intensity (MFI) of specific markers was normalized to the respective isotype control by division and is presented as relative fluorescence intensity (RFI). Proliferation of viable T-cells was determined by the decline of CFSE ($CFSE^{low}$) and *Lm* infection rates in viable hMDMs were assessed by DsRed or EGFP expressing *Lm* as described previously (Crauwels et al., 2015). For T-cell proliferation and *Lm* infection rates, values of the respective controls were subtracted for each donor and condition (Δ), respectively, which enabled donor-specific evaluation of different treatments.

2.2.5 Immunofluorescence

7 d after infection, 0.2x10^6 cells were seeded per well in a 12-well chamber slide. Subsequent to incubation (30 min, 37°C) allowing adherence to the slide, cells were fixed in 100 µl IF fixation solution (10 min, 4°C). Thereafter, wells were washed twice with 100 µl 1x PBS and permeabilized with IF permeabilization solution (10 min, 4°C). After washing twice with 100 µl 1x PBS, 100 µl IF blocking buffer were added (10 min, 4°C). Cells were washed twice and 100 µl IF antibody staining solution were added for 30 min (4°C). Fluorescent-labeled antibodies were diluted in IF staining buffer as recommended by the manufacturers. Excess of antibodies was removed by washing wells once with 1x PBS and nuclear staining was carried out for 10 min using 100 µl of diluted Hoechst 34580 (1 µg/ml in 1x PBS). After complete removal of supernatant, a cover slip was applied with 3 drops of

ProLong Gold Antifade Mountant. The chamber slide was stored in the dark at 4°C. Analysis was carried out at a 63x magnification using a Zeiss Axio Observer.Z1 microscope.

2.2.6 ELISA

24 h or 7 d after infection, cell culture supernatants were collected in 96-well plates (duplicates) and frozen at -80°C. They were thawed and analyzed for the presence of human sTNFα, IL-10 or IFNγ using DuoSet ELISA Kits according to the manufacturer's protocol. Human C5a levels were examined with the LEGEND MAX C5a ELISA Kit according to the manufacturer's instructions (exception: provide 20 µl Buffer B + 80 µl sample/standard and incubate over night at 4°C). The optical density was measured with a microplate reader and cytokine concentrations were determined by comparing optical densities to the respective standard curve.

2.2.7 Diff-Quik staining

At least 10^5 hMDMs were sedimented on glass slides by centrifugation at 75x g for 5 min. Afterwards, slides were air-dried, fixed with methanol (2 min, RT) and stained (2 min, RT) using Diff-Quik solution I and II (Medion Diagnostics). Excess dye was washed away with water. Analysis of cytospin slides was performed using a Zeiss AxioPhot microscope and a 100x magnification.

2.2.8 Statistical analysis

All data are shown as mean ± SD. The number of independent experiments and donors (*n*) is depicted in each figure. Statistical significance was determined by the Wilcoxon signed-rank test (two-tailed, paired) using Graph-Pad Prism. A value of $*P < 0.05$; $**P < 0.01$; $***P < 0.001$ and $****P < 0.0001$ was considered statistically significant.

3 Results

3.1 Characterization of infected hMDM/PBL co-cultures

3.1.1 *Leishmania major* growth characteristics

The virulent inoculum of *L. major* consists of viable and apoptotic parasites (van Zandbergen et al., 2006). In order to select the appropriate parasite culture for subsequent infection experiments, which contains both viable and apoptotic *Leishmania*, we first investigated the time frame of logarithmic (log phase) or stationary (stat phase) parasite growth by counting parasites under a microscope (**Figure 7A**). During the first 3 days of cultivation (log phase) the number of parasites rapidly increased from $2.6x10^6$ *Lm*/ml to $7.4x10^7$ *Lm*/ml. Afterwards, cell counts rose more slowly (in this thesis we termed this transition phase) until the maximum of $1.6x10^8$ *Lm*/ml on day 6 to 8 (stat phase) was reached. We additionally determined culture composition by separately counting viable and apoptotic parasites (**Figure 7B**). The percentage of apoptotic cells decreased during the first 3 days (stat phase) of cultivation from 43% to the minimum of 1%. Then, during the transition phase, the proportion of apoptotic parasites increased again until the stat phase (day 6-8) was reached, where *L. major* cultures comprise 50-60% apoptotic parasites. To mimic natural infection conditions in our experiments, we used *L. major* of the stat phase that were cultivated *in vitro* for 6-8 days and thus were composed of a higher proportion of apoptotic parasites in comparison to the log phase.

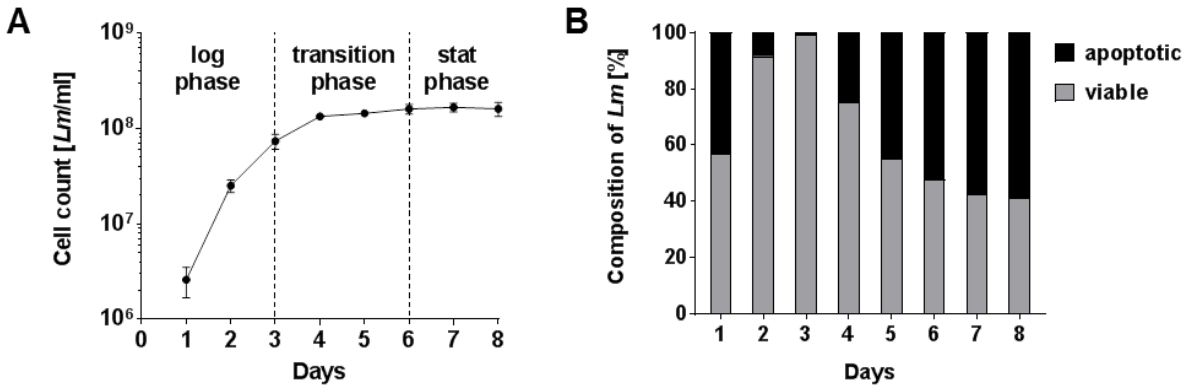

Figure 7: Growth characteristics of *L. major* parasites. *L. major* promastigotes were cultured in blood agar plates over a period of 8 days. (A) Parasite growth was determined by counting total *Leishmania* under the microscope every 24 hours. (B) To analyze the composition of *Leishmania* cultures, the percentage of viable and apoptotic parasites was determined. Data are presented as mean ± SD and were obtained in 1-3 independent experiments (*n*=1-3).

3.1.2 Infection of human macrophages with *L. major*

In our *in vitro* infection model, we used hMDMs as host cells of *L. major* parasites. Human blood cells were obtained from healthy individuals that had not been exposed to *Leishmania* before. Monocytes were separated from these blood cells by plastic adherence and hMDMs were generated by incubation with GM-CSF. We confirmed infection with *L. major* by analyzing hMDMs 24 hours after the addition of parasites (MOI=20). Diff-Quik stained cytospins from infected samples, compared to non-infected controls, visualized the uptake of *L. major* into hMDMs (**Figure 8A**). Quantification was carried out by flow cytometry using transgenic *L. major* that expressed either a red (DsRed) or green (EGFP) fluorescent protein. We determined *L. major* infection rates in comparison to non-infected control samples and found that 24 hours after parasite addition 26±13% of hMDMs were infected with *L. major* (**Figure 8B**). Diff-Quik staining and flow cytometric analysis demonstrated susceptibility of hMDMs to infection with *L. major* and confirmed successful uptake of parasites into host cells.

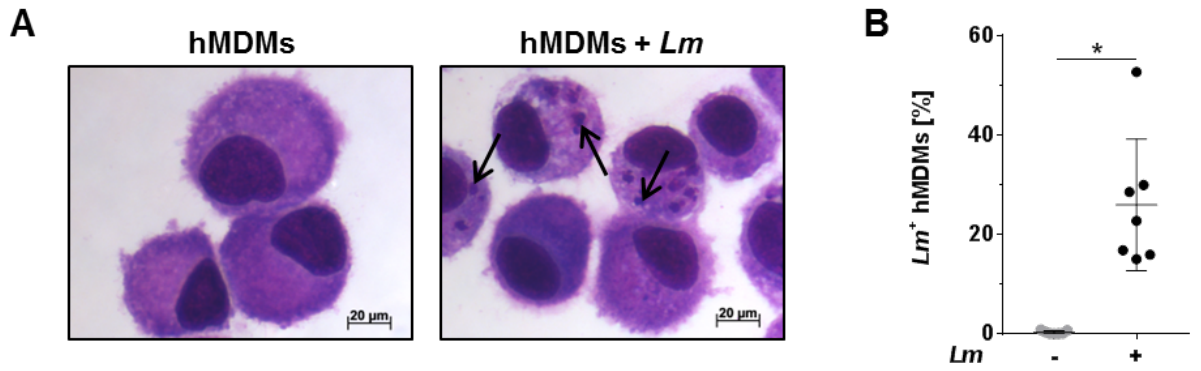

Figure 8: *L. major* infection rates in hMDMs. Macrophages were infected with fluorescent *L. major* (MOI=20) and analyzed after 24 hours. (A) Infected and non-infected hMDMs were stained with Diff-Quik and images were taken at 100x magnification using a Zeiss AxioPhot microscope. Representative micrographs are depicted. Black arrows indicate *L. major* parasites. (B) Infection rates in hMDMs were quantified 24 hours after infection by flow cytometry in comparison to non-infected controls. Data are presented as mean ± SD (n=7) and were obtained in 2 independent experiments. The Wilcoxon signed-rank test was performed to evaluate statistical significance. *$P < 0.05$.

3.1.3 T-cell proliferation in response to *L. major* infection of macrophages

We co-cultured *L. major*-infected or non-infected hMDMs with CFSE-labeled autologous PBLs, comprising approximately 70-90% T-cells (**Figure 9A**), to study the consequences on T-cell proliferation and infection rates in hMDMs. Using flow cytometry, proliferation of T-cells was assessed by the decline of CFSE and infection rates were determined through detection

of fluorescent *L. major* parasites. Gating strategies applied to analyze flow cytometric data are depicted (**Figure 9B, C**).

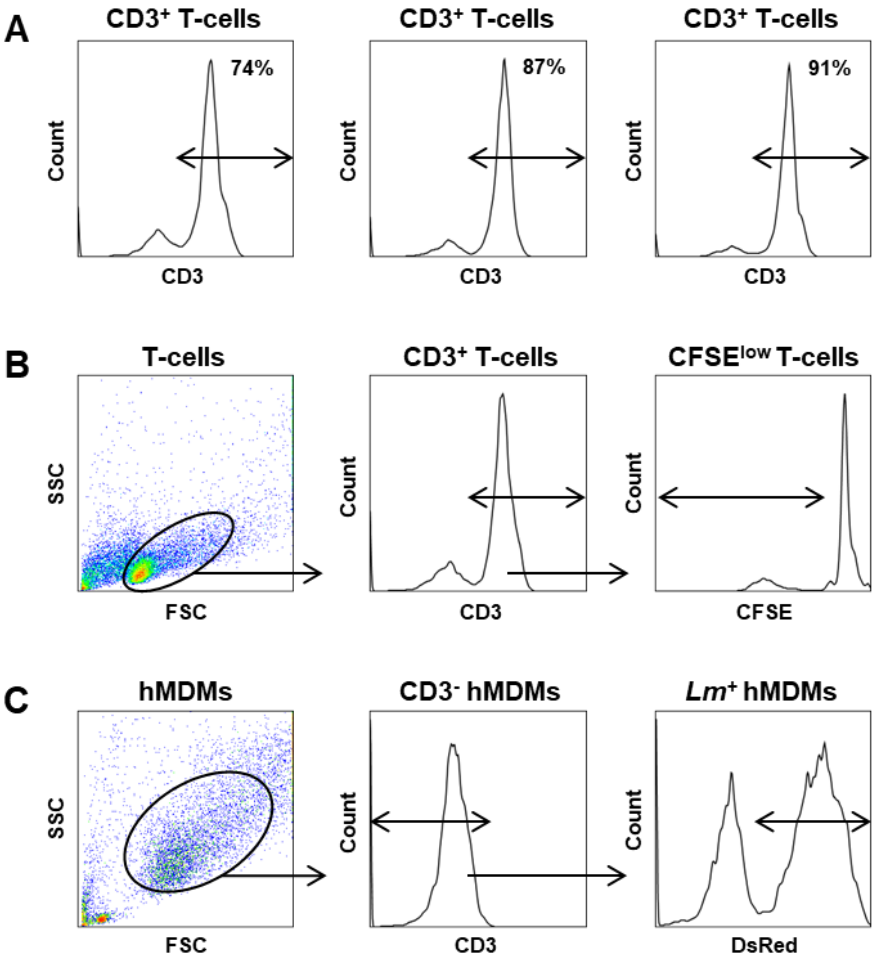

Figure 9: Gating strategies used to determine T-cell proliferation and *L. major* infection rates. (A) PBLs comprise approximately 70-90% T-cells: T-cells within PBLs were determined according to their SSC/FSC properties and anti-CD3 antibody co-staining. (B) T-cell proliferation: $CD3^+$ T-cells were gated as described in (A). Proliferation of T-cells was determined by the reduction of CFSE ($CFSE^{low}$). (C) *L. major* infection rate: Macrophages were gated according to their SSC/FSC properties and $CD3^+$ T-cells were excluded using anti-CD3 antibody co-staining. The percentage of infected hMDMs was assessed using *L. major* that expressed EGFP or DsRed.

We observed a significant increase of $CD3^+$ T-cell proliferation (10±7%) in response to *L. major* infection of hMDMs compared to non-infected controls (3±2%) (**Figure 10A**). As a consequence of T-cell proliferation, the percentage of *L. major*-infected hMDMs was significantly reduced (44±13%) in the presence of PBLs compared to their absence (68±14%) (**Figure 10B**). Phenotypic characterization of $CD3^+$ T-cells revealed that *L. major*-induced proliferating ($CFSE^{low}$) T-cells expressed CD4 (14±13% of total T-cell population). Only 2±1% of total T-cells expressed CD8 and proliferated upon infection. The percentage of non-

proliferating ($CFSE^{high}$) $CD4^+$ T-cells in the *L. major*-infected co-culture was 56±10% and the proportion of $CFSE^{high}$ $CD8^+$ T-cells was 28±9% (**Figure 10C**). In the absence of *L. major*, the percentage of proliferating $CD4^+$ T-cells was reduced (4±3%) and thus, the proportion of non-proliferating $CD4^+$ T-cells was increased (63±9%). Non-infected co-cultures additionally comprised 1±2% $CFSE^{low}$ $CD8^+$ and 30±8% $CFSE^{high}$ $CD8^+$ T-cells. These data demonstrated that a $CD4^+$ T-cell response was able to reduce the number of infected macrophages. In contrast, $CD8^+$ T-cells did not proliferate upon *L. major* infection of hMDMs.

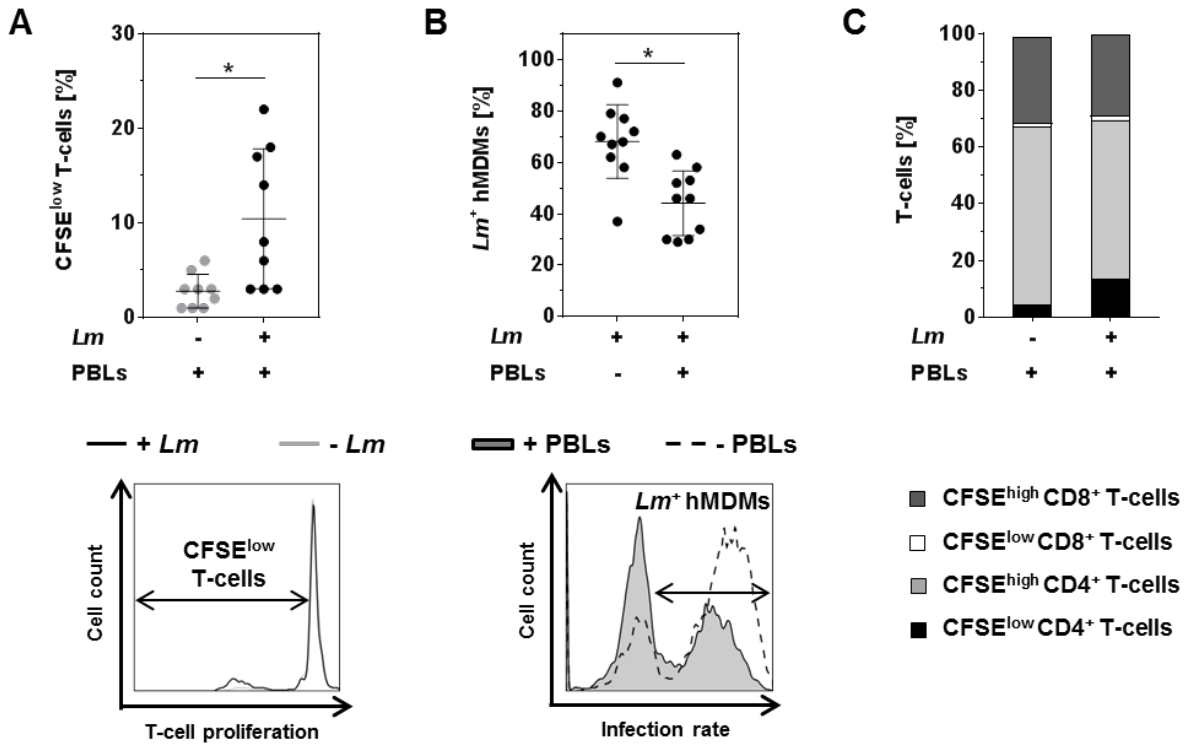

Figure 10: Proliferation of $CD4^+$ T-cells reduces the number of *L. major*-infected macrophages. *L. major*-infected/non-infected hMDMs (MOI=20) were incubated in the absence or presence of CFSE-labeled autologous PBLs. 7 days post-infection, T-cell proliferation (A, C) and infection rates (B) were measured by flow cytometry with T-cells being defined by anti-CD3 antibody co-staining. (A, B) Representative histograms show T-cell proliferation in the non-infected (grey line) in comparison to the *L. major*-infected co-culture (black line) and infection rates in hMDMs in the absence (black dashed line) compared to the presence of PBLs (black solid). (C) CD4 and CD8 subset distribution was determined for proliferating ($CFSE^{low}$) and non-proliferating ($CFSE^{high}$) $CD3^+$ T-cells. At least 3 independent experiments were conducted of which data are presented as mean ± SD ($n \geq 9$). To determine statistical significance, the Wilcoxon signed-rank test was performed.*$P < 0.05$.

3.1.4 Upregulation of T-cell activation markers upon *L. major* infection

Besides T-cell proliferation, activation of T-cells can be determined by the expression of specific surface markers. Hence, we investigated surface expression of the T-cell activation markers CD25, CD69 and programmed death-1 (PD-1) on either whole T-cell populations or on proliferating T-cells (BRENCHLEY et al., 2002; Sabins et al., 2016). Surface expression was determined by flow cytometry and is depicted as the ratio of the MFI of specific markers to the MFI of isotype controls (RFI). We found that CD25 (mean RFI: 17±9) was significantly upregulated on whole T-cells in the infected hMDM/PBL co-culture compared to non-infected controls (mean RFI: 10±7) (**Figure 11A**). In contrast, CD69 expression on T-cells (mean RFI: 19±3 vs 13±6) did not change significantly upon *L. major* infection of hMDMs (**Figure 11B**). Analysis of the proliferating population revealed that T-cells from non-infected hMDM/PBL co-cultures, showing minimal proliferation, expressed PD-1 (mean RFI: 5±2). This expression was significantly upregulated (**Figure 11C**) upon infection of hMDMs (mean RFI: 11±3). Overall, increased activation of T-cells was detected due to infection of hMDMs with *L. major*.

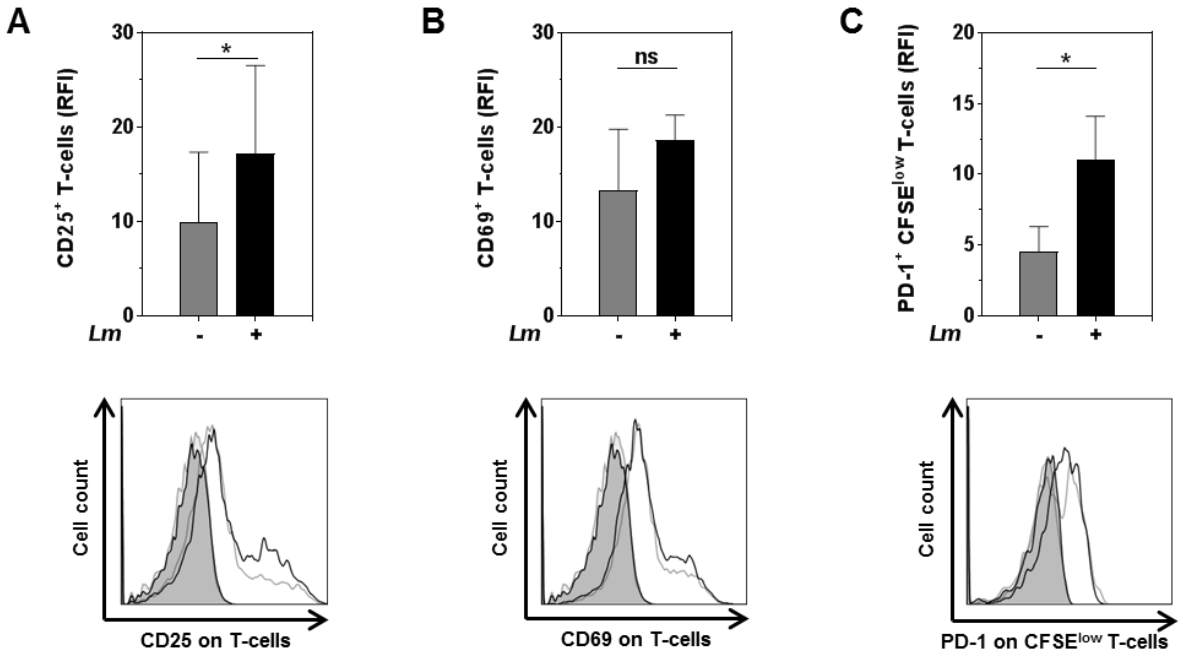

Figure 11: Increased expression of T-cell activation markers upon *L. major* infection of hMDMs. Non-infected or *L. major*-infected hMDMs (MOI=20) were incubated in the presence of CFSE-labeled autologous PBLs. 7 days after infection, expression of CD25 (A) and CD69 (B) was determined on whole T-cell populations by flow cytometry with T-cells being defined by anti-CD3 antibody co-staining. (C) Expression of PD-1 was assessed for $CFSE^{low}$ T-cells. RFI is depicted as the ratio of the MFI of specific markers to the MFI of isotype controls. Representative histograms show cell surface expression on T-cells in the infected (black line) or non-infected culture (grey line) in comparison to isotype controls (black/grey solid). At least 3 independent experiments were conducted of which data are presented as mean ± SD ($n \geq 5$). To determine statistical significance, the Wilcoxon signed-rank test was performed.*$P < 0.05$.

3.1.5 Naive T-cells respond to *L. major* infection of macrophages

As indicated above (**3.1.3**), T-cells proliferated upon *L. major* infection of hMDMs, although blood cells were obtained from healthy donors. Previous studies suggest cross-reactive memory T-cells, rather than naive T-cells, to respond to *Leishmania* parasites (Kemp et al., 1992). Using flow cytometry, we investigated the memory phenotype of proliferating T-cells by analyzing CD45RO expression in the presence or absence of an infection. We found that T-cells from non-infected hMDM/PBL co-cultures, showing low basal proliferation, expressed CD45RO (mean RFI: 28±20) (**Figure 12A**). This expression was significantly upregulated (mean RFI: 38±21) upon infection of hMDMs, supporting the assumption that $CD45RO^+$ memory T-cells respond to *L. major*.

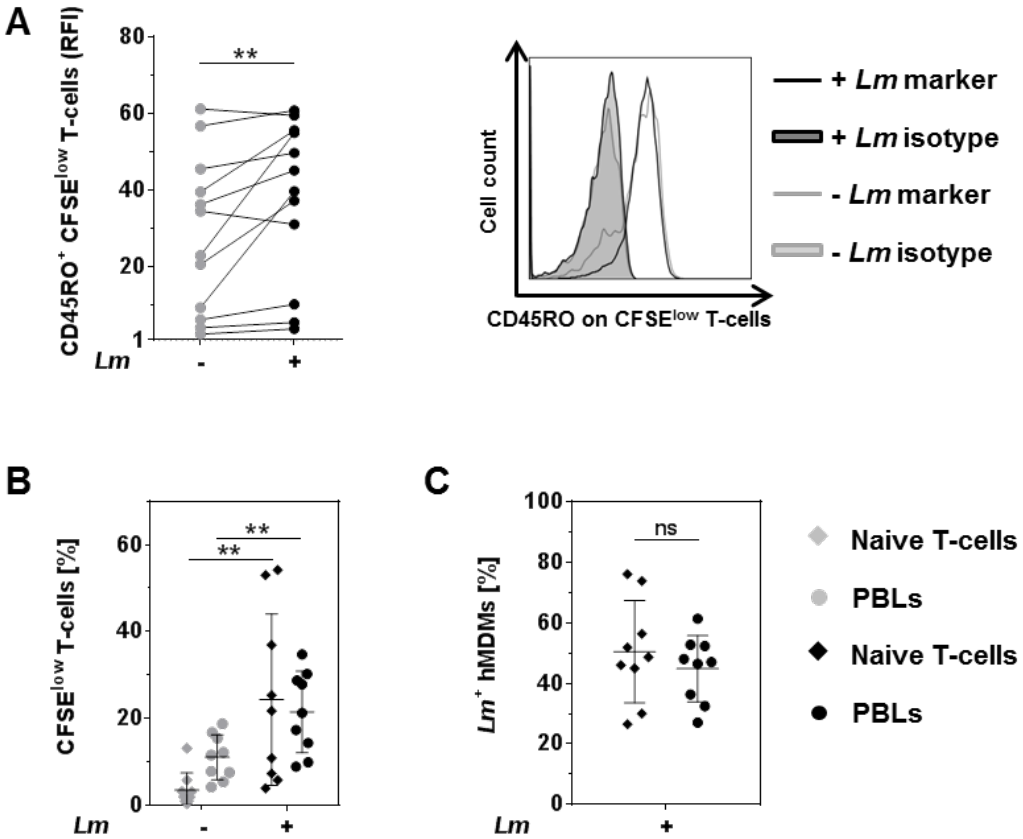

Figure 12: Natural reactivity of T-cells towards *L. major*. *L. major*-infected/non-infected hMDMs (MOI=20) were incubated in the presence of CFSE-labeled autologous PBLs. 7 days after infection, T-cell proliferation (A, B) and infection rates (C) were measured by flow cytometry with T-cells being defined by anti-CD3 antibody co-staining. (A) CD45RO expression on proliferating T-cells was assessed using flow cytometry. Representative histograms show cell surface expression on proliferating T-cells in the infected (black line) or non-infected culture (grey line) in comparison to isotype controls (black/grey solid). T-cell proliferation (B) and infection rates (C) in the hMDM/PBL co-culture were compared to values obtained with MACS-separated naive $CD3^+$ T-cells co-cultured with $CD14^+$ hMDMs. At least 3 independent experiments were conducted of which data are presented as mean ± SD ($n \geq 8$). To determine statistical significance, the Wilcoxon signed-rank test was performed.*$P < 0.05$; **$P < 0.01$.

To further characterize the T-cell response towards parasites, studies with MACS-purified naive CD45RA$^+$ T-cells and CD14$^+$ hMDMs were performed. These experiments revealed that naive T-cells from *Leishmania*-unexposed individuals considerably proliferate (24±20% vs 3±4%) in response to infection (**Figure 12B**). Thereupon, the number of infected hMDMs is reduced (50±17%) to a similar extent as after the co-incubation with PBLs (45±11%) (**Figure 12C**).

We additionally analyzed CD45RO expression on MACS-purified naive T-cells and compared results to those obtained with T-cells from PBLs. In contrast to PBLs, non-proliferating naive T-cells in the non-infected and infected co-culture did not express CD45RO, confirming successful MACS-separation of CD45RO$^-$ T-cells (**Figure 13A, B**). Interestingly, in the co-culture with naive T-cells, CD45RO expression was upregulated upon T-cell proliferation, both in the absence (**Figure 13A**) and presence (**Figure 13B**) of *L. major*. According to these findings, non-exposed individuals possessed a natural reactivity to *L. major* parasites, contributing to disease control. Upon proliferation, CD45RO levels are increased on T-cells.

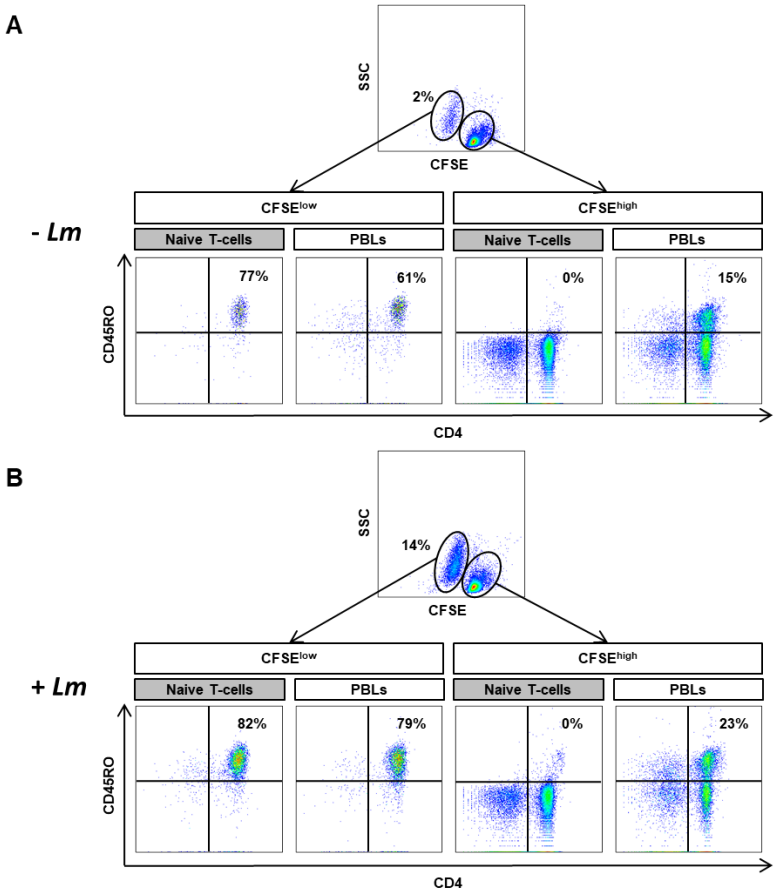

Figure 13: CD45RO expression on CD4$^+$ T-cells. Non-infected (A) and *L. major*-infected (B) hMDMs were incubated with CFSE-labeled autologous PBLs or naive CD3$^+$ T-cells obtained by MACS. 7 days after infection, CD45RO expression on CFSE^{low} or CFSE^{high} T-cells was determined by flow cytometry using anti-CD3/CD4 antibody co-staining.

3.2 Blockade of TNFα signaling in infected hMDM/PBL co-cultures

3.2.1 Expression of mTNFR1, mTNFR2 and TNFα by macrophages or T-cells

To evaluate the importance of TNFα signaling in our *in vitro* model of human cutaneous leishmaniasis, we assessed sTNFα levels in supernatants of infected or non-infected hMDMs by ELISA. Compared to non-infected controls (68±59 pg/ml), the release of sTNFα was significantly increased (234±235 pg/ml) in the presence of *L. major* (**Figure 14**).

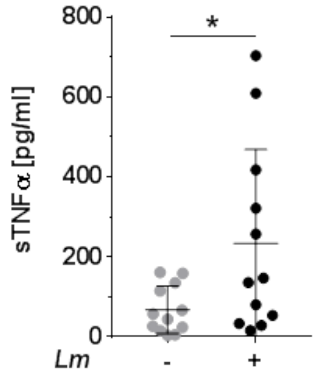

Figure 14: Elevated levels of sTNFα in supernatants of hMDMs upon *L. major* infection. Macrophages were infected with *L. major* (MOI=20) and the concentration of sTNFα in cell supernatants, in the presence or absence of parasites, was measured by ELISA after 24 hours. Data are presented as mean ± SD (*n*=12) and were obtained in 4 independent experiments. The Wilcoxon signed-rank test was performed to evaluate statistical significance. *$P < 0.05$.

Prior to cleavage by TNFα-converting enzyme, which releases the soluble form, TNFα is expressed as membrane-integrated protein (Kalliolias and Ivashkiv, 2016). We further examined cell surface expression of mTNFα and its receptors mTNFR1 and mTNFR2 on non-infected or infected hMDMs. In order to investigate the influence of *L. major* infection on mTNFR or mTNFα expression on T-cells, we co-incubated hMDMs with autologous PBLs in the presence or absence of parasites. In general, we detected that hMDMs and T-cells more frequently expressed mTNFR2 than mTNFR1 on their cell surface irrespective of infection (**Figure 15A, B**). Infection slightly reduced mTNFR2 expression on hMDMs (mean RFI: 11±7 vs 30±19), whereas mTNFR2 levels were significantly increased on T-cells (mean RFI: 13±5 vs 10±4) after co-incubation with *L. major*-infected hMDMs. Surface expression of mTNFα was not detected on hMDMs and T-cells, neither in the absence nor in the presence of *L. major* (**Figure 15A, B**).

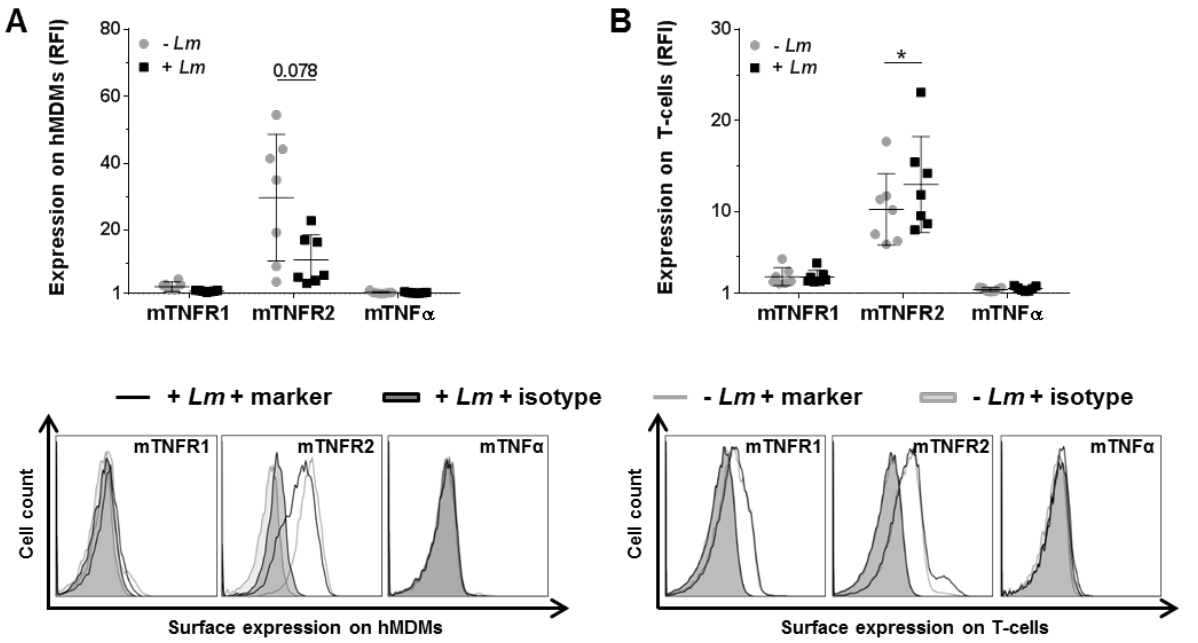

Figure 15: Expression of mTNFα and mTNFRs by hMDMs or T-cells after *L. major* infection. (A) Macrophages were infected with *L. major* (MOI=20) and surface expression of mTNFR1, mTNFR2 or mTNFα was analyzed by flow cytometry after 24 hours. (B) To determine surface expression on T-cells, PBLs were co-incubated with infected/non-infected hMDMs and measured by flow cytometry 7 days post-infection, with T-cells being defined by anti-CD3 antibody co-staining. Histograms show expression on hMDMs or T-cells in the non-infected (grey line) or infected culture (black line) in comparison to the isotype controls (black/grey solid). Data are presented as mean ± SD ($n \geq 7$) and were obtained in at least 2 independent experiments. The Wilcoxon signed-rank test was performed to evaluate statistical significance. *$P < 0.05$.

3.2.2 Expression of mTNFα by hMDMs upon inhibition of TACE

Levels of mTNFα were monitored on *L. major*-infected hMDMs every 24 hours over a period of 7 days (**Figure 16A**). However, mTNFα expression was not detected on the surface of hMDMs as exemplarily shown for 3 hours (mean RFI: 1.1), 2 days (mean RFI: 1.0) and 6 days (mean RFI: 1.0). TNFα is initially expressed as membrane-integrated form that is cleaved by TACE and subsequently released into supernatants (**1.2.1**). Previous results demonstrated secretion of sTNFα upon infection of hMDMs (**3.2.1**). In order to increase mTNFα expression on hMDMs, mTNFα processing to sTNFα was prevented using the TACE inhibitor TAPI-1. We treated *L. major*-infected hMDMs with 10 µM or 100 µM TAPI-1 as recommended by the manufacturer and analyzed mTNFα expression on hMDMs by flow cytometry. However, independent of the concentration applied, levels of mTNFα did not increase after TAPI-1 treatment in comparison to non-treated controls (**Figure 16B**). Furthermore, the addition of 100 µM TACE inhibitor negatively affected cell viability as demonstrated in the scatter plot of FSC vs SSC.

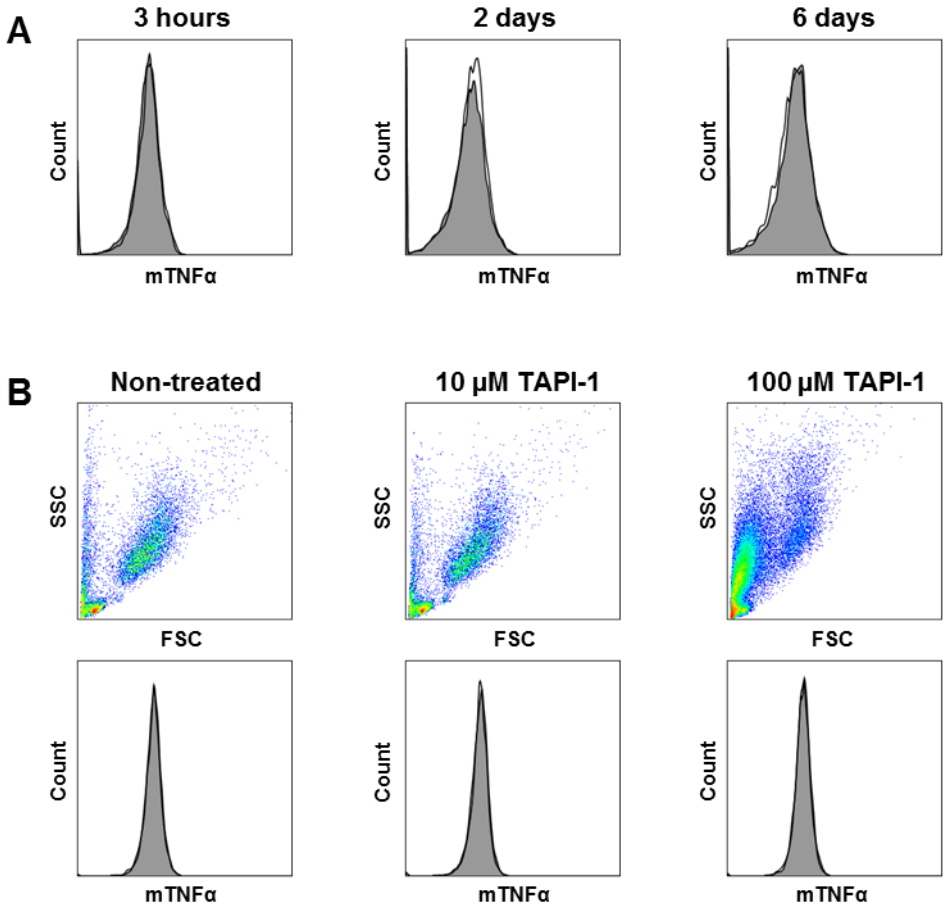

Figure 16: Expression of mTNFα on *L. major*-infected hMDMs after inhibition of TACE. (A) Macrophages were infected with *L. major*. Expression of mTNFα was assessed by flow cytometry over a period of 7 days. Representative histograms show mTNFα expression on infected hMDMs after 3 hours, 2 days and 6 days. (B) 10 µM or 100 µM TAPI-1, inhibiting mTNFα processing, were added after infection of hMDMs with *L. major*. After 24 hours, surface expression of mTNFα was analyzed by flow cytometry. Histograms show expression of mTNFα on infected hMDMs (black line) in comparison to the isotype controls (black solid).

3.2.3 T-cell proliferation and infection rates upon anti-TNFα treatment

As mTNFα seemed to be negligible in our *in vitro* model, we continued with the investigation of sTNFα-mediated effects. To determine the impact of sTNFα neutralization on *Leishmania* infection by different TNFα blockers, we compared the chimeric antibody Remicade®, its biosimilar Remsima®, the fully human antibody Humira® and the PEGylated Fab-derived inhibitor Cimzia®. Anti-TNFα agents were used in equimolar amounts with a concentration of 20 µg/ml for Remicade® (Re), Remsima® (Rs), Humira® (Hu) and 13 µg/ml for Cimzia® (Ci). First, hMDM/PBL co-cultures, treated with the different anti-TNFα agents, were tested by ELISA to examine the ability to neutralize sTNFα. We found that *L. major*-induced sTNFα (1053±650 pg/ml vs 216±111 pg/ml) was effectively neutralized by all TNFα inhibitors (Re:

43±75 pg/ml; Rs: 31±60 pg/ml; Hu: 98±93 pg/ml; Ci: 25±27 pg/ml) so that little or no sTNFα was measurable in cell culture supernatants 7 days after infection (**Figure 17**).

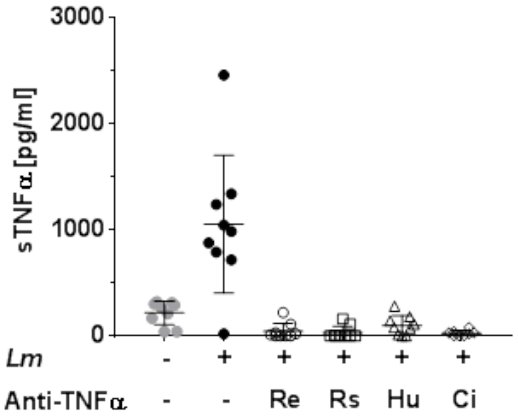

Figure 17: TNFα blockers similarly neutralize sTNFα. The anti-TNFα agents Remicade® (Re), Remsima® (Rs), Humira® (Hu) and Cimzia® (Ci) were added 24 hours after *L. major* infection (MOI=20) and hMDMs were incubated in the presence of CFSE-labeled autologous PBLs. The concentration of sTNFα in the supernatants of hMDM/PBL co-cultures was measured by ELISA 7 days after infection. Results are presented as mean ± SD ($n \geq 7$) and 4 separate experiments were conducted.

Subsequently, the influence of anti-TNFα agents on T-cell proliferation and *L. major* infection rates in hMDMs was determined and compared by flow cytometry. In order to illustrate donor-specific effects of different treatments, values of the respective controls were subtracted for each donor and condition (Δ). We found that *L. major*-induced T-cell proliferation was significantly reduced in the presence of Remicade® (-4±3%), Remsima® (-3±3%) or Humira® (-3±3%) (**Figure 18A**). Concomitantly, the percentage of *L. major*-infected hMDMs increased significantly (Re: +14±7%, Rs: +14±9%, Hu: +11±12%), demonstrating the immunosuppressive effects of TNFα inhibitors (**Figure 18B**). Remarkably, blockade of sTNFα by Cimzia® did not reduce, but significantly increase T-cell proliferation (+6±6%) compared to non-treated controls (**Figure 18A**). Moreover, infection rates in hMDMs did not change significantly (+5±9%) after treatment with Cimzia® (**Figure 18B**). Raw data obtained for T-cell proliferation and *L. major* infection rates after treatment with anti-TNFα agents are shown in **Figure 18C and D**.

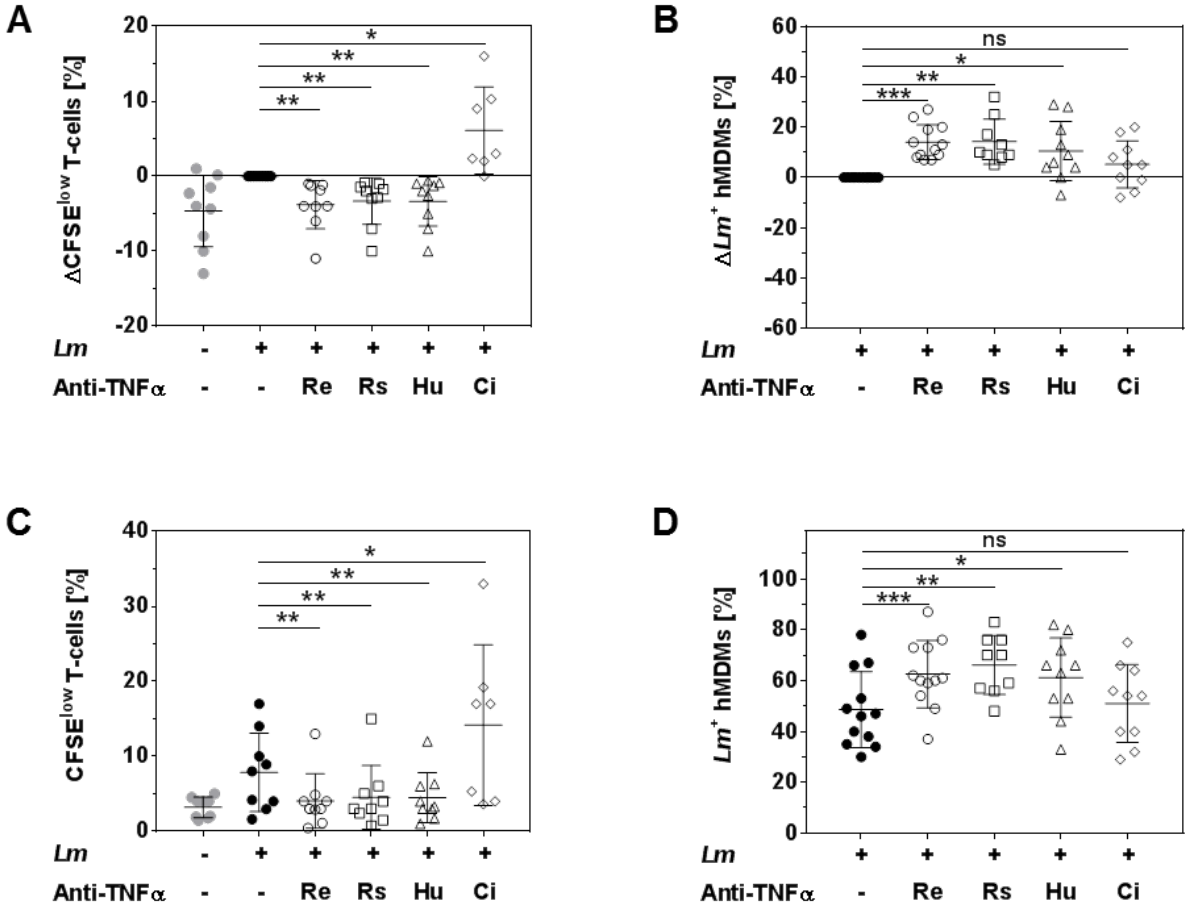

Figure 18: Treatment with TNFα blockers demonstrates diverging effects on T-cell proliferation and infection rates. *L. major*-infected/non-infected hMDMs (MOI=20) were incubated in the presence of CFSE-labeled autologous PBLs and the anti-TNFα agents Remicade® (Re), Remsima® (Rs), Humira® (Hu) and Cimzia® (Ci). 7 days after infection, T-cell proliferation (A, C) and infection rates in hMDMs (B, D) were analyzed by flow cytometry. (A, B) Values of the respective controls were subtracted for each donor and condition to illustrate differences (Δ). (C, D) Raw data of T-cell proliferation and *L. major* infection rates are depicted without subtracting values from controls. Results are presented as mean ± SD ($n \geq 7$) and at least 4 separate experiments were conducted. The Wilcoxon signed-rank test was performed to evaluate statistical significance.*$P < 0.05$; **$P < 0.01$; ***$P < 0.001$.

We also quantified the percentage of infected hMDMs in the absence of PBLs to identify and compare whether previously observed effects of anti-TNFα treatment were mediated by T-cells. Altogether, *L. major* infection rates in these samples did not change significantly after treatment with either of the four TNFα blockers compared to non-treated controls (**Figure 19A, B**). This demonstrated a T-cell-dependent impact of sTNFα on *Leishmania* infection.

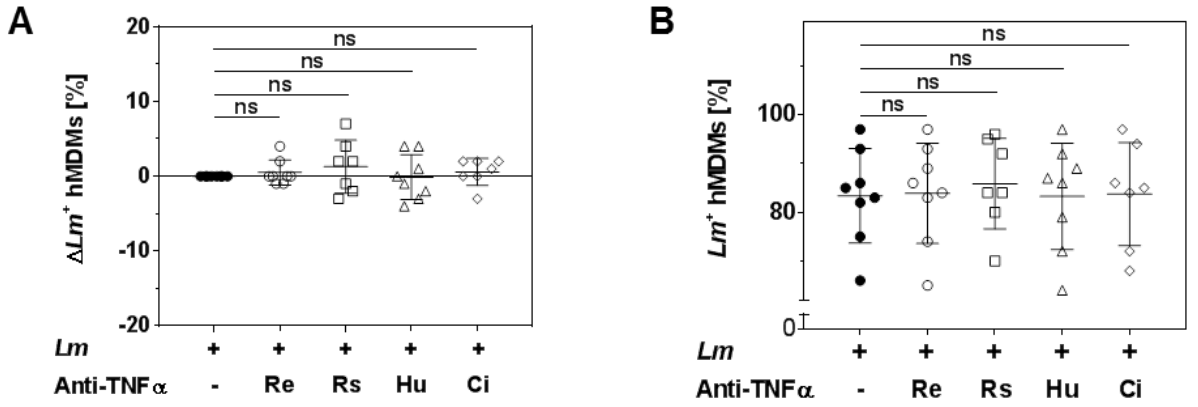

Figure 19: *L. major* infection rates in hMDMs after sTNFα blockade in the absence of PBLs. (A) Macrophages were infected with *L. major* (MOI=20). The TNFα inhibitors Remicade® (Re), Remsima® (Rs), Humira® (Hu) and Cimzia® (Ci) were added 24 hours after infection and cells were incubated in the absence of PBLs. 7 days after infection, the number of infected hMDMs was determined by flow cytometry. Values of the respective controls were subtracted for each donor and condition (Δ). (B) Raw data of infection rates are depicted without subtracting values from controls. Data are presented as mean ± SD ($n \geq 7$) and were obtained in 4 independent experiments. Statistical analysis was carried out using the Wilcoxon signed-rank test. ns $P > 0.05$.

In previous experiments, PBLs were used as source of T-cells, which might in addition to T-cells comprise B-cells and NK-cells (Filippis Christodoulos, 2018). To assess whether effects of anti-TNFα agents, exclusively depended on hMDMs and T-cells, we next applied Remicade® or Cimzia® treatment to MACS-purified $CD14^+$ hMDMs and $CD3^+$ T-cells. Upon treatment with Remicade®, we detected significantly reduced T-cell proliferation (-18±13%) (**Figure 20A**) and increased infection rates (+10±7%) (**Figure 20B**). In contrast, sTNFα blockade by Cimzia® did not significantly reduce T-cell proliferation (-1±4%) or increase the number of infected hMDMs (+4±6%) (**Figure 20A, B**). The result for T-cell proliferation is inconsistent with the PBL-based T-cell assay, where an increase in proliferation had been observed after treatment with Cimzia® (**Figure 18A, C**). Our experiments, based on MACS-purified hMDM/T-cell co-cultures, confirmed the previously obtained findings that, in contrast to Remicade®, Cimzia® does not dampen T-cell proliferation and does not adversely influence *L. major* infection rates. Thus, effects mediated by TNFα inhibitors were exclusively hMDM- and T-cell-dependent.

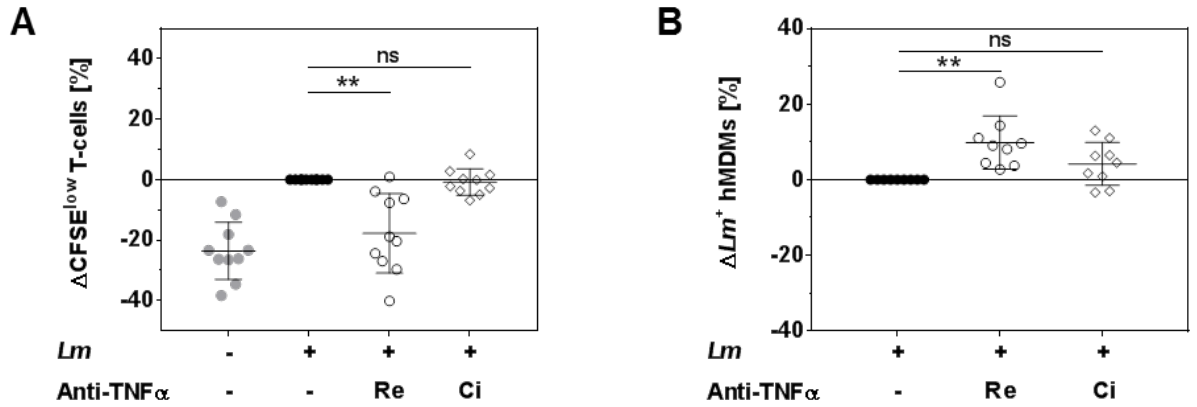

Figure 20: Effects mediated by Cimzia® or Remicade® treatment depend on hMDMs and T-cells. $CD14^+$ hMDMs and untouched $CD3^+$ T-cells were enriched by MACS. Macrophages were infected with fluorescent *L. major* (MOI=20) and after 24 hours, CFSE-labeled autologous T-cells and Remicade® or Cimzia® were added. 7 days after infection, T-cell proliferation (A) and infection rates in hMDMs (B) were analyzed by flow cytometry. Data are depicted as differences (Δ) as values of the respective controls were subtracted for each donor and condition. Results are presented as mean ± SD ($n \geq 9$) and 5 separate experiments were conducted. The Wilcoxon signed-rank test was performed to evaluate statistical significance. ns $P > 0.05$; $^{**}P < 0.01$.

3.2.4 Titration of Remicade® and Cimzia®

In contrast to the other TNFα blockers used in our studies, Cimzia® contains only one binding site for sTNFα. We therefore analyzed the sTNFα-neutralizing capacity of different concentrations of Cimzia® or Remicade® by ELISA. Overall, no or little sTNFα was detectable after treatment with 1 µg/ml Remicade® (103±94 pg/ml), 10 µg/ml Remicade® (75±81 pg/ml), 20 µg/ml Remicade® (40±50 pg/ml), 1 µg/ml Cimzia® (15±22 pg/ml), 6 µg/ml Cimzia® (0±0 pg/ml), 13 µg/ml Cimzia® (0±0 pg/ml) or 26 µg/ml Cimzia® (0±0 pg/ml), indicating that all tested concentrations of Remicade® and Cimzia® efficiently neutralized sTNFα (**Figure 21**). Interestingly, despite only one binding site, average sTNFα levels after treatment with Cimzia® were comparatively lower as after treatment with Remicade®. Furthermore, 6-26 µg/ml Cimzia® neutralized sTNFα equally well, whereas levels of sTNFα were lowest upon blockade with 20 µg/ml instead of 1 µg/ml or 10 µg/ml Remicade®.

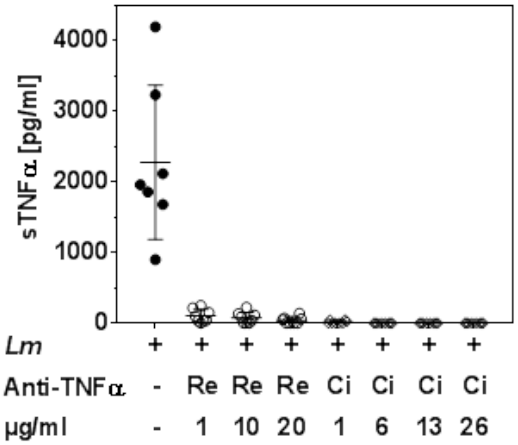

Figure 21: Neutralization of sTNFα by different concentrations of Cimzia® or Remicade®. Different concentrations of Cimzia® or Remicade® were added 24 hours after infection and hMDMs were incubated in the presence of CFSE-labeled autologous PBLs. After 7 days, the concentration of sTNFα was measured by ELISA. 3 separate experiments were performed of which results are presented as mean ± SD ($n \geq 7$).

We additionally analyzed T-cell proliferation and the percentage of infected hMDMs upon treatment with different concentrations of Cimzia® or Remicade®. In comparison to non-treated controls, proliferation of T-cells decreased after sTNFα blockade with 1 µg/ml (-9±7%), 10 µg/ml (-10±8%) or 20 µg/ml (-9±9%) Remicade® (**Figure 22A**). As a result, infection rates in hMDMs considerably increased upon Remicade® treatment (1 µg/ml: +8±5%; 10 µg/ml: +10±6%; 20 µg/ml: +9±6%) (**Figure 22B**). In contrast to Remicade®, T-cell proliferation either increased or remained unchanged after sTNFα neutralization with 1 µg/ml (+1±4%), 6 µg/ml (+4±3%), 13 µg/ml (+4±4%) or 26 µg/ml (+0±5%) Cimzia® (**Figure 22A**). Consequently, *L. major* infection rates only slightly increased (1 µg/ml: +3±4%; 6 µg/ml: +3±3%; 13 µg/ml: +4±4%; 26 µg/ml: +4±4%) upon Cimzia® treatment (**Figure 22B**). Taken together, diverging effects on T-cell proliferation and infection rates mediated by Remicade® or Cimzia® treatment maintained over a wide range of concentrations. However, Cimzia® proved to have a slightly better neutralizing capacity towards sTNFα in comparison with Remicade®. For this reason, further experiments were conducted using the highest concentration of Remicade® (20 µg/ml) and equimolar amounts of Cimzia® (13 µg/ml).

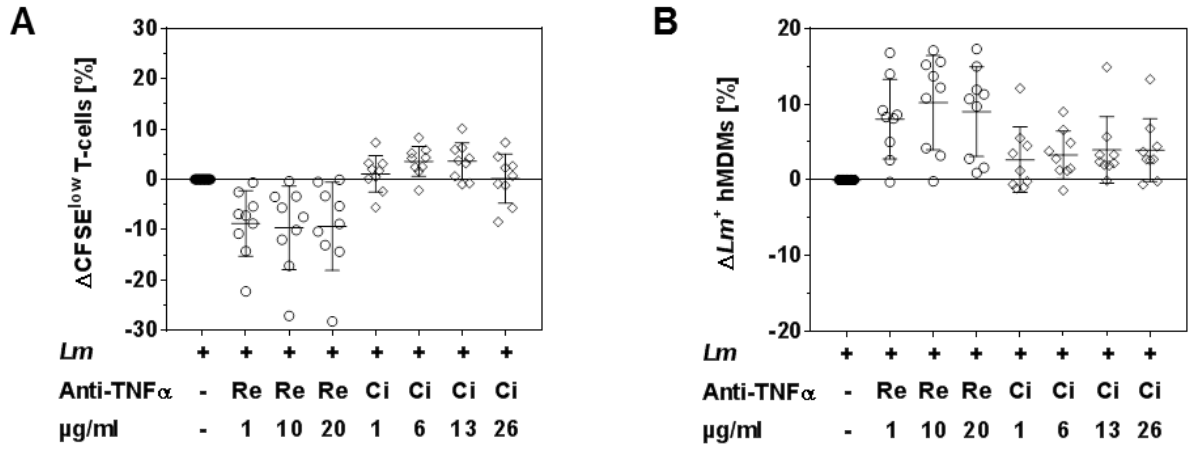

Figure 22: T-cell proliferation and infection rates after treatment with different concentrations of Cimzia® or Remicade®. Macrophages were infected with fluorescent *L. major* (MOI=20) and incubated with CFSE-labeled autologous PBLs. Different concentrations of Cimzia® or Remicade® were added and T-cell proliferation (A) and the number of infected hMDMs (B) were analyzed by flow cytometry after 7 days. Data are shown as differences (Δ) by subtracting values of the respective controls for each donor and condition. 3 separate experiments were performed of which results are presented as mean ± SD (*n*=9).

3.2.5 Relevance of mTNFα in infected hMDM/PBL co-cultures

We above (**Figure 18**) showed the relevance of sTNFα for T-cell activation and parasite control in our *in vitro* model. In contrast, mTNFα expression was not detected on infected hMDMs, neither at varying incubation time points nor upon inhibition of TACE (**3.2.2**). To verify the irrelevance of mTNFα during *L. major* infection, we treated infected hMDM/PBL co-cultures with Remicade® and analyzed membrane-bound Remicade® by flow cytometry using a fluorescent-labeled anti-IgG Fc secondary antibody. As expected, Remicade® was not detected on hMDMs or T-cells (**Figure 23**), demonstrating the independence of mTNFα for the control of parasites.

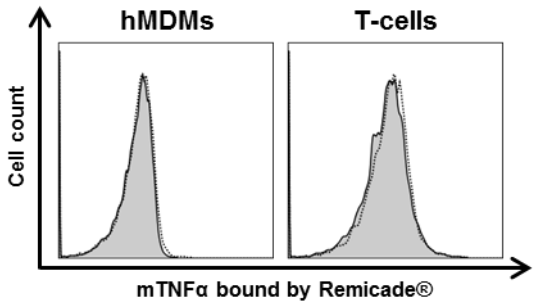

Figure 23: Cell surface binding of Remicade® on hMDMs or T-cells. *L. major*-infected hMDMs were incubated with Remicade® and PBLs for 7 days. Binding of Remicade® to hMDMs and T-cells was measured by flow cytometry using anti-human IgG Fc secondary antibody staining. Remicade®-treated cells (black dotted line) in comparison to non-treated cells (black solid) are shown.

3.2.6 T-cell proliferation and infection rates upon blockade of mTNFRs

With the aim to distinguish between mTNFR1- and mTNFR2-dependent cell activation in the hMDM/PBL co-culture, either of the mTNFRs was blocked with antibodies and the impact on T-cell proliferation and *L. major* infection rates was investigated by flow cytometry. In comparison with non-treated controls, T-cell proliferation did not change significantly after mTNFR1 (+1±5%) or mTNFR2 (-3±5%) blockade (**Figure 24A**). Similarly, no significant differences in infection rates were detected upon treatment with anti-mTNFR1 (+5±7%) or anti-mTNFR2 (+3±6%) antibodies (**Figure 24B**). Thus, blocking single mTNFRs, instead of the ligand sTNFα, showed only minor effects on parasite control in hMDMs.

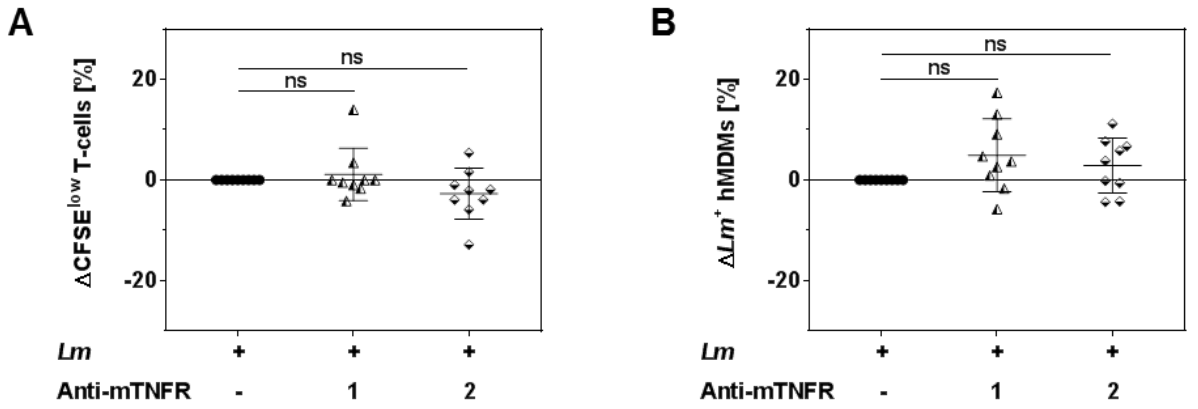

Figure 24: T-cell proliferation and infection rates in hMDMs after mTNFR blockade. *L. major*-infected hMDMs were incubated with CFSE-labeled autologous PBLs and mTNFRs were blocked with antibodies. 7 days after infection, T-cell proliferation (A) and infection rates (B) were measured by flow cytometry. Values of the respective controls were subtracted for each donor and condition to illustrate differences (Δ). 4 separate experiments were performed of which data are shown as mean ± SD (*n*=9). To analyze statistical significance, the Wilcoxon signed-rank test was performed. ns $P > 0.05$.

3.2.7 T-cell proliferation and infection rates upon neutralization of IFNγ

In addition to TNFα, we studied the importance of IFNγ in our *in vitro* model as several reports had previously described IFNγ to play a major role in *L. major* infection control (Kaye and Scott, 2011). For this purpose, T-cell expansion and the percentage of infected hMDMs were examined by flow cytometry after neutralization of IFNγ by antibodies. In comparison to non-treated controls, neither T-cell expansion (+0±5%) (**Figure 25A**) nor infection rates in hMDMs (+1±9%) (**Figure 25B**) changed significantly upon anti-IFNγ treatment. Thus, parasite control in the infected hMDM/PBL co-cultures was independent of IFNγ. In line with these

results, IFNγ was not detectable in supernatants of infected co-cultures by ELISA (data not shown).

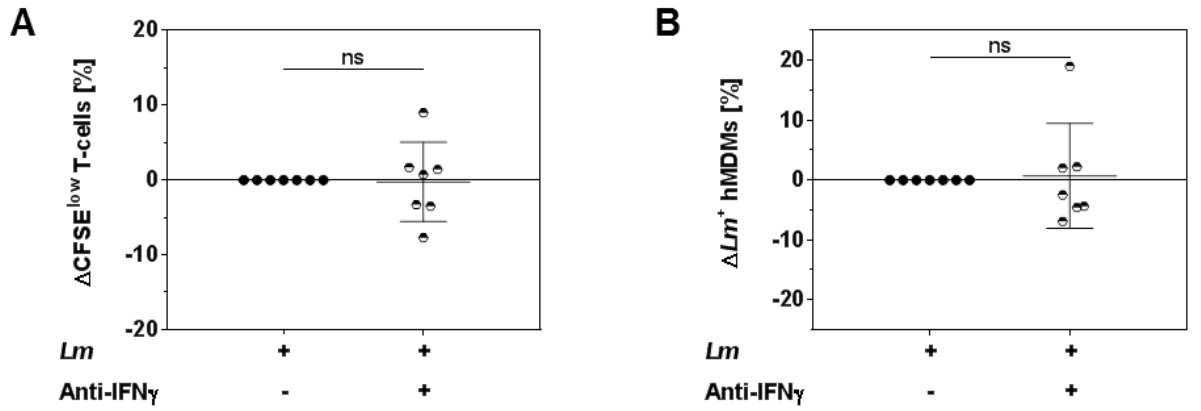

Figure 25: T-cell proliferation and infection rates in hMDMs after IFNγ blockade. *L. major*-infected hMDMs were incubated with CFSE-labeled autologous PBLs and IFNγ was neutralized with antibodies. T-cell proliferation (A) and infection rates in hMDMs (B) were measured by flow cytometry 7 days post-infection. Values of the respective controls were subtracted for each donor and condition (Δ). Data are shown as mean ± SD (*n*=7) and were obtained in 3 separate experiments. The Wilcoxon signed-rank test was performed. ns $P > 0.05$.

3.3 T-cell phenotype, effector function and cell viability upon anti-TNFα treatment

3.3.1 Phenotype of *L. major*-induced T-cells

We have previously shown that PD-1 expression on proliferating T-cells was significantly increased in infected hMDM/PBL co-cultures (**3.1.4**). In order to determine the impact of sTNFα blockade on T-cell activation, PD-1 expression on proliferating T-cells was examined after anti-TNFα treatment with Remicade® or Cimzia® (**Figure 26**). By flow cytometry, we found that PD-1 levels were significantly reduced in Remicade®- (mean RFI: 7±4) compared to non-treated (mean RFI: 11±3) samples. However, treatment with Cimzia® maintained T-cell activation as shown by unaltered PD-1 levels (mean RFI: 11±4) in comparison with the non-treated condition.

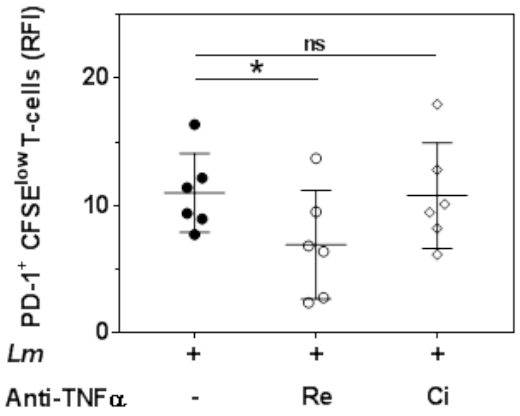

Figure 26: PD-1 expression on T-cells after treatment with Remicade® or Cimzia®. Macrophages were infected with *L. major* (MOI=20). 24 hours after infection, Remicade® or Cimzia® were added and cells were incubated in the presence of CFSE-labeled autologous PBLs. 7 days post-infection, expression of PD-1 was assessed on $CFSE^{low}$ T-cells. 3 independent experiments were conducted of which data are presented as mean ± SD (*n*=6). To determine statistical significance, the Wilcoxon signed-rank test was performed.*$P < 0.05$.

Levels of the memory marker CD45RO were increased on proliferating T-cells after infection of hMDMs with *L. major* (**3.1.5**). By flow cytometry, we investigated the memory phenotype of *L. major*-induced proliferating T-cells upon neutralization of sTNFα by Remicade® or Cimzia® (**Figure 27**). Compared to non-treated controls (mean RFI: 38±21), CD45RO expression significantly decreased after Remicade® treatment (mean RFI: 22±15). By contrast, CD45RO levels remained unaltered upon sTNFα neutralization by Cimzia® (mean RFI: 41±40).

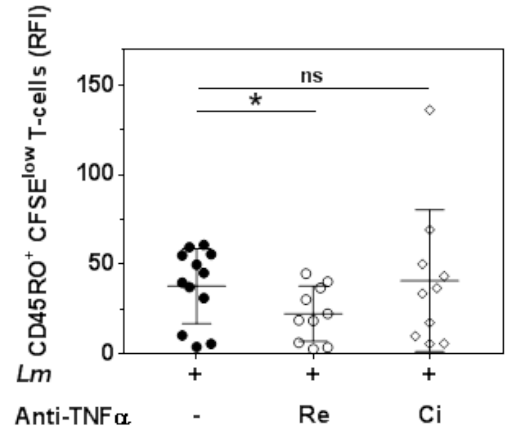

Figure 27: CD45RO expression on T-cells after treatment with Remicade® or Cimzia®. *L. major*-infected hMDMs were treated with Remicade® or Cimzia® and incubated in the presence of CFSE-labeled autologous PBLs. 7 days after infection, CD45RO expression on proliferating T-cells was assessed by flow cytometry. 5 independent experiments were conducted of which data are presented as mean ± SD (*n*≥10). To determine statistical significance, the Wilcoxon signed-rank test was performed.*$P < 0.05$.

3.3.2 Cytolytic protein expression in *L. major*-induced T-cells

Cytolytic molecules such as perforin (PF), granulysin (GL) and granzymes are required for protective immunity against intracellular pathogens. They are expressed in effector T-cells and released upon antigen stimulation (Barry and Bleackley, 2002). We quantified the intracellular levels of perforin, granulysin, granzyme A (GrA) and granzyme B (GrB) in proliferating T-cells and assessed the effect of either Remicade® or Cimzia® treatment by flow cytometry. The gating strategy used to determine cytolytic protein expression is exemplarily shown for granzyme B (**Figure 28**).

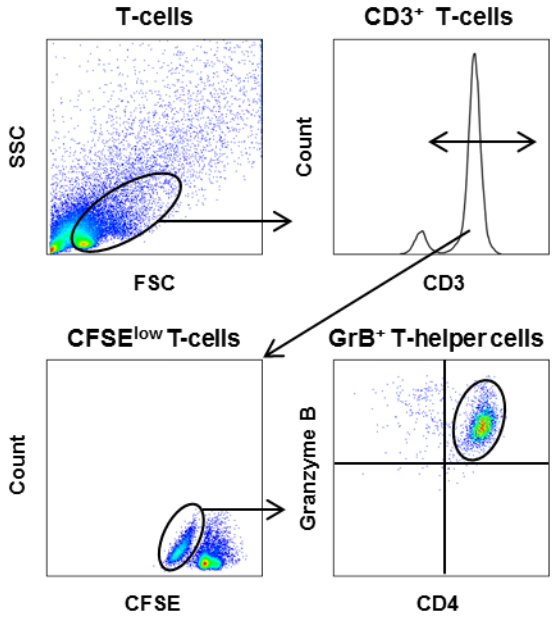

Figure 28: Gating strategy used to determine cytolytic protein expression in T-cells. Expression of cytolytic molecules in T-cells exemplarily shown for granzyme B: Fixed T-cells were defined by their size (SSC/FSC) and anti-CD3 antibody staining. Amongst proliferating T-cells ($CFSE^{low}$) the percentage of granzyme B and CD4 double-positive T-helper cells was assessed.

Expression of perforin (+5±6%), granulysin (+8±8%), granzyme A (+26±8%) and granzyme B (+30±14%) was significantly upregulated in proliferating $CD4^+$ T-cells in the infected co-culture compared to non-infected controls (**Figure 29A-D**). This upregulation was largely reversed (PF: -3±4%, GL: -5±7%, GrA: -10±7%, GrB: -19±13%) after neutralization of sTNFα by Remicade®, with perforin, granzyme A and granzyme B being significantly reduced compared to non-treated controls (**Figure 29A-D**). In contrast, neutralization of sTNFα by Cimzia® did not interfere with the *L. major*-induced upregulation of perforin (+4±4%), granzyme A (+7±6%) and granzyme B (+6±12%) (**Figure 29A, C, D**). Only granulysin levels (-4±4%) were lowered and comparable to those measured after treatment with Remicade® (**Figure 29B**).

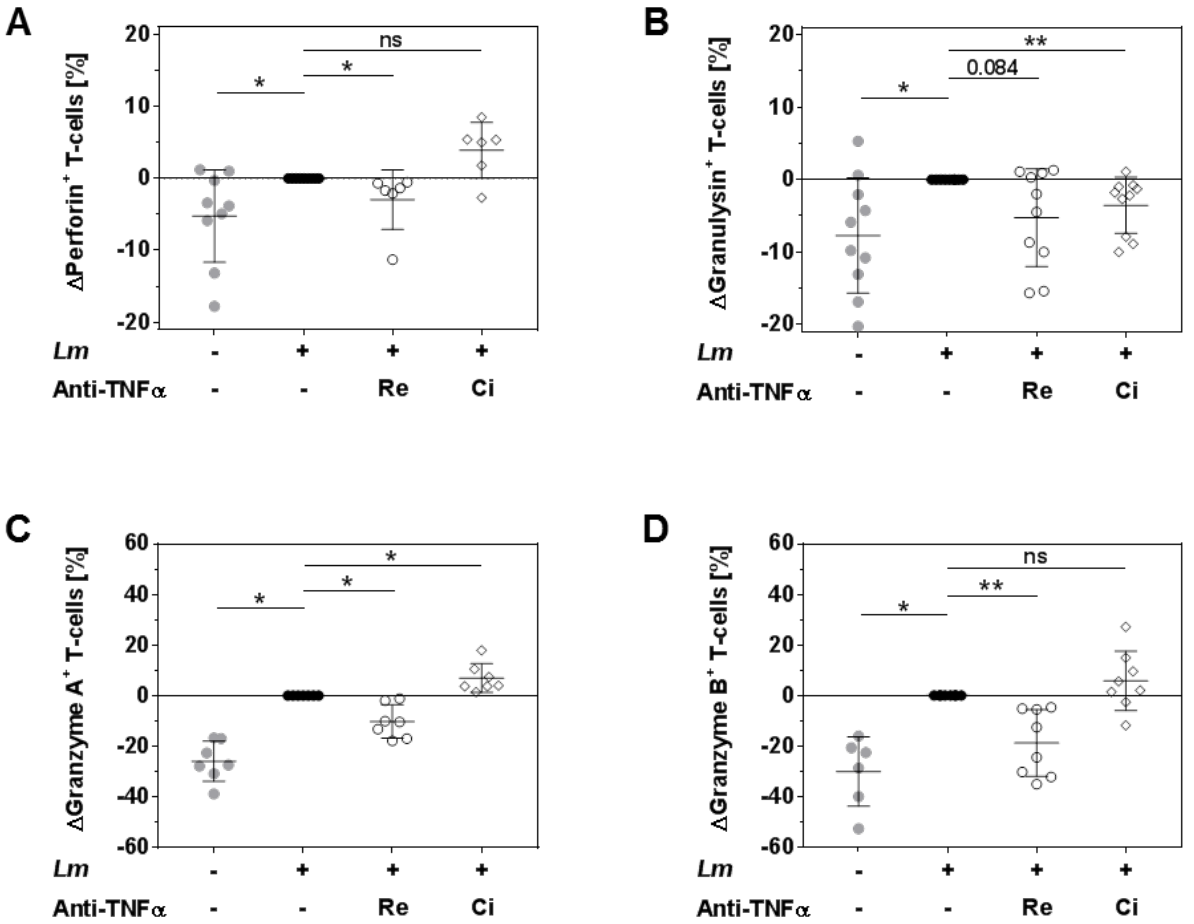

Figure 29: Intracellular expression of cytolytic proteins in proliferating CD4$^+$ T-cells after anti-TNFα treatment. Non-infected or *L. major*-infected hMDMs were co-incubated with CFSE-labeled autologous PBLs and sTNFα was neutralized by Remicade® or Cimzia®. Proliferating CD4$^+$ T-cells expressing perforin (A), granulysin (B), granzyme A (C) or granzyme B (D) were detected using anti-CD3 and anti-CD4 antibody co-staining in intracellular flow cytometry 7 days after infection. To illustrate differences (Δ), values of the respective controls were subtracted for each donor and condition. Data are presented as mean ± SD ($n \geq 6$) and were obtained in at least 3 independent experiments. To analyze statistical significance, the Wilcoxon signed-rank test was performed.*$P < 0.05$; **$P < 0.01$.

Using non-infected or infected hMDM/PBL co-cultures, we identified a very low number of proliferating T-cells to express CD8 (**Figure 10C**). These proliferating CD8$^+$ T-cells were further investigated by intracellular flow cytometry to determine expression of cytolytic molecules. As expected, overall levels of perforin, granulysin, granzyme A or granzyme B in proliferating CD8$^+$ T-cells were very low (<10%). Moreover, infection of hMDMs with *L. major* or neutralization of sTNFα with Remicade® or Cimzia® showed no significant effects on cytolytic protein expression (**Figure 30A-D**).

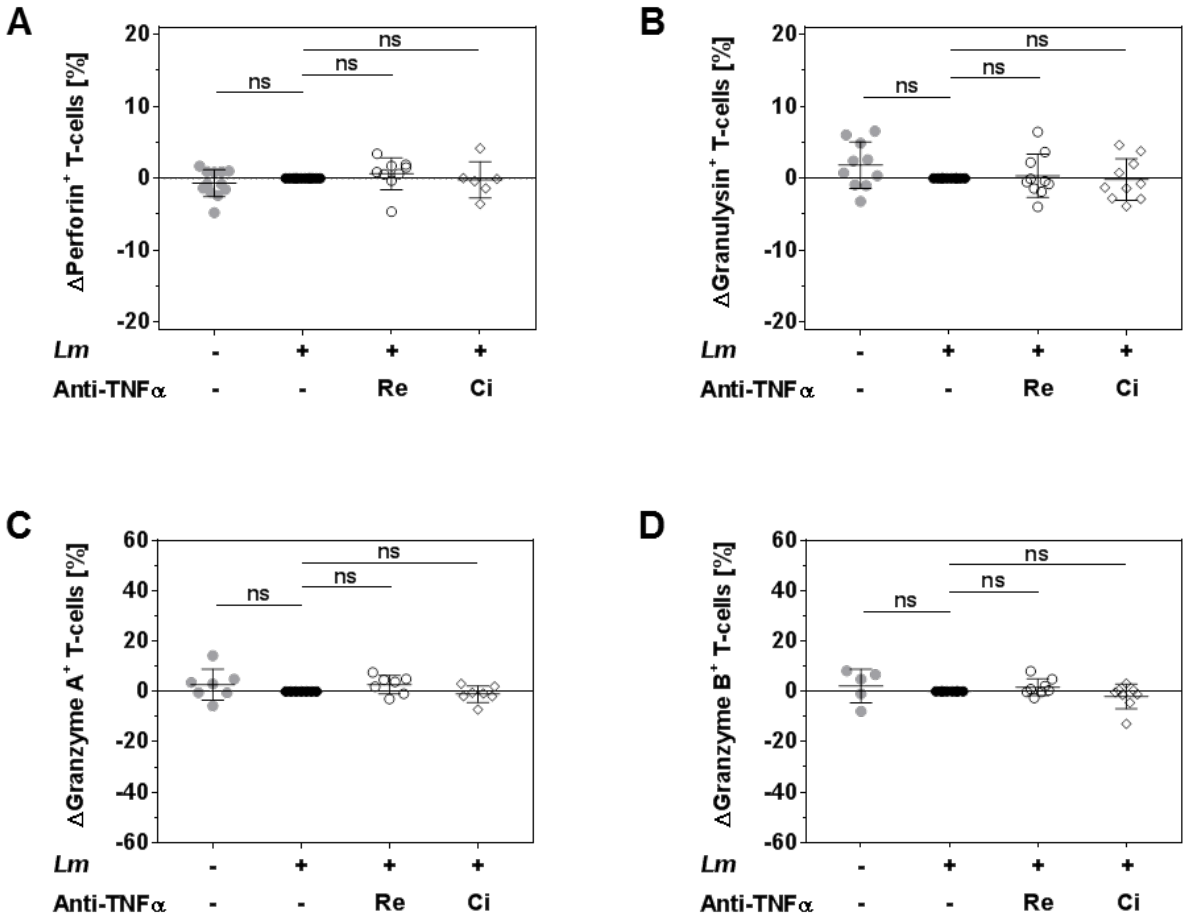

Figure 30: Intracellular expression of cytolytic proteins in proliferating CD8$^+$ T-cells after anti-TNFα treatment. Non-infected or *L. major*-infected hMDMs were co-incubated with CFSE-labeled autologous PBLs and sTNFα was neutralized by Remicade® or Cimzia®. 7 days post-infection, proliferating CD8$^+$ T-cells expressing perforin (A), granulysin (B), granzyme A (C) or granzyme B (D) were determined using anti-CD3 and anti-CD8 antibody co-staining in intracellular flow cytometry. Values of the respective controls were subtracted for each donor and condition (Δ). Data are presented as mean ± SD ($n \geq 5$) and were obtained in at least 3 independent experiments. The Wilcoxon signed-rank test was performed. ns $P > 0.05$.

Infected hMDM/PBL co-cultures were analyzed by immunofluorescence to investigate whether T-cells, positive for cytolytic proteins, reside in close proximity to infected hMDMs. Results are exemplarily shown for granzyme A (**Figure 31**). We were able to detect hMDMs that were surrounded by T-cells, but signals of granzyme A were weak and partially overlapped with DsRed signals of *L. major*. Thus, we could not exactly distinguish between parasites and cytolytic proteins.

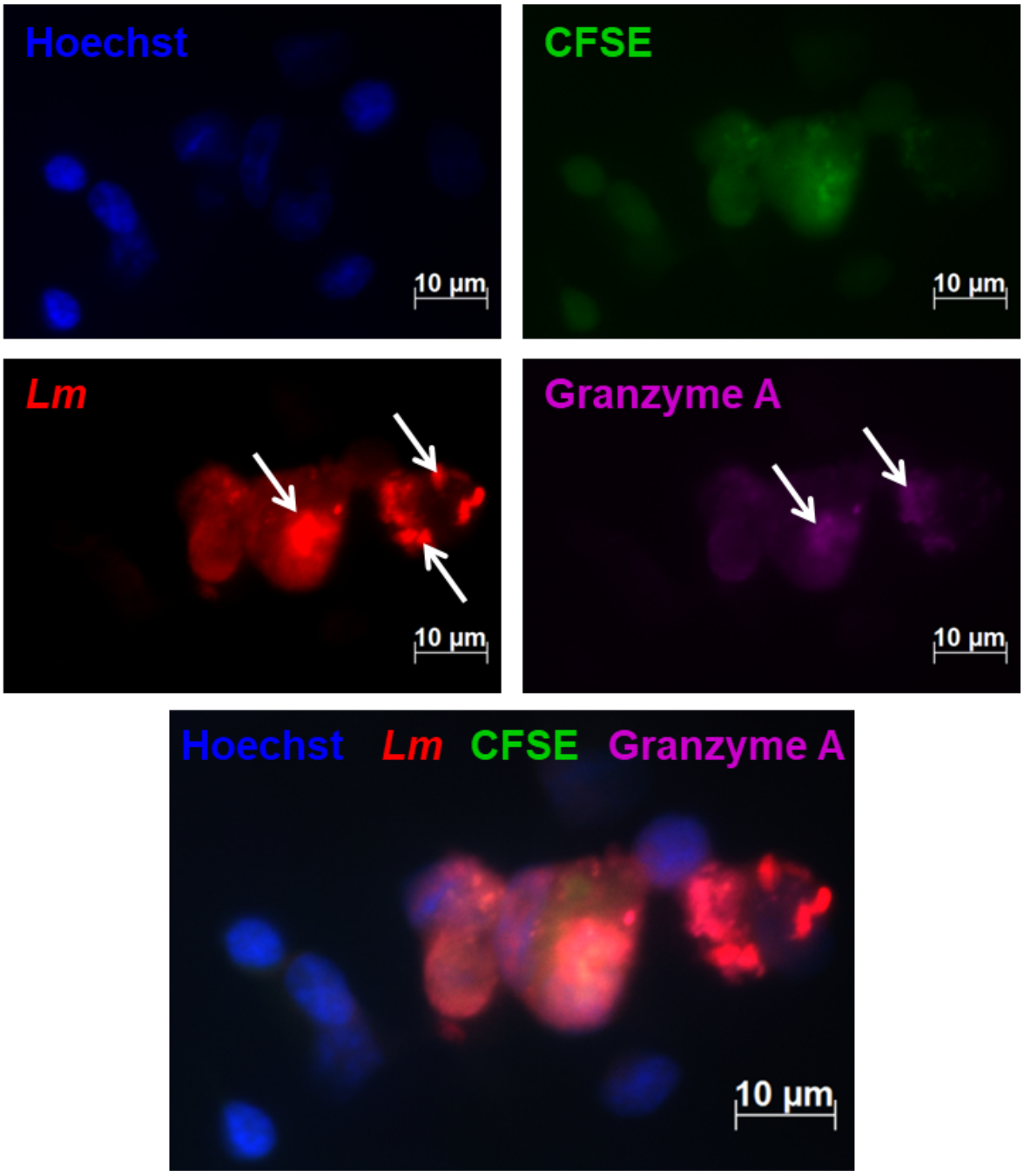

Figure 31: Granzyme A expression in T-cells and hMDMs. Macrophages were infected with fluorescent *L. major* (red) and co-incubated with autologous PBLs. Primary human cells were labeled with CFSE (green). After 7 days, cells were fixed, permeabilized and stained with an anti-granzyme A antibody (purple). Nuclei were counterstained with Hoechst 34580 (blue). Images were taken with a Zeiss Axio Observer.Z1 microscope and a 63x magnification.

3.3.3 Cell viability of infected macrophages and co-cultured T-cells

Expression of cytolytic proteins as shown in **Figure 29A-D** can affect cell viability due to induction of apoptosis (Barry and Bleackley, 2002). To assess whether treatment with

Remicade® or Cimzia® caused this kind of cytolytic molecule-mediated cell death, flow cytometry was applied and the number of dead cells in the hMDM/PBL co-cultures was determined by PI staining. 7 days after infection with *L. major*, the percentage of PI^+ hMDMs (13±6%) (**Figure 32A**) and PI^+ T-cells (18±9%) (**Figure 32B**) in the infected hMDM/PBL co-culture was low. Furthermore, values of Remicade®- or Cimzia®-treated samples were comparable to non-treated controls, demonstrating that sTNFα blockade did not affect host or effector cell viability.

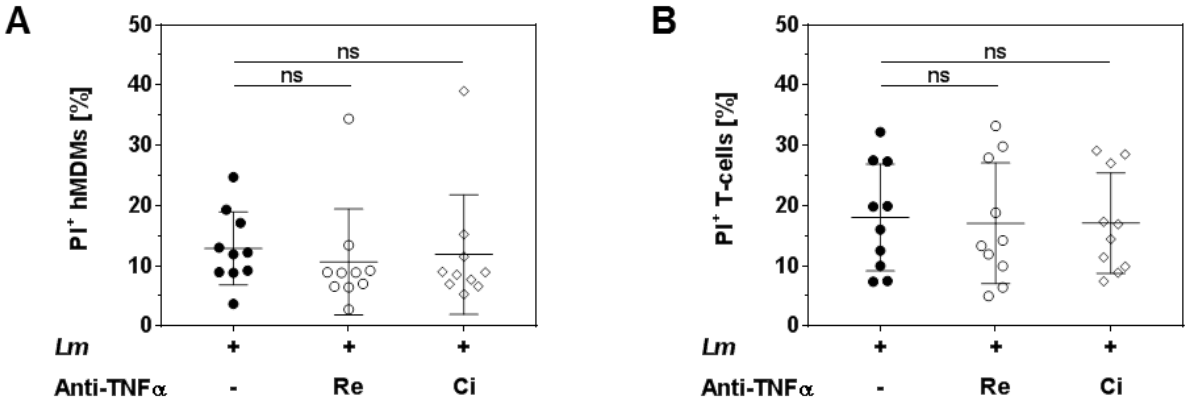

Figure 32: Cell viability of T-cells or hMDMs after treatment with Remicade® or Cimzia®. Macrophages were infected with *L. major* (MOI=20). After 24 hours, Remicade® or Cimzia® were added and cells were co-incubated with CFSE-labeled autologous PBLs. 7 days post-infection, the percentage of PI^+ hMDMs (A) and PI^+ T-cells (B) was determined by anti-CD3 antibody co-staining in flow cytometry. Data are presented as mean ± SD (*n*=10) and were obtained in 4 independent experiments. The Wilcoxon signed-rank test was performed to evaluate statistical significance. ns $P > 0.05$.

3.4 Role of structural features for diverging effects of Cimzia®

3.4.1 Relevance of Fc interactions for parasite control

In contrast to the Fab-derived drug Cimzia®, Remicade® is capable of binding to FcγRs *via* its Fc region (**1.2.3**). Signaling through FcγRs can alter cell activation and consequently might influence T-cell proliferation or *L. major* infection rates (Thalayasingam and Isaacs, 2011; Chan et al., 2015). By flow cytometry, we detected that infected hMDMs highly expressed FcγRs (**Figure 33**) with CD64 levels being the highest (mean RFI: 16±6), followed by CD32 (mean RFI: 13±10) and CD16 (mean RFI: 5±3).

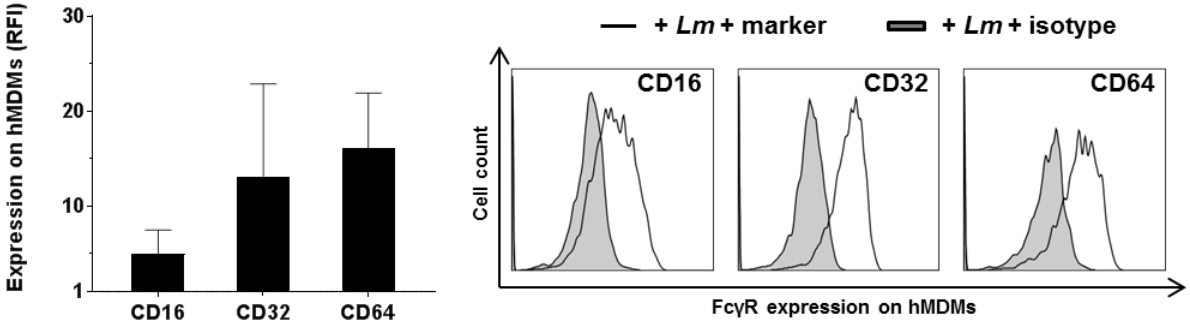

Figure 33: Fcγ receptor expression on macrophages. 24 hours after *L. major* infection, FcγR expression (CD16, CD32 and CD64) on hMDMs was analyzed using flow cytometry. Representative histograms show expression of FcγRs (black line) on infected hMDMs in comparison to the isotype control (black solid). Results are presented as mean ± SD ($n \geq 6$) and were obtained in 3 independent experiments.

To exclude that interaction of FcγRs and the Remicade® Fc moiety influenced T-cell proliferation or infection rates, we saturated FcγRs on hMDMs by pre-incubation with the IgG preparation Polyglobin® (Weissmuller et al., 2012). Blockade of FcγRs after 7 days was confirmed by flow cytometry using fluorescent-labeled anti-IgG Fc secondary $F(ab')_2$ antibodies (**Figure 34A**). Polyglobin® IgG antibodies were bound to the cell surface of hMDMs *via* FcγRs and thus FcγRs were effectively blocked (**Figure 34B**).

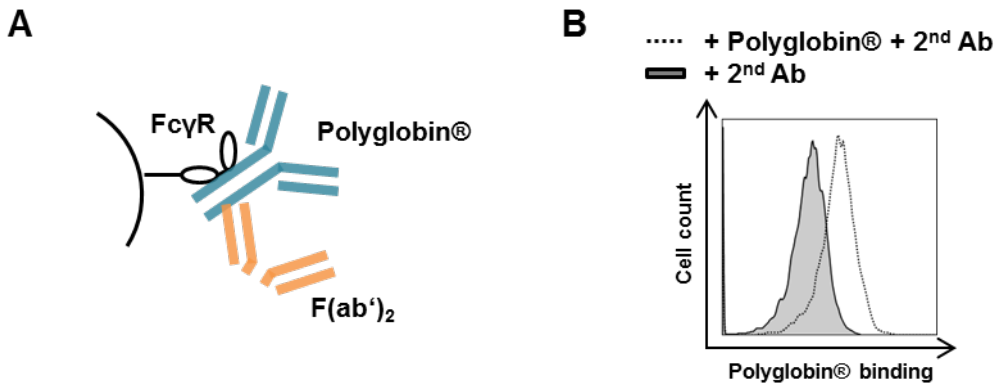

Figure 34: Fcγ receptor blockade by Polyglobin®. *L. major*-infected macrophages were pre-incubated with Polyglobin® after which PBLs were added. (A) After 7 days, binding of Polyglobin® antibodies to FcγRs on hMDMs was confirmed by flow cytometry using anti-human IgG Fc secondary $F(ab')_2$ antibody staining. (B) *L. major*-infected and Polyglobin®-treated cells (black dotted line) in comparison to non-treated cells (black solid) are shown.

To investigate whether interaction with FcγRs influenced Remicade®-mediated effects, T-cell expansion and the number of infected hMDMs were compared in the absence to the presence of Polyglobin®. By flow cytometry, we found that neutralization of sTNFα by Remicade® equally reduced T-cell proliferation in the presence (-11±11%) or absence of the

IgG preparation (-12±11%) (**Figure 35A**). Likewise, infection rates increased in the presence of Remicade® with (+8±8%) or without (+7±9%) FcγR blockade (**Figure 35B**). Pre-incubation with Polyglobin® devoid of sTNFα blockade showed no significant impact on T-cell expansion (-3±6%) and the number of infected hMDMs (+1±5%) in comparison with non-treated controls. These results demonstrated that effects mediated by Remicade® did not depend on Fc-FcγR interaction. Consequently, a different feature had to be responsible for the diverging effects of Cimzia®.

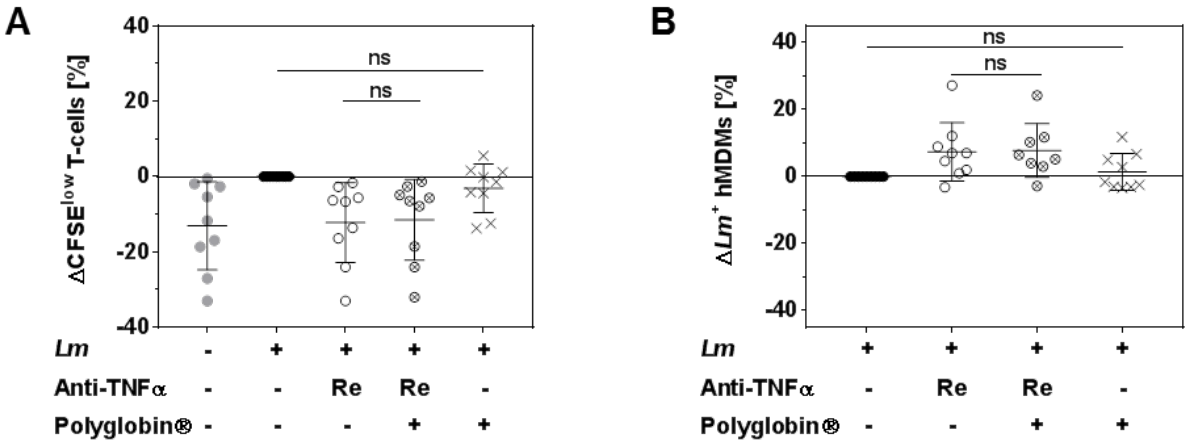

Figure 35: T-cell proliferation and infection rates upon Fcγ receptor blockade. *L. major*-infected or non-infected hMDMs were pre-incubated with Polyglobin® after which PBLs and Remicade® were added. 7 days post-infection, T-cell proliferation (A) and infection rates in hMDMs (B) were assessed by flow cytometry and values of the respective controls were subtracted for each donor and condition to illustrate differences (Δ). Results are presented as mean ± SD ($n \geq 8$) and were obtained in 4 independent experiments. Statistical analysis was carried out using the Wilcoxon signed-rank test. ns $P > 0.05$.

3.4.2 Relevance of PEGylation for parasite control

Another major difference between the tested anti-TNFα agents is the conjugated PEG moiety of Cimzia® (**1.2.3**), which is added to therapeutic proteins to increase stability and half-life (Harris and Chess, 2003). We sought to examine whether this PEG portion could explain the higher T-cell proliferation and lower *L. major* infection rates in hMDMs after treatment with Cimzia® compared to Remicade®. To this end, Remicade® was PEGylated (20-fold) with the amine-reactive MS-PEG and the resulting PEG-Remicade® or Cimzia® was compared to the non-PEGylated form of Remicade®. At first, co-culture supernatants were investigated by ELISA to test whether PEG-Remicade® is still capable of neutralizing sTNFα. The comparison of Remicade®- (18±34 pg/ml) with PEG-Remicade®-treated (29±30 pg/ml) samples proved effective neutralization of sTNFα with no significant differences between

tested TNFα inhibitors (**Figure 36**). Treatment with MS-PEG alone (1120±942 pg/ml) did not alter sTNFα levels in cell supernatants of the infected hMDM/PBL co-culture compared to non-treated controls (1286±1051 pg/ml).

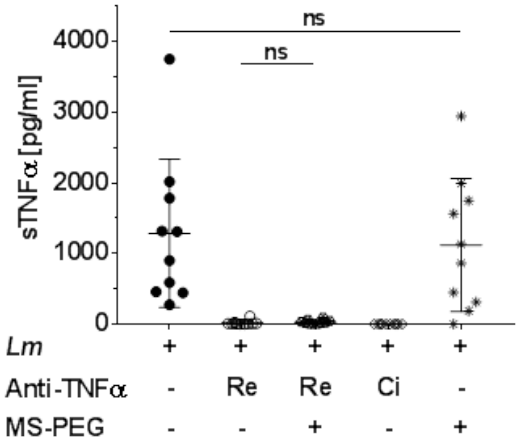

Figure 36: Effective neutralization of sTNFα by PEG-Remicade®. Macrophages were infected with *L. major* (MOI=20) and after 24 hours CFSE-labeled autologous PBLs were added. Co-cultures were treated with Remicade®, PEGylated Remicade® or Cimzia® to neutralize sTNFα. 7 days after infection, sTNFα levels in cell supernatants were measured by ELISA. 4 independent experiments were conducted of which data are shown as mean ± SD (*n*=10). The Wilcoxon signed-rank test was performed to evaluate statistical significance. ns $P > 0.05$.

Subsequent to the neutralization capacity, T-cell proliferation and infection rates in hMDMs were measured by flow cytometry. Similar to Cimzia® (+10±6%), a significantly higher T-cell proliferation (**Figure 37A**) was observed in the presence of PEG-Remicade® (+4±4%) compared to non-PEGylated Remicade®. Likewise, the percentage of *L. major*-infected hMDMs was significantly reduced after treatment with Cimzia® (-6±4%) or PEG-Remicade® (-4±3%) (**Figure 37B**). T-cell proliferation (**Figure 37A**) of non-treated samples (+10±9%) compared to MS-PEG-treated samples (+9±7%) and infection rates (**Figure 37B**) of non-treated (-8±6%) in comparison with MS-PEG-treated samples (-11±5%) showed no significant impact of MS-PEG alone.

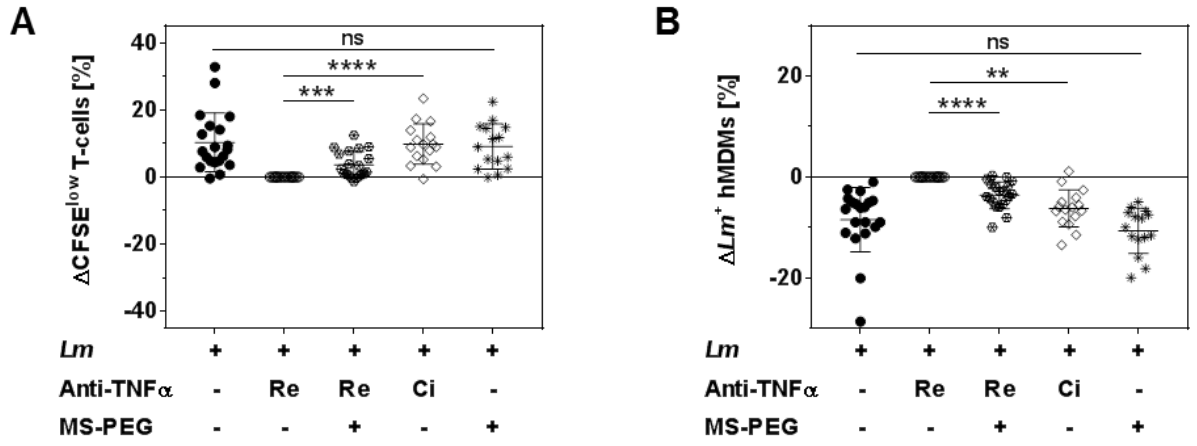

Figure 37: Increased T-cell proliferation and reduced infection rates in hMDMs after PEGylation of Remicade®. The *L. major*-infected hMDM/PBL co-culture was treated with Remicade®, PEGylated Remicade® or Cimzia® to neutralize sTNFα. 7 days post-infection, samples were measured by flow cytometry to assess T-cell proliferation (A) as well as the percentage of infected hMDMs (B). T-cell proliferation and infection rates are presented as differences (Δ); values of the respective controls were subtracted for each donor and condition. 6 independent experiments were conducted of which data are shown as mean ± SD ($n \geq 15$). The Wilcoxon signed-rank test was performed to evaluate statistical significance. $^{**}P < 0.01$; $^{***}P < 0.001$; $^{****}P < 0.0001$.

We above demonstrated increased T-cell proliferation and reduced *L. major* infection rates after treatment with PEG-Remicade® compared to non-PEGylated Remicade® (**Figure 37**). PEGylation was carried out by incubating Remicade® with 20-fold molar excess of MS-PEG as recommended by the manufacturer. We then titrated the amount of MS-PEG to investigate whether different ratios of MS-PEG could enhance the impact of PEG-Remicade® on T-cell proliferation and infection rates. However, using 1-fold (+0±1%), 10-fold (+1±2%), 40-fold (+1±1%) or 80-fold (+1±1%) molar excess of MS-PEG for the PEGylation of Remicade®, T-cell proliferation remained unchanged compared to Remicade®-treated samples (**Figure 38A**). Similarly, unaltered or even increased numbers of infected hMDMs (1-fold: +2±5%; 10-fold: +3±4%; 40-fold: -1±3%; 80-fold: +0±3%) were measured upon treatment with differently PEGylated Remicade® (**Figure 38B**). According to these findings, we continued with 20-fold PEGylated Remicade® as this variant proved to have a direct effect on T-cell proliferation and consequently *L. major* infection rates in hMDMs.

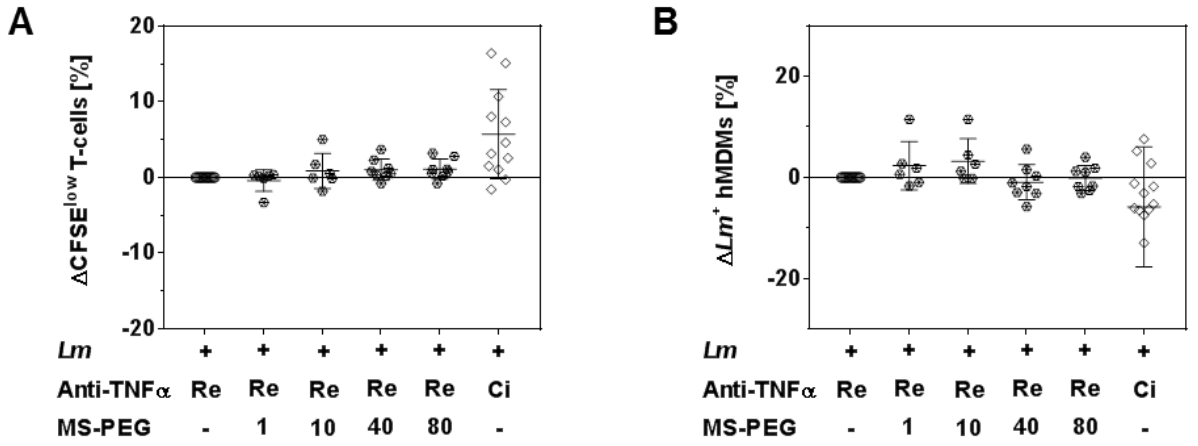

Figure 38: Titration of MS-PEG. The *L. major*-infected hMDM/PBL co-culture was treated with Remicade®, PEGylated Remicade® or Cimzia® to neutralize sTNFα. PEGylation of Remicade® was carried out with 1-fold, 10-fold, 40-fold or 80-fold molar excess of MS-PEG. After 7 days, samples were measured by flow cytometry to determine T-cell proliferation (A) and the number of infected hMDMs (B). T-cell proliferation and infection rates are presented as differences (Δ). At least 2 independent experiments were conducted of which data are shown as mean ± SD ($n \geq 6$).

3.4.3 IL-10 levels upon anti-TNFα treatment

We next investigated the consequences of PEGylated TNFα inhibitors on anti-inflammatory cytokine production. For this purpose, levels of IL-10 were determined in supernatants of hMDM/PBL co-cultures using ELISA. IL-10 is a major regulatory cytokine and its secretion can suppress inflammation by inhibiting T-cell function or by suppressive T-cell activity (Kemper and Atkinson, 2007; Saraiva and O'Garra, 2010). We detected significantly elevated levels of IL-10 after treatment with Cimzia® (538±323 pg/ml) in comparison with Remicade® (84±89 pg/ml) (**Figure 39**). Treatment with PEGylated Remicade® only slightly increased (139±155 pg/ml) the release of IL-10 compared to the non-PEGylated form. Levels of IL-10 in non-treated (124±117 pg/ml) and MS-PEG-treated (125±121 pg/ml) samples were comparable. From this we conclude that the differences in IL-10 levels detected here might be involved in the diverging effects of anti-TNFα drugs on T-cell proliferation and infection rates.

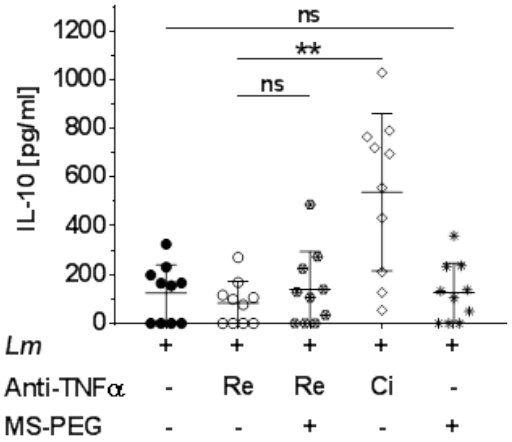

Figure 39: Increased levels of IL-10 upon sTNFα blockade by Cimzia®. *L. major*-infected hMDM/PBL co-cultures were treated with Remicade®, PEGylated Remicade® or Cimzia® to neutralize sTNFα. 7 days post-infection, IL-10 levels in cell supernatants were measured by ELISA. Data are shown as mean ± SD (*n*=10) and were obtained in 4 independent experiments. Statistical analysis was carried out using the Wilcoxon signed-rank test. $^{**}P < 0.01$.

3.4.4 Complement activation upon anti-TNFα treatment

As reported previously (Verhoef et al., 2014), PEG is able to activate complement. In order to investigate mechanisms underlying PEG-induced T-cell expansion, we characterized the capacity of PEGylated TNFα inhibitors to activate the complement system by measuring the release of C5a, a marker of terminal complement activation (Molino et al., 2012). Remarkably, C5a levels were significantly higher in the presence of Cimzia® (69±67 pg/ml) compared to Remicade® (25±26 pg/ml) (**Figure 40**). Accordingly, the comparison of PEGylated with non-PEGylated Remicade® demonstrated a significantly increased release of C5a (55±47 pg/ml) after treatment with PEG-Remicade®. C5a levels after incubation with MS-PEG were slightly but not significantly increased (42±69 pg/ml) compared to non-treated controls (17±14 pg/ml). Altogether, these data confirm a complement-mediated stimulation of the immune response that is caused by the PEG moiety of Cimzia® or PEG-Remicade®.

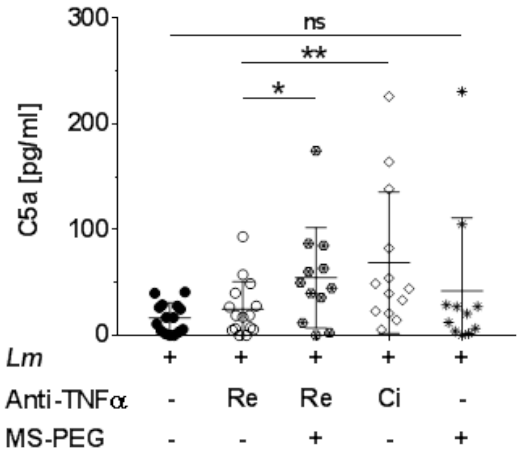

Figure 40: Increased levels of C5a upon treatment with Cimzia® or PEG-Remicade®. Macrophages were infected with *L. major* (MOI=20) and after 24 hours CFSE-labeled autologous PBLs were added. Co-cultures were treated with Remicade®, PEGylated Remicade® or Cimzia® to neutralize sTNFα. 7 days after infection, C5a levels in cell supernatants were determined by ELISA. 4 independent experiments were conducted of which data are shown as mean ± SD ($n \geq 13$). The Wilcoxon signed-rank test was performed to evaluate statistical significance.*$P < 0.05$; **$P < 0.01$.

4 Discussion

Although TNFα blockers have revolutionized therapy of autoimmune diseases, one of their major adverse effects is the significant risk of serious infections. Several reports describe a higher incidence of leishmaniasis to be linked to the treatment with Remicade®, Humira®, Enbrel® and Simponi®. To validate our hypothesis that therapeutic anti-TNFα agents can differently affect *Leishmania* infection, we succeeded in the development of an *in vitro* model that provides new insights into anti-TNFα-induced loss of parasite control in humans. Based on *L. major*-infected hMDMs co-cultured with autologous PBLs, we investigated the effects on *L. major* induced T-cells and infection rates in macrophages mediated by different TNFα inhibitors. We demonstrate that neutralization of TNFα by the anti-TNFα antibodies Remicade®, Remsima® and Humira® negatively affects infection control by the immune system. Treatment with these agents significantly reduced *Leishmania*-induced T-cell proliferation and increased the number of infected macrophages. Assessing the relevance of both mTNFα and sTNFα, we found that secreted TNFα has a prominent role for infection control whereas in this model no clear role was found for the membrane-integrated form due to the lack of expression on cell surfaces. These findings show that neutralization of sTNFα is the predominant mode of action of TNFα blockers in our *in vitro* model. Blockade of mTNFα as well as mTNFα-dependent ADCC- or CDC-mediated cell death as effector function of TNFα inhibitors could thus be excluded.

In contrast to the other anti-TNFα agents examined, blockade of sTNFα by Cimzia® did not affect T-cell proliferation and consequently infection was under control. Moreover, compared to Remicade®, Cimzia® did not impair the T-cell activation and phenotype as well as the expression of cytolytic effector molecules in proliferating T-cells. Investigating the structural differences of anti-TNFα agents that might result in diverging effects on parasite control, confirmed that Remicade®-mediated effects on T-cell proliferation and *L. major* infection rates were not mediated *via* Fc-FcγR interaction. However, our data reveal that Cimzia® supports parasite control through its conjugated PEG moiety as PEGylation of Remicade® improved the clearance of intracellular *Leishmania*. This effect could be linked to complement activation, with C5a expression being increased upon treatment with PEGylated TNFα blockers. **Figure 41** schematically summarizes the obtained results in this work.

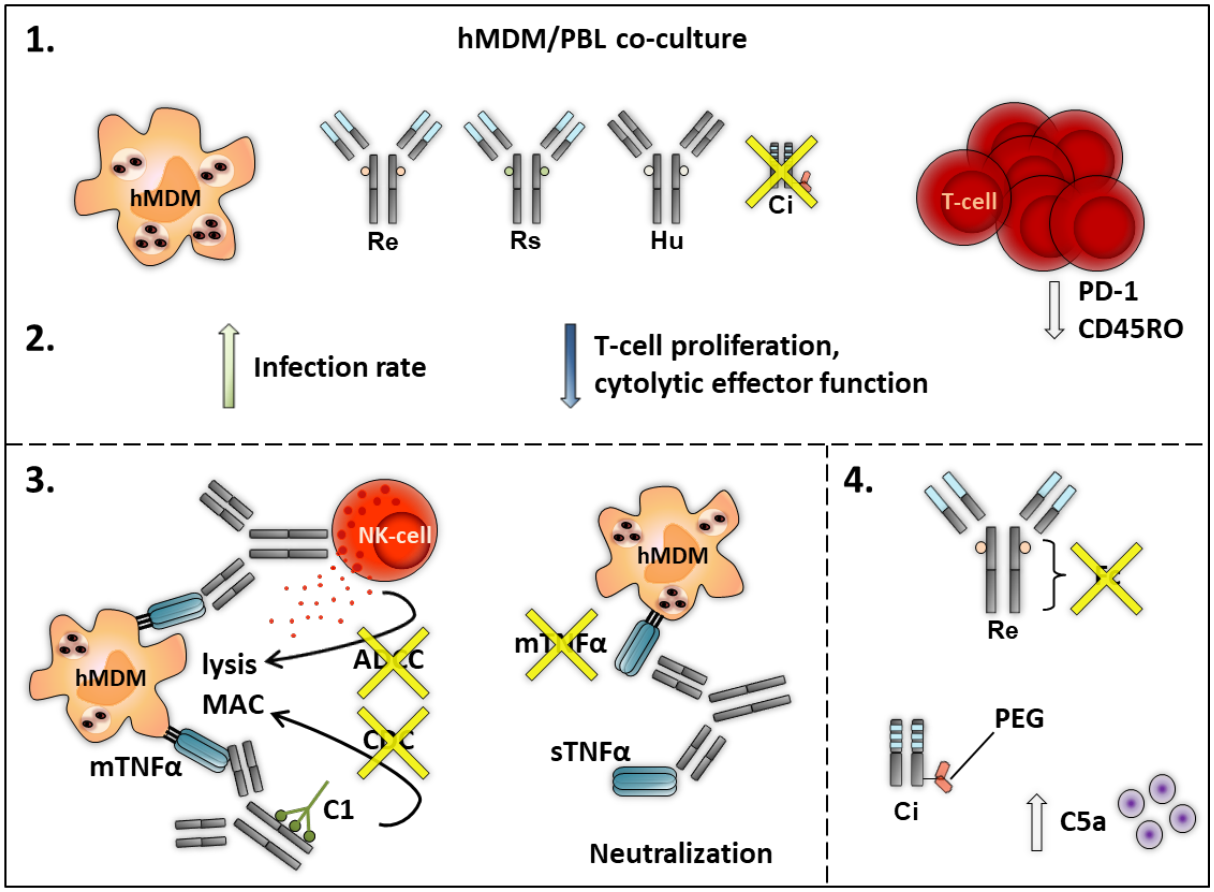

Figure 41: Summary of the obtained research data. (1) We developed an *in vitro* model of human leishmaniasis that is based on *L. major*-infected hMDMs co-cultured with autologous PBLs. (2) In contrast to Cimzia®, neutralization of TNFα by Remicade® (Re), Remsima® (Rs) and Humira® (Hu) significantly reduces *Leishmania*-induced T-cell proliferation and increases the number of infected macrophages. Furthermore, compared to Remicade®, Cimzia® does not impair the T-cell activation and phenotype as well as the expression of cytolytic effector molecules. (3) Neutralization of sTNFα is the predominant mode of action of TNFα blockers as mTNFα is not expressed on cell surfaces. Consequently, mTNFα-dependent ADCC or CDC is not induced. (4) The effects on T-cell proliferation and *L. major* infection rates by Remicade® treatment are not mediated *via* Fc-FcγR interaction. Cimzia® supports parasite control through its conjugated PEG moiety, which can be linked to complement activation as C5a expression is increased.

4.1 Characterization of *L. major*-infected hMDM/PBL co-cultures

In the present work, a TNFα-dependent *in vitro* model was established in order to compare different anti-TNFα agents and to analyze their impact on human leishmaniasis. We first characterized this *in vitro* model based on hMDM/PBL co-cultures and found that infection of macrophages with *L. major* increased the release of sTNFα into cell supernatants. Interestingly, measured sTNFα concentrations strongly differed among the tested donors. This effect was also observed by Castellano et al. in *L. braziliensis* antigen-stimulated PBMC cultures that were obtained from leishmaniasis patients or healthy controls (Castellano et al., 2009). Heterogeneity in cytokine production by human blood donors might be explained by several parameters such as environmental factors as well as the genetic predisposition or the immune status of tested individuals.

It has been shown *in vitro* that sTNFα co-stimulates the expression of NFκB and IL-2Rα (CD25) in primary human T-cells and thereby induces T-cell proliferation (Pimentel-Muiños et al., 1994). Indeed, we monitored $CD4^+$ T-cell proliferation concomitant to increased sTNFα secretion upon *L. major* infection and in agreement to previous reports, this proliferation enhanced parasite control in macrophages (Crauwels et al., 2015; Scott and Novais, 2016). Consistent with the induction of $CD4^+$ T-cell proliferation, infected samples showed an increased expression of the activation markers CD25 and PD-1 on T-cells. Levels of CD25 increase 24 hours after activating stimulation and expression remains high until day 7 (Bajnok et al., 2017). At this time point, we performed measurements of activation markers in our experiments. By contrast, CD69 is described as a very early T-cell activation marker. It is upregulated within hours of TCR signaling but expression quickly declines after 24 hours (Bajnok et al., 2017). In our model, we did not detect significant differences in CD69 levels between infected and non-infected hMDM/PBL co-cultures as levels of CD69 might have already declined when measuring its expression on day 7. Thus, CD25, instead of CD69, is the appropriate marker to monitor T-cell activation in our infection model.

Most German donors are vaccinated against tetanus and thus T-cell proliferation can be observed in cell cultures obtained from healthy subjects and treated with the recall antigen tetanus toxoid (Zaunders et al., 2009; Crauwels et al., 2015). Unexpectedly, in our studies, T-cells were activated in response to *L. major* infection, although blood cells were obtained from healthy donors who had not been exposed to parasites before. These activated T-cells

displayed high levels of the memory marker CD45RO. Prior reports suggest cross-reactive memory T-cells, rather than naive T-cells, to respond to *Leishmania* (Kemp et al., 1992). However, using MACS-purified $CD45RA^+$ T-cells, we demonstrated the ability of naive T-cells to recognize *L. major* and to proliferate whereupon CD45RO is upregulated. Consistent with these data, Sassi et al. showed proliferation of PBMCs from healthy adults or cord blood of newborns in response to membrane-derived antigen (MLA) from *L. major* or *L. infantum*. This proliferation required $CD4^+$ T-cells and antigen-processing by macrophages, it was restricted to MHC-II and mediated by proteins in MLA (Sassi et al., 2005).

Thus, according to our findings, individuals possess a natural reactivity to *Leishmania* parasites contributing to disease control. Variations in reactivity and intrinsic differences of immune cells might result in different disease outcomes. Several studies underline this assumption. *L. braziliensis* or *L. amazonensis* antigen-stimulated naive PBMCs of healthy donors showed responses ranging between high IFNγ and low IFNγ production (Scorza et al., 2017). Furthermore, infection rates and parasite burden in hMDMs obtained from subclinically infected patients were lower after *in vitro* exposure to *L. braziliensis* compared to patients with CL (Giudice et al., 2012). Though human individuals exhibit a natural reactivity towards *Leishmania*, studies investigating blood of donors with a history of leishmaniasis should complement our investigations.

4.2 Blockade of TNFα signaling in infected hMDM/PBL co-cultures

Subsequent to successful characterization, we used our leishmaniasis model to compare the chimeric antibody Remicade®, its biosimilar Remsima®, the fully human antibody Humira® and the PEGylated Fab-derived inhibitor Cimzia®. The application of equimolar amounts of TNFα inhibitors confirmed that all tested agents effectively neutralized sTNFα. Interestingly, despite only one binding site, the neutralizing capacity of Cimzia® seemed slightly better compared to the other inhibitors. As a consequence of sTNFα blockade, infection rates in human macrophages substantially increased upon treatment with Remicade®, Remsima® and Humira®. This increase resulted from reduced T-cell proliferation and it demonstrates the negative impact of various anti-TNFα agents on parasite control in human leishmaniasis.

Infection is a major adverse effect of immunosuppressive anti-TNFα treatment. Our findings corroborate clinical reports that link reactivation of leishmaniasis or a higher susceptibility for an initial infection with *Leishmania* parasites to the application of Remicade® or Humira® as well as further TNFα blockers Enbrel® and Simponi® (Leonardis et al., 2009; Guarneri et al., 2017). When purified T-cells instead of PBLs were co-incubated, comparable results were obtained, confirming that anti-TNFα-mediated effects exclusively depended on hMDMs and T-cells. Noteworthy, anti-TNFα agents tested in our experiments had no effect on *L. major* infection rates in the absence of PBLs, illustrating the importance of T-cell activation for parasite control in humans. In this aspect, our human model differs from data obtained in mice that showed enhanced parasite killing in sTNFα-treated and lipopolysaccharide-stimulated macrophages in the absence of T-cells (Liew et al., 1990b; F Y Liew, C Parkinson, S Millott, A Severn, and M Carrier, 1990). Furthermore, Fromm et al. demonstrated a highly active Th1 phenotype, despite TNFα knock-out, by analyzing expression levels of the transcription factor Tbet in T-cells that were isolated from the spleen of C57BL/6 mice after *L. major* infection (Fromm et al., 2015).

When assessing the relevance of membrane-integrated or secreted TNFα in our infection model, we demonstrated a prominent role of sTNFα for parasite control. The membrane integrated form seemed to be rapidly cleaved as mTNFα could not be detected on cell surfaces, neither at different time points nor after treatment with the TACE inhibitor TAPI-1. This suggests that neutralization of sTNFα rather than mTNFα-dependent ADCC- or CDC-mediated cell death is the predominant mode of action of anti-TNFα agents in our *in vitro* model. Despite differing amino acid sequence, species origin or glycosylation profile, tested TNFα inhibitors are described to have similar binding affinities towards sTNFα (Mitoma et al., 2016). This might explain the fact that the comparison of Remicade®, Remsima® and Humira® revealed no substantial differences regarding T-cell proliferation and *L. major* infection rates. Of note, and in contrast to the other anti-TNFα agents studied, treatment with Cimzia® maintained T-cell proliferation and parasite control despite effective sTNFα blockade. This issue is intriguing and is discussed below.

In addition to the anti-TNFα agents tested here, it might be of interest to investigate and compare the obtained data to Enbrel® using our *in vitro* model of leishmaniasis. This TNFα inhibitor showed similar binding affinity towards sTNFα but comprises a strongly differing

structure compared to other anti-TNFα agents. Moreover, clinical reports indicate that infections, especially tuberculosis, occurred more frequently in patients treated with Remicade® than with Enbrel® (Wallis and Ehlers, 2005).

In order to determine the receptor primarily responsible for TNFα signaling in our *in vitro* model, we neutralized mTNFR1 or mTNFR2. Blockade of mTNFR2 only slightly reduced T-cell proliferation and anti-mTNFR1 or anti-mTNFR2 treatment slightly increased *L. major* infection rates compared to controls. These data indicate that mTNFRs might compensate for the loss of each other and thus blocking both receptors simultaneously should be further investigated. Our findings, which did not reveal a prominent role for either mTNFR1 or mTNFR2, are in contrast to observations made in mice. Studies with *L. major*-infected C57BL/6 mice emphasize the relevance of mTNFR1 and mTNFα for disease control (Fromm et al., 2015).

In addition to TNFα in mouse infection models, IFNγ is also described to stimulate macrophages to kill intracellular pathogens (Liew et al., 1990a; Novais et al., 2014). We analyzed the relevance of IFNγ for parasite control in human cells, but in contrast to previous reports, we found that T-cell proliferation and infection rates were independent of this cytokine.

4.3 T-cell phenotype, effector function and cell viability upon anti-TNFα treatment

When performing the sTNFα neutralization experiments, we focused on Cimzia® due to its diverging effects compared to the other TNFα inhibitors tested. Remicade®, the most extensively studied anti-TNFα antibody, was used as reference agent. Neutralization of sTNFα by Remicade® revealed significantly reduced proliferation of T-cells, whereas Cimzia® treatment maintained T-cell proliferation. We investigated the T-cell phenotype upon anti-TNFα treatment and found that proliferating $CD4^+$ T-cells expressed significantly lower levels of PD-1 and CD45RO after treatment with Remicade® compared to non-treated controls. Furthermore, the overall expression of cytolytic proteins was reduced after the addition of Remicade®, which indicates reduced effector function of proliferating T-cells. In line with our

findings, inhibition of the TNFα-dependent expression of granzyme A by T-cells was previously demonstrated after Remicade® treatment (Dahlén et al., 2013). In contrast to Remicade®, application of Cimzia® did not interfere with the T-cell phenotype and effector function as shown by overall unaltered PD-1, CD45RO and cytolytic effector molecule expression.

Cytolytic proteins play a pivotal role in combating intracellular infections. They are released by T-cells leading to pore-formation in target cell membranes and to target cell lysis by several, not yet fully understood mechanisms (Barry and Bleackley, 2002). Of note, our experiments revealed increased levels of cytolytic molecules in *L. major*-induced proliferating $CD4^+$ T-cells, although antimicrobial and cytotoxic activity has mainly been attributed to $CD8^+$ T-cells (Soghoian and Streeck, 2010; Voskoboinik et al., 2015). In agreement with recent studies showing that $CD4^+$ T-cells can also display cytolytic functions (Grossman et al., 2004; Bastian et al., 2008; Soghoian and Streeck, 2010), we assume that *L. major*-induced proliferating $CD4^+$ T-cells release cytolytic proteins that mediate killing of intracellular parasites. Similarly, a role of cytolytic molecules in parasite control has been previously described by Dotiwala and colleagues for *in vitro* infection with *L. major*, *Trypanosoma cruzi* and *Toxoplasma gondii*. Granulysin and granzymes enter infected host cells with the help of perforin. Then, granulysin delivers granzymes to the intracellular parasite, where granzymes induce parasite death independently of host cell death (Dotiwala et al., 2016).

The role of cytolytic $CD8^+$ T-cells in human leishmaniasis is controversial. Expression of granzyme A and granzyme B positively correlated with lesion progression in patients (da Silva Santos and Brodskyn, 2014). By contrast, an increase in *L. braziliensis*-reactive $CD8^+$ T-cells was observed during the healing process of CL (Da-Cruz et al., 2002). In our study, proliferation of cytolytic $CD4^+$ T-cells was induced upon infection with *L. major*. Induction of cytolytic $CD8^+$ T-cells was negligible. In order to exclude cell death of primary human cells mediated by cytolytic effector molecules, cells were stained with PI. Thus, we could demonstrate that cytolytic proteins expressed by $CD4^+$ T-cells do not impair cell viability. Macrophages and co-cultured T-cells displayed low PI positivity and values were comparable in the absence or presence of anti-TNFα agents.

4.4 Role of structural features for diverging effects of Cimzia®

With the aim to elucidate underlying mechanisms that lead to enhanced parasite control upon treatment with Cimzia®, we focused on structural differences between tested anti-TNFα agents. In contrast to all other TNFα inhibitors tested, Cimzia® lacks an Fc region that could intact with FcγRs on macrophages (Goel and Stephens, 2010). Signaling through these receptors alters the activation status of cells bearing them (Thalayasingam and Isaacs, 2011; Chan et al., 2015). By pre-incubation with the IgG preparation Polyglobin®, we confirmed that Remicade®-mediated effects on T-cell proliferation and *L. major* infection rates were not mediated *via* Fc-FcγR interaction, but exclusively depended on sTNFα neutralization. As discussed above, these findings support the conclusion that comparing Fc-mediated mechanisms of action (ADCC or CDC) by TNFα inhibitors using this *in vitro* model is not possible.

Our results partially agree with research from Vos et al. who also found Remicade® but not Cimzia® treatment to reduce T-cell proliferation. Inconsistent with our data, the inhibition of proliferation was abolished after blockade of FcγRs (Vos et al., 2011). Changes in the experimental set-up might explain these variations.

Among the tested anti-TNFα agents, Cimzia® was the only TNFα blocker being modified with a PEG moiety. PEG is commonly used to increase half-life and stability and to reduce immunogenicity as well as aggregation of therapeutic proteins (Harris and Chess, 2003). It is described to have no adverse biological effects, although several studies revealed unanticipated immunogenicity of PEG (Garay et al., 2012). To this end, it would be interesting to examine and compare Cimzia®-mediated effects in the absence and presence of a PEG moiety. However, as we could not test non-PEGylated Cimzia®, we PEGylated Remicade® to determine the effects that were mediated by the PEG moiety. PEG-Remicade® proved effective sTNFα blockade, which was comparable to non-PEGylated Remicade®. Interestingly, T-cell proliferation and parasite control upon PEG-Remicade® treatment was significantly increased compared to Remicade®-treated samples. These findings confirm an immunostimulatory effect of PEG-Remicade® in the absence of sTNFα, which is similar to Cimzia® treatment.

We analyzed the consequences of PEGylated TNFα inhibitors on anti-inflammatory cytokine production by measuring levels of the major regulatory cytokine IL-10 (Kemper and

Atkinson, 2007; Saraiva and O'Garra, 2010). The release of IL-10 was significantly increased after treatment with Cimzia® in comparison to Remicade® or non-treated controls. Treatment with PEGylated Remicade® slightly increased the release of IL-10 compared to the non-PEGylated form. These differences in IL-10 levels detected here might be involved in the diverging effects of anti-TNFα drugs on T-cell proliferation and infection rates. High IL-10 levels, which regulate/suppress excessive inflammation, support our theory that, despite sTNFα neutralization, Cimzia® supplementary enhanced the immune response through a yet unknown mechanism. IL-10 was initially described as Th2 or regulatory T-cell (Treg) cytokine, albeit recent studies have demonstrated that many other cells of the adaptive immune system such as Th1 and Th17 produce IL-10 (Saraiva and O'Garra, 2010). Examination of cell type-specific transcription factors such as Tbet (Th1), GATA3 (Th2), RORγt (Th17) as well as FoxP3 (Treg) and multiple cytokines might provide further insights into T-cell phenotypes and changes mediated by the application of Cimzia®.

Several reports describe the development of anti-PEG antibodies and activation of complement upon exposure to PEG. Underlying mechanisms and involved factors remain elusive, though some researchers assume PEG as ingredient in food or cosmetics to correlate with this phenomenon (Verhoef et al., 2014). Anti-PEG antibodies are associated with the rapid clearance of the therapeutic PEG-asparaginase and were found in patients treated with PEGylated uricase (Armstrong et al., 2007; Sundy et al., 2011). Elevated C3a and C5a plasma levels were measured in mice injected with repeated doses of PEGylated-thioaptamer and *in vitro* experiments demonstrated that PEGylated nanocapsules induced increased C4 consumption and C5a levels in human serum (Molino et al., 2012; Morita et al., 2016). PEG alone demonstrated the generation of complement activation products such as C4d, C3a-desArg and SC5b-9 in human serum (Hamad et al., 2008).

In fact, concomitant to increased T-cell proliferation, we found elevated levels of C5a in cell supernatants upon treatment with PEGylated Remicade® or Cimzia®. In agreement to previous studies, showing that C3a and C5a promote $CD4^+$ T-cell expansion, our findings strongly indicate complement to play a major role in cell activation and *L. major* infection control in the absence of sTNFα (Cravedi et al., 2013). Complement activation depends on the concentration and molecular weight of PEG (Hamad et al., 2008). Thus, variations in the

structure or size of the PEG moiety might explain deviations between PEG-Remicade® and Cimzia®.

Undesirable activation of the immune or complement system by PEG can result in clearance of PEGylated pharmaceuticals or potential hypersensitivity reactions (Verhoef et al., 2014). However, Cimzia® demonstrated efficacy in clinical trials and is effectively and generally well-tolerated used in therapy for almost 10 years (Deeks, 2016).

The complement system has been traditionally regarded as innate system that controls invading pathogens by chemotaxis, opsonization and lysis (Dunkelberger and Song, 2010). However, recent studies, including our investigations, revealed that complement has been largely underestimated in the past. It can modulate the adaptive immune response as T-cell activation can be directly induced by complement components or indirectly *via* complement-activated APCs such as macrophages (Hawlisch et al., 2004; Kemper and Atkinson, 2007; Kwan et al., 2012; Cravedi et al., 2013). Therefore, we assume that increased T-cell proliferation after treatment with PEGylated anti-TNFα agents is a result of complement activation. Further investigations should be carried out to confirm our hypothesis. Besides C5a, C3a is an important anaphylatoxin, which mediates cell activation and inflammation and whose secretion should be further examined (Kemper and Atkinson, 2007). Expression of complement receptors such as C3aR and C5aR on macrophages and T-cells should be determined and their relevance for cell activation and parasite control could be investigated by application of specific receptor antagonists. Furthermore, blockade of certain complement pathways by specific inhibitors such as decay acceleration factor (DAF) or factor H, which inhibit C3 convertases, can help to reveal complement-mediated effects (Merle et al., 2015).

The paradigm that complement is only released to serum after its production in the liver has changed in recent years. Noteworthy, immune cells themselves can produce and release complement proteins locally (Lubbers et al., 2017). Macrophages and T-cells, which we used in our *in vitro* assay, are thus practically able to initiate full signaling through complement pathways with one exception: the formation of the MAC involving C6-C9. This illustrates that activation of macrophages and T-cells rather than target cell death by the MAC is mediated through complement in our experiments.

4.5 Concluding remarks

Taken together, we provide an *in vitro* model of human leishmaniasis that allows direct comparison of different therapeutic anti-TNFα agents and conclusions on the impairment of pathogen control. Herein, we demonstrated significant differences between the treatment with Cimzia® and other anti-TNFα agents. We showed that PEGylation of Remicade® promoted immunostimulation and parasite control, an effect that we proved to be even more pronounced for Cimzia®. Our data strongly indicate PEG-mediated complement activation to maintain T-cell activation, effector function and parasite killing in hMDMs in the absence of sTNFα. Further examinations need to follow this study to determine detailed molecular mechanism of complement activation by PEG and its supportive role for *L. major* infection control. Considering that reactivation of a latent infection or a higher susceptibility for a new infection with *Leishmania* is a severe adverse effect of immunosuppressive anti-TNFα treatment, careful characterization of TNFα blockers and investigation of adverse effects is indispensable. Our findings contribute to a better understanding of the effectiveness of different TNFα inhibitors and will be helpful for the assessment of immunosuppressive anti-TNFα agents. Based on our results, we propose that anti-TNFα therapy using Cimzia® may be advantageous for patients living in high-incidence areas of leishmaniasis.

5 References

Aggarwal, B.B., Gupta, S.C., and Kim, J.H. (2012). Historical perspectives on tumor necrosis factor and its superfamily. 25 years later, a golden journey. Blood *119*, 651-665.

Aggarwal, B.B., Henzel, W.J., Moffat, B., Kohr, W.J., and Harkins, R.N. (1985a). Primary structure of human lymphotoxin derived from 1788 lymphoblastoid cell line. The Journal of biological chemistry *260*, 2334-2344.

Aggarwal, B.B., Kohr, W.J., Hass, P.E., Moffat, B., Spencer, S.A., Henzel, W.J., Bringman, T.S., Nedwin, G.E., Goeddel, D.V., and Harkins, R.N. (1985b). Human tumor necrosis factor. Production, purification, and characterization. The Journal of biological chemistry *260*, 2345-2354.

Alexander, J., and Brombacher, F. (2012). T helper1/t helper2 cells and resistance/susceptibility to leishmania infection. Is this paradigm still relevant? Frontiers in immunology *3*, 80.

Ali, T., Kaitha, S., Mahmood, S., Ftesi, A., Stone, J., and Bronze, M.S. (2013). Clinical use of anti-TNF therapy and increased risk of infections. Drug, healthcare and patient safety *5*, 79-99.

Armstrong, J.K., Hempel, G., Koling, S., Chan, L.S., Fisher, T., Meiselman, H.J., and Garratty, G. (2007). Antibody against poly(ethylene glycol) adversely affects PEG-asparaginase therapy in acute lymphoblastic leukemia patients. Cancer *110*, 103-111.

Aronson, N., Herwaldt, B.L., Libman, M., Pearson, R., Lopez-Velez, R., Weina, P., Carvalho, E., Ephros, M., Jeronimo, S., and Magill, A. (2017). Diagnosis and Treatment of Leishmaniasis. Clinical Practice Guidelines by the Infectious Diseases Society of America (IDSA) and the American Society of Tropical Medicine and Hygiene (ASTMH). The American journal of tropical medicine and hygiene *96*, 24-45.

Arthritis Foundation (2017). Arthritis By The Numbers. Book of Trusted Facts & Figures. 2017; v1.3. http://www.arthritis.org/Documents/Sections/About-Arthritis/arthritis-facts-stats-figures.pdf.

Atreya, R., Zimmer, M., Bartsch, B., Waldner, M.J., Atreya, I., Neumann, H., Hildner, K., Hoffman, A., Kiesslich, R., and Rink, A.D., et al. (2011). Antibodies against tumor necrosis factor (TNF) induce T-cell apoptosis in patients with inflammatory bowel diseases via TNF receptor 2 and intestinal $CD14^{+}$ macrophages. Gastroenterology *141*, 2026-2038.

Bagalas, V., Kioumis, I., Argyropoulou, P., and Patakas, D. (2007). Visceral leishmaniasis infection in a patient with rheumatoid arthritis treated with etanercept. Clinical rheumatology *26*, 1344-1345.

Bajnok, A., Ivanova, M., Rigó, J., and Toldi, G. (2017). The Distribution of Activation Markers and Selectins on Peripheral T Lymphocytes in Preeclampsia. Mediators of inflammation *2017*, 8045161.

Bal, A., Unlu, E., Bahar, G., Aydog, E., Eksioglu, E., and Yorgancioglu, R. (2007). Comparison of serum IL-1 beta, sIL-2R, IL-6, and TNF-alpha levels with disease activity parameters in ankylosing spondylitis. Clinical rheumatology *26*, 211-215.

Barral-Netto, M., Badaró, R., Barral, A., Almeida, R.P., Santos, S.B., Badaró, F., Pedral-Sampaio, D., Carvalho, E.M., Falcoff, E., and Falcoff, R. (1991). Tumor necrosis factor (cachectin) in human visceral leishmaniasis. The Journal of infectious diseases *163*, 853-857.

Barry, M., and Bleackley, R.C. (2002). Cytotoxic T lymphocytes. All roads lead to death. Nature reviews. Immunology *2*, 401-409.

Bastian, M., Braun, T., Bruns, H., Rollinghoff, M., and Stenger, S. (2008). Mycobacterial Lipopeptides Elicit CD4+ CTLs in Mycobacterium tuberculosis-Infected Humans. The Journal of Immunology *180*, 3436-3446.

Bogdan, C. (2012). Leishmaniasis in rheumatology, haematology and oncology: epidemiological, immunological and clinical aspects and caveats. Annals of the rheumatic diseases *71 Suppl 2*, i60-6.

Bogdan, C., and Röllinghoff, M. (1998). The immune response to Leishmania. Mechanisms of parasite control and evasion. International journal for parasitology *28*, 121-134.

Bongartz, T., Sutton, A.J., Sweeting, M.J., Buchan, I., Matteson, E.L., and Montori, V. (2006). Anti-TNF antibody therapy in rheumatoid arthritis and the risk of serious infections and malignancies: systematic review and meta-analysis of rare harmful effects in randomized controlled trials. JAMA *295*, 2275-2285.

Bradley, J.R. (2008). TNF-mediated inflammatory disease. The Journal of pathology *214*, 149-160.

BRENCHLEY, J.M., DOUEK, D.C., AMBROZAK, D.R., CHATTERJI, M., BETTS, M.R., DAVIS, L.S., and KOUP, R.A. (2002). Expansion of activated human naive T-cells precedes effector function. Clin Exp Immunol *130*, 432-440.

Carneiro, P.P., Conceição, J., Macedo, M., Magalhães, V., Carvalho, E.M., and Bacellar, O. (2016). The Role of Nitric Oxide and Reactive Oxygen Species in the Killing of Leishmania braziliensis by Monocytes from Patients with Cutaneous Leishmaniasis. PloS one *11*, e0148084.

Carswell, E.A., Old, L.J., Kassel, R.L., Green, S., Fiore, N., and Williamson, B. (1975). An endotoxin-induced serum factor that causes necrosis of tumors. Proceedings of the National Academy of Sciences of the United States of America *72*, 3666-3670.

Castellano, L.R., Filho, D.C., Argiro, L., Dessein, H., Prata, A., Dessein, A., and Rodrigues, V. (2009). Th1/Th2 immune responses are associated with active cutaneous leishmaniasis and clinical cure is associated with strong interferon-gamma production. Human immunology *70*, 383-390.

Catala, A., Roe, E., Dalmau, J., Pomar, V., Munoz, C., Yelamos, O., and Puig, L. (2015). Anti-tumour necrosis factor-induced visceral and cutaneous leishmaniasis: case report and review of the literature. Dermatology (Basel, Switzerland) *230*, 204-207.

CDC (2017). Centers for Disease Control and Prevention. IBD prevalence in the United States. https://www.cdc.gov/ibd/data-statistics.htm.

Chan, K.R., Ong, E.Z., Mok, D.Z.L., and Ooi, E.E. (2015). Fc receptors and their influence on efficacy of therapeutic antibodies for treatment of viral diseases. Expert review of anti-infective therapy *13*, 1351-1360.

Chaudhari, K., Rizvi, S., and Syed, B.A. (2016). Rheumatoid arthritis. Current and future trends. Nature reviews. Drug discovery *15*, 305-306.

Coates, L.C., FitzGerald, O., Helliwell, P.S., and Paul, C. (2016). Psoriasis, psoriatic arthritis, and rheumatoid arthritis. Is all inflammation the same? Seminars in arthritis and rheumatism *46*, 291-304.

Courret, N., Fréhel, C., Gouhier, N., Pouchelet, M., Prina, E., Roux, P., and Antoine, J.-C. (2002). Biogenesis of Leishmania-harbouring parasitophorous vacuoles following phagocytosis of the metacyclic promastigote or amastigote stages of the parasites. Journal of cell science *115*, 2303-2316.

Crauwels, P., Bohn, R., Thomas, M., Gottwalt, S., Jäckel, F., Krämer, S., Bank, E., Tenzer, S., Walther, P., and Bastian, M., et al. (2015). Apoptotic-like Leishmania exploit the host´s autophagy machinery to reduce T-cell-mediated parasite elimination. Autophagy *11*, 285-297.

Cravedi, P., Leventhal, J., Lakhani, P., Ward, S.C., Donovan, M.J., and Heeger, P.S. (2013). Immune cell-derived C3a and C5a costimulate human T cell alloimmunity. American journal of transplantation : official journal of the American Society of Transplantation and the American Society of Transplant Surgeons *13*, 2530-2539.

da Silva Santos, C., and Brodskyn, C.I. (2014). The Role of CD4 and CD8 T Cells in Human Cutaneous Leishmaniasis. Frontiers in public health *2*, 165.

Da-Cruz, A.M., Bittar, R., Mattos, M., Oliveira-Neto, M.P., Nogueira, R., Pinho-Ribeiro, V., Azeredo-Coutinho, R.B., and Coutinho, S.G. (2002). T-cell-mediated immune responses in patients with cutaneous or mucosal leishmaniasis. Long-term evaluation after therapy. Clinical and diagnostic laboratory immunology *9*, 251-256.

Dahlén, R., Strid, H., Lundgren, A., Isaksson, S., Raghavan, S., Magnusson, M.K., Simrén, M., Sjövall, H., and Öhman, L. (2013). Infliximab inhibits activation and effector functions of peripheral blood T cells in vitro from patients with clinically active ulcerative colitis. Scandinavian journal of immunology *78*, 275-284.

Deeks, E.D. (2016). Certolizumab Pegol. A Review in Inflammatory Autoimmune Diseases. BioDrugs : clinical immunotherapeutics, biopharmaceuticals and gene therapy *30*, 607-617.

Desjeux, P. (2004). Leishmaniasis. Current situation and new perspectives. Comparative immunology, microbiology and infectious diseases *27*, 305-318.

Dotiwala, F., Mulik, S., Polidoro, R.B., Ansara, J.A., Burleigh, B.A., Walch, M., Gazzinelli, R.T., and Lieberman, J. (2016). Killer lymphocytes use granulysin, perforin and granzymes to kill intracellular parasites. Nature medicine *22*, 210-216.

Dunkelberger, J.R., and Song, W.-C. (2010). Complement and its role in innate and adaptive immune responses. Cell research *20*, 34-50.

El-Tahan, R.R., Ghoneim, A.M., and El-Mashad, N. (2016). TNF-α gene polymorphisms and expression. SpringerPlus *5*, 1508.

EMA (2013). Assessment report Remsima. http://www.ema.europa.eu/docs/en_GB/document_library/EPAR_-_Public_assessment_report/human/002576/WC500151486.pdf.

EMA (2017). Biosimilars in the EU. Information guide for healthcare professionals. http://www.ema.europa.eu/docs/en_GB/document_library/Leaflet/2017/05/WC500226648.pdf.

European Medicines Agency (2017). European public assessment reports. http://www.ema.europa.eu/ema/index.jsp?curl=pages/medicines/landing/epar_search.jsp&mid=WC0b01ac058001d124.

F Y Liew, C Parkinson, S Millott, A Severn, and M Carrier (1990). Tumour necrosis factor (TNF alpha) in leishmaniasis. I. TNF alpha mediates host protection against cutaneous leishmaniasis.

Fabre, S., Gibert, C., Lechiche, C., Dereure, J., Jorgensen, C., and Sany, J. (2005). Visceral leishmaniasis infection in a rheumatoid arthritis patient treated with infliximab. Clinical and experimental rheumatology *23*, 891-892.

Fakhoury, M., Negrulj, R., Mooranian, A., and Al-Salami, H. (2014). Inflammatory bowel disease. Clinical aspects and treatments. Journal of inflammation research *7*, 113-120.

Fehres, C.M., Unger, W.W.J., Garcia-Vallejo, J.J., and van Kooyk, Y. (2014). Understanding the biology of antigen cross-presentation for the design of vaccines against cancer. Frontiers in immunology *5*, 149.

Filippis Christodoulos (2018). PD-1 checkpoint inhibition in Leishmania infection of primary human cells. Dissertation (Mainz).

Fonseca, S.G., Romão, P.R.T., Figueiredo, F., Morais, R.H., Lima, H.C., Ferreira, S.H., and Cunha, F.Q. (2003). TNF-alpha mediates the induction of nitric oxide synthase in macrophages but not in neutrophils in experimental cutaneous leishmaniasis. European journal of immunology *33*, 2297-2306.

Franklin, G., Greenspan, J., and Chen, S. (2009). Anti-tumor necrosis factor-alpha therapy provokes latent leishmaniasis in a patient with rheumatoid arthritis. Annals of clinical and laboratory science *39*, 192-195.

Fromm, P.D., Kling, J.C., Remke, A., Bogdan, C., and Körner, H. (2015). Fatal Leishmaniasis in the Absence of TNF Despite a Strong Th1 Response. Frontiers in microbiology *6*, 1520.

Galdino, H., Maldaner, A.E., Pessoni, L.L., Soriani, F.M., Pereira, L.I.d.A., Pinto, S.A., Duarte, F.B., Gomes, C.M., Fleuri, A.K.A., and Dorta, M.L., et al. (2014). Interleukin 32γ (IL-32γ) is highly expressed in cutaneous and mucosal lesions of American Tegumentary Leishmaniasis patients. Association with tumor necrosis factor (TNF) and IL-10. BMC infectious diseases *14*, 249.

Garay, R.P., El-Gewely, R., Armstrong, J.K., Garratty, G., and Richette, P. (2012). Antibodies against polyethylene glycol in healthy subjects and in patients treated with PEG-conjugated agents. Expert opinion on drug delivery *9*, 1319-1323.

Gaze, S.T., Dutra, W.O., Lessa, M., Lessa, H., Guimarães, L.H., Jesus, A.R.d., Carvalho, L.P., Machado, P., Carvalho, E.M., and Gollob, K.J. (2006). Mucosal leishmaniasis patients display an activated inflammatory T-cell phenotype associated with a nonbalanced monocyte population. Scandinavian journal of immunology *63*, 70-78.

Ginhoux, F., and Jung, S. (2014). Monocytes and macrophages. Developmental pathways and tissue homeostasis. Nature reviews. Immunology *14*, 392-404.

Giudice, A., Vendrame, C., Bezerra, C., Carvalho, L.P., Delavechia, T., Carvalho, E.M., and Bacellar, O. (2012). Macrophages participate in host protection and the disease pathology associated with Leishmania braziliensis infection. BMC infectious diseases *12*, 75.

Goel, N., and Stephens, S. (2010). Certolizumab pegol. mAbs *2*, 137-147.

Goffe, B., and Cather, J.C. (2003). Etanercept. An overview. Journal of the American Academy of Dermatology *49*, S105-11.

Gollob, K.J., Antonelli, L.R.V., and Dutra, W.O. (2005). Insights into CD4+ memory T cells following Leishmania infection. Trends in parasitology *21*, 347-350.

Gollob, K.J., Viana, A.G., and Dutra, W.O. (2014). Immunoregulation in human American leishmaniasis. Balancing pathology and protection. Parasite immunology *36*, 367-376.

Grossman, W.J., Verbsky, J.W., Tollefsen, B.L., Kemper, C., Atkinson, J.P., and Ley, T.J. (2004). Differential expression of granzymes A and B in human cytotoxic lymphocyte subsets and T regulatory cells. Blood *104*, 2840-2848.

Guarneri, C., Bevelacqua, V., Patterson, J.W., and Tchernev, G. (2017). Cutaneous and visceral leishmaniasis during anti-TNFα therapy. Wien Med Wochenschr *167*, 78-82.

Guedes-Barbosa, L.S., Pereira da Costa, I., Fernandes, V., Henrique da Mota, L.M., Menezes, I. de, and Aaron Scheinberg, M. (2013). Leishmaniasis during anti-tumor necrosis factor therapy: report of 4 cases and review of the literature (additional 28 cases). Seminars in arthritis and rheumatism *43*, 152-157.

Gupta, G., Oghumu, S., and Satoskar, A.R. (2013). Mechanisms of immune evasion in leishmaniasis. Advances in applied microbiology *82*, 155-184.

Hailu, A., van Baarle, D., Knol, G.J., Berhe, N., Miedema, F., and Kager, P.A. (2005). T cell subset and cytokine profiles in human visceral leishmaniasis during active and asymptomatic or sub-clinical infection with Leishmania donovani. Clinical immunology (Orlando, Fla.) *117*, 182-191.

Hakimi, S., Rivière, S., Del Giudice, P., Dereure, J., and Le Quellec, A. (2010). Localized Cutaneous Leishmaniasis due to Leishmania infantum in a Patient Treated with Infliximab. Dermatology (Basel, Switzerland) *220*, 63-65.

Hamad, I., Hunter, A.C., Szebeni, J., and Moghimi, S.M. (2008). Poly(ethylene glycol)s generate complement activation products in human serum through increased alternative pathway turnover and a MASP-2-dependent process. Molecular immunology *46*, 225-232.

Harashima, S., Horiuchi, T., Hatta, N., Morita, C., Higuchi, M., Sawabe, T., Tsukamoto, H., Tahira, T., Hayashi, K., and Fujita, S., et al. (2001). Outside-to-inside signal through the membrane TNF-alpha induces E-selectin (CD62E) expression on activated human CD4+ T cells. Journal of immunology (Baltimore, Md. : 1950) *166*, 130-136.

Harris, J.M., and Chess, R.B. (2003). Effect of pegylation on pharmaceuticals. Nature reviews. Drug discovery *2*, 214-221.

Hawlisch, H., Wills-Karp, M., Karp, C.L., and Köhl, J. (2004). The anaphylatoxins bridge innate and adaptive immune responses in allergic asthma. Molecular immunology *41*, 123-131.

Horiuchi, T., Mitoma, H., Harashima, S.-i., Tsukamoto, H., and Shimoda, T. (2010). Transmembrane TNF-. Structure, function and interaction with anti-TNF agents. Rheumatology *49*, 1215-1228.

Horta, M.F., Mendes, B.P., Roma, E.H., Noronha, F.S.M., Macêdo, J.P., Oliveira, L.S., Duarte, M.M., and Vieira, L.Q. (2012). Reactive oxygen species and nitric oxide in cutaneous leishmaniasis. Journal of parasitology research *2012*, 203818.

Jeziorski, E., Dereure, J., Mac Bullen, G., Blanchet, C., Ludwig, C., Costes, V., and Rodière, M. (2015). Mucosal relapse of visceral leishmaniasis in a child treated with anti-TNFα. International journal of infectious diseases : IJID : official publication of the International Society for Infectious Diseases *33*, 135-136.

Kagami, S., Rizzo, H.L., Lee, J.J., Koguchi, Y., and Blauvelt, A. (2010). Circulating Th17, Th22, and Th1 cells are increased in psoriasis. The Journal of investigative dermatology *130*, 1373-1383.

Kalliolias, G.D., and Ivashkiv, L.B. (2016). TNF biology, pathogenic mechanisms and emerging therapeutic strategies. Nature reviews. Rheumatology *12*, 49-62.

Kane, M.M., and Mosser, D.M. (2000). Leishmania parasites and their ploys to disrupt macrophage activation. Current opinion in hematology *7*, 26-31.

Kannicht, C., Ramström, M., Kohla, G., Tiemeyer, M., Casademunt, E., Walter, O., and Sandberg, H. (2013). Characterisation of the post-translational modifications of a novel, human cell line-derived recombinant human factor VIII. Thrombosis research *131*, 78-88.

Kaye, P., and Scott, P. (2011). Leishmaniasis: complexity at the host-pathogen interface. Nature reviews. Microbiology *9*, 604-615.

Kemp, M., Hansen, M.B., and Theander, T.G. (1992). Recognition of Leishmania antigens by T lymphocytes from nonexposed individuals. Infection and immunity *60*, 2246-2251.

Kemper, C., and Atkinson, J.P. (2007). T-cell regulation: with complements from innate immunity. Nature reviews. Immunology *7*, 9-18.

Keshavarz Valian, H., Nateghi Rostami, M., Tasbihi, M., Miramin Mohammadi, A., Eskandari, S.E., Sarrafnejad, A., and Khamesipour, A. (2013). CCR7+ central and CCR7- effector memory CD4+ T cells in human cutaneous leishmaniasis. Journal of clinical immunology *33*, 220-234.

Kharazmi, A., Kemp, K., Ismail, A., Gasim, S., Gaafar, A., Kurtzhals, J.A., El Hassan, A.M., Theander, T.G., and Kemp, M. (1999). T-cell response in human leishmaniasis. Immunology Letters *65*, 105-108.

Konara, C.S., Barnard, R.T., Hine, D., Siegel, E., and Ferro, V. (2016). The Tortoise and the Hare: Evolving Regulatory Landscapes for Biosimilars. Trends in biotechnology *34*, 70-83.

Kwan, W.-h., van der Touw, W., and Heeger, P.S. (2012). Complement regulation of T cell immunity. Immunologic research *54*, 247-253.

Leonardis, F. de, Govoni, M., Lo Monaco, A., and Trotta, F. (2009). Visceral leishmaniasis and anti-TNF-alpha therapy: case report and review of the literature. Clinical and experimental rheumatology *27*, 503-506.

Liew, F.Y., Li, Y., and Millott, S. (1990a). Tumor necrosis factor-alpha synergizes with IFN-gamma in mediating killing of Leishmania major through the induction of nitric oxide. Journal of immunology (Baltimore, Md. : 1950) *145*, 4306-4310.

Liew, F.Y., Li, Y., and Millott, S. (1990b). Tumour necrosis factor (TNF-alpha) in leishmaniasis. II. TNF-alpha-induced macrophage leishmanicidal activity is mediated by nitric oxide from L-arginine. Immunology *71*, 556-559.

Linehan, S.A., Martinez-Pomares, L., and Gordon, S. (2000). Mannose receptor and scavenger receptor. Two macrophage pattern recognition receptors with diverse functions in tissue homeostasis and host defense. Advances in experimental medicine and biology *479*, 1-14.

Lubbers, R., van Essen, M.F., van Kooten, C., and Trouw, L.A. (2017). Production of complement components by cells of the immune system. Clinical and experimental immunology *188*, 183-194.

Maeda, M., Watanabe, N., Neda, H., Yamauchi, N., Okamoto, T., Sasaki, H., Tsuji, Y., Akiyama, S., Tsuji, N., and Niitsu, Y. (1992). Serum tumor necrosis factor activity in inflammatory bowel disease. Immunopharmacology and immunotoxicology *14*, 451-461.

Mantzaris, G.J. (2016). Anti-TNFs: Originators and Biosimilars. Digestive diseases (Basel, Switzerland) *34*, 132-139.

McConville, M.J., Turco, S.J., Ferguson, M.A., and Sacks, D.L. (1992). Developmental modification of lipophosphoglycan during the differentiation of Leishmania major promastigotes to an infectious stage. The EMBO journal *11*, 3593-3600.

Merle, N.S., Church, S.E., Fremeaux-Bacchi, V., and Roumenina, L.T. (2015). Complement System Part I - Molecular Mechanisms of Activation and Regulation. Frontiers in immunology *6*, 262.

Micallef, C., and Azzopardi, C.M. (2014). Atypical cutaneous leishmaniasis in the immunosuppressed. BMJ case reports *2014*.

Minozzi, S., Bonovas, S., Lytras, T., Pecoraro, V., González-Lorenzo, M., Bastiampillai, A.J., Gabrielli, E.M., Lonati, A.C., Moja, L., and Cinquini, M., et al. (2016). Risk of infections using anti-TNF agents in rheumatoid arthritis, psoriatic arthritis, and ankylosing spondylitis. A systematic review and meta-analysis. Expert opinion on drug safety *15*, 11-34.

Misslitz, A., Mottram, J.C., Overath, P., and Aebischer, T. (2000). Targeted integration into a rRNA locus results in uniform and high level expression of transgenes in Leishmania amastigotes. Molecular and biochemical parasitology *107*, 251-261.

Mitoma, H., Horiuchi, T., Tsukamoto, H., Tamimoto, Y., Kimoto, Y., Uchino, A., To, K., Harashima, S.-i., Hatta, N., and Harada, M. (2008). Mechanisms for cytotoxic effects of anti-tumor necrosis factor agents on transmembrane tumor necrosis factor alpha-expressing cells: comparison among infliximab, etanercept, and adalimumab. Arthritis and rheumatism *58*, 1248-1257.

Mitoma, H., Horiuchi, T., Tsukamoto, H., and Ueda, N. (2016). Molecular mechanisms of action of anti-TNF-α agents - Comparison among therapeutic TNF-α antagonists. Cytokine.

Molino, N.M., Bilotkach, K., Fraser, D.A., Ren, D., and Wang, S.-W. (2012). Complement activation and cell uptake responses toward polymer-functionalized protein nanocapsules. Biomacromolecules *13*, 974-981.

Moradin, N., and Descoteaux, A. (2012). Leishmania promastigotes. Building a safe niche within macrophages. Frontiers in cellular and infection microbiology *2*, 121.

Morita, Y., Kamal, M., Kang, S.-A., Zhang, R., Lokesh, G.L., Thiviyanathan, V., Hasan, N., Woo, S., Zhao, D., and Leslie, M., et al. (2016). E-selectin Targeting PEGylated-thioaptamer Prevents Breast Cancer Metastases. Molecular therapy. Nucleic acids *5*, e399.

Mpofu, S., Fatima, F., and Moots, R.J. (2005). Anti-TNF-alpha therapies. They are all the same (aren't they?). Rheumatology *44*, 271-273.

Murch, S.H., Braegger, C.P., Walker-Smith, J.A., and MacDonald, T.T. (1993). Location of tumour necrosis factor alpha by immunohistochemistry in chronic inflammatory bowel disease. Gut *34*, 1705-1709.

Nateghi Rostami, M., Seyyedan Jasbi, E., Khamesipour, A., and Miramin Mohammadi, A. (2015). Plasma levels of tumor necrosis factor-alpha (TNF-α), TNF-α soluble receptor type 1 (sTNFR I) and IL-22 in human leishmaniasis. Tropical biomedicine *32*, 478-484.

Neefjes, J., Jongsma, M.L.M., Paul, P., and Bakke, O. (2011). Towards a systems understanding of MHC class I and MHC class II antigen presentation. Nature reviews. Immunology *11*, 823-836.

Nelson, A.L. (2010). Antibody fragments. Hope and hype. mAbs *2*, 77-83.

Nesbitt, A., Fossati, G., Bergin, M., Stephens, P., Stephens, S., Foulkes, R., Brown, D., Robinson, M., and Bourne, T. (2007). Mechanism of action of certolizumab pegol (CDP870). In vitro comparison with other anti-tumor necrosis factor α agents. Inflammatory Bowel Diseases *13*, 1323-1332.

Novais, F.O., Nguyen, B.T., Beiting, D.P., Carvalho, L.P., Glennie, N.D., Passos, S., Carvalho, E.M., and Scott, P. (2014). Human classical monocytes control the intracellular stage of Leishmania braziliensis by reactive oxygen species. The Journal of infectious diseases *209*, 1288-1296.

Ochoa, M.C., Minute, L., Rodriguez, I., Garasa, S., Perez-Ruiz, E., Inogés, S., Melero, I., and Berraondo, P. (2017). Antibody-dependent cell cytotoxicity. Immunotherapy strategies enhancing effector NK cells. Immunology and cell biology *95*, 347-355.

Oliveira, F., Bafica, A., Rosato, A.B., Favali, C.B.F., Costa, J.M., Cafe, V., Barral-Netto, M., and Barral, A. (2011). Lesion size correlates with Leishmania antigen-stimulated TNF-levels in human cutaneous leishmaniasis. The American journal of tropical medicine and hygiene *85*, 70-73.

Oliveira, W.N., Ribeiro, L.E., Schrieffer, A., Machado, P., Carvalho, E.M., and Bacellar, O. (2014). The role of inflammatory and anti-inflammatory cytokines in the pathogenesis of human tegumentary leishmaniasis. Cytokine *66*, 127-132.

Pasut, G. (2014). Pegylation of biological molecules and potential benefits. Pharmacological properties of certolizumab pegol. BioDrugs : clinical immunotherapeutics, biopharmaceuticals and gene therapy *28 Suppl 1*, S15-23.

Peters, N.C., Egen, J.G., Secundino, N., Debrabant, A., Kimblin, N., Kamhawi, S., Lawyer, P., Fay, M.P., Germain, R.N., and Sacks, D. (2008). In vivo imaging reveals an essential role for neutrophils in leishmaniasis transmitted by sand flies. Science *321*, 970-974.

Pimentel-Muiños, F.X., Muñoz-Fernández, M.A., and Fresno, M. (1994). Control of T lymphocyte activation and IL-2 receptor expression by endogenously secreted lymphokines. Journal of immunology (Baltimore, Md. : 1950) *152*, 5714-5722.

Polando, R., Dixit, U.G., Carter, C.R., Jones, B., Whitcomb, J.P., Ballhorn, W., Harintho, M., Jerde, C.L., Wilson, M.E., and McDowell, M.A. (2013). The roles of complement receptor 3 and Fcγ receptors during Leishmania phagosome maturation. Journal of leukocyte biology *93*, 921-932.

Qadoumi, M., Becker, I., Donhauser, N., Röllinghoff, M., and Bogdan, C. (2002). Expression of inducible nitric oxide synthase in skin lesions of patients with american cutaneous leishmaniasis. Infection and immunity *70*, 4638-4642.

Rai, E., and Wakeland, E.K. (2011). Genetic predisposition to autoimmunity--what have we learned? Seminars in immunology *23*, 67-83.

Ribeiro-de-Jesus, A., Almeida, R.P., Lessa, H., Bacellar, O., and Carvalho, E.M. (1998). Cytokine profile and pathology in human leishmaniasis. Brazilian journal of medical and biological research = Revista brasileira de pesquisas medicas e biologicas *31*, 143-148.

Rioux, J.A., Lanotte, G., Serres, E., Pratlong, F., Bastien, P., and Perieres, J. (1990). Taxonomy of Leishmania. Use of isoenzymes. Suggestions for a new classification. Annales de parasitologie humaine et comparee *65*, 111-125.

Ritter, U., Frischknecht, F., and van Zandbergen, G. (2009). Are neutrophils important host cells for Leishmania parasites? Trends in parasitology *25*, 505-510.

Ruiz, J.H., and Becker, I. (2007). CD8 cytotoxic T cells in cutaneous leishmaniasis. Parasite Immunol *29*, 671-678.

Sabins, N.C., Harman, B.C., Barone, L.R., Shen, S., and Santulli-Marotto, S. (2016). Differential Expression of Immune Checkpoint Modulators on In Vitro Primed CD4(+) and CD8(+) T Cells. Frontiers in immunology *7*, 221.

Sacks, D.L. (1989). Metacyclogenesis in Leishmania promastigotes. Experimental Parasitology *69*, 100-103.

Salmon-Ceron, D., Tubach, F., Lortholary, O., Chosidow, O., Bretagne, S., Nicolas, N., Cuillerier, E., Fautrel, B., Michelet, C., and Morel, J., et al. (2011). Drug-specific risk of non-tuberculosis opportunistic infections in patients receiving anti-TNF therapy reported to the 3-year prospective French RATIO registry. Annals of the rheumatic diseases *70*, 616-623.

Saraiva, M., and O'Garra, A. (2010). The regulation of IL-10 production by immune cells. Nature reviews. Immunology *10*, 170-181.

Sarma, J.V., and Ward, P.A. (2011). The complement system. Cell and tissue research *343*, 227-235.

Sassi, A., Largueche-Darwaz, B., Collette, A., Six, A., Laouini, D., Cazenave, P.A., and Dellagi, K. (2005). Mechanisms of the Natural Reactivity of Lymphocytes from Noninfected Individuals to Membrane-Associated Leishmania infantum Antigens. Journal of immunology (Baltimore, Md. : 1950) *174*, 3598-3607.

Scallon, B., Cai, A., Solowski, N., Rosenberg, A., Song, X.-Y., Shealy, D., and Wagner, C. (2002). Binding and functional comparisons of two types of tumor necrosis factor antagonists. The Journal of pharmacology and experimental therapeutics *301*, 418-426.

Scorza, B.M., Carvalho, E.M., and Wilson, M.E. (2017). Cutaneous Manifestations of Human and Murine Leishmaniasis. International journal of molecular sciences *18*.

Scott, P., and Novais, F.O. (2016). Cutaneous leishmaniasis: immune responses in protection and pathogenesis. Nature reviews. Immunology *16*, 581-592.

Sedger, L.M., and McDermott, M.F. (2014). TNF and TNF-receptors: From mediators of cell death and inflammation to therapeutic giants - past, present and future. Cytokine & growth factor reviews *25*, 453-472.

Sehgal, G., Zhang, K., Todd, R.F., Boxer, L.A., and Petty, H.R. (1993). Lectin-like inhibition of immune complex receptor-mediated stimulation of neutrophils. Effects on cytosolic calcium release and superoxide production. Journal of immunology (Baltimore, Md. : 1950) *150*, 4571-4580.

Shaikh, S.A. (2007). Ankylosing spondylitis. Recent breakthroughs in diagnosis and treatment. The Journal of the Canadian Chiropractic Association *51*, 249-260.

Silva, M.T., and Correia-Neves, M. (2012). Neutrophils and macrophages. The main partners of phagocyte cell systems. Frontiers in immunology *3*, 174.

Singh, S., Kumar, N., Dwiwedi, P., Charan, J., Kaur, R., Sidhu, P., and Chugh, V.K. (2017). Monoclonal Antibodies. A Review. Current clinical pharmacology.

Soghoian, D.Z., and Streeck, H. (2010). Cytolytic CD4(+) T cells in viral immunity. Expert review of vaccines *9*, 1453-1463.

Stebut, E. von, and Tenzer, S. (2017). Cutaneous leishmaniasis. Distinct functions of dendritic cells and macrophages in the interaction of the host immune system with Leishmania major. International journal of medical microbiology : IJMM.

Steverding, D. (2017). The history of leishmaniasis. Parasites & vectors *10*, 82.

Strome, S.E., Sausville, E.A., and Mann, D. (2007). A mechanistic perspective of monoclonal antibodies in cancer therapy beyond target-related effects. The oncologist *12*, 1084-1095.

Sundy, J.S., Baraf, H.S.B., Yood, R.A., Edwards, N.L., Gutierrez-Urena, S.R., Treadwell, E.L., Vázquez-Mellado, J., White, W.B., Lipsky, P.E., and Horowitz, Z., et al. (2011). Efficacy and tolerability of pegloticase for the treatment of chronic gout in patients refractory to conventional treatment: two randomized controlled trials. JAMA *306*, 711-720.

Tauber, A.I. (2003). Metchnikoff and the phagocytosis theory. Nature reviews. Molecular cell biology *4*, 897-901.

Tektonidou, M.G., and Skopouli, F.N. (2008). Visceral leishmaniasis in a patient with psoriatic arthritis treated with infliximab. Reactivation of a latent infection? Clinical rheumatology *27*, 541-542.

Thalayasingam, N., and Isaacs, J.D. (2011). Anti-TNF therapy. Best practice & research. Clinical rheumatology *25*, 549-567.

Theillet, F.-X., Smet-Nocca, C., Liokatis, S., Thongwichian, R., Kosten, J., Yoon, M.-K., Kriwacki, R.W., Landrieu, I., Lippens, G., and Selenko, P. (2012). Cell signaling, post-translational protein modifications and NMR spectroscopy. Journal of biomolecular NMR *54*, 217-236.

Theodos, C.M., Povinelli, L., Molina, R., Sherry, B., and Titus, R.G. (1991). Role of tumor necrosis factor in macrophage leishmanicidal activity in vitro and resistance to cutaneous leishmaniasis in vivo. Infection and immunity *59*, 2839-2842.

Tsigankov, P., Gherardini, P.F., Helmer-Citterich, M., Späth, G.F., Myler, P.J., and Zilberstein, D. (2014). Regulation dynamics of Leishmania differentiation. Deconvoluting signals and identifying phosphorylation trends. Molecular & cellular proteomics : MCP *13*, 1787-1799.

van Kuijk, A.W.R., Reinders-Blankert, P., Smeets, T.J.M., Dijkmans, B.A.C., and Tak, P.P. (2006). Detailed analysis of the cell infiltrate and the expression of mediators of synovial inflammation and joint destruction in the synovium of patients with psoriatic arthritis. Implications for treatment. Annals of the rheumatic diseases *65*, 1551-1557.

van Zandbergen, G., Bollinger, A., Wenzel, A., Kamhawi, S., Voll, R., Klinger, M., Müller, A., Hölscher, C., Herrmann, M., and Sacks, D., et al. (2006). Leishmania disease development depends on the presence of apoptotic promastigotes in the virulent inoculum. Proceedings of the National Academy of Sciences of the United States of America *103*, 13837-13842.

van Zandbergen, G., Hermann, N., Laufs, H., Solbach, W., and Laskay, T. (2002). Leishmania Promastigotes Release a Granulocyte Chemotactic Factor and Induce Interleukin-8 Release but Inhibit Gamma Interferon-Inducible Protein 10 Production by Neutrophil Granulocytes. Infection and immunity *70*, 4177-4184.

van Zandbergen, G., Klinger, M., Mueller, A., Dannenberg, S., Gebert, A., Solbach, W., and Laskay, T. (2004). Cutting Edge. Neutrophil Granulocyte Serves as a Vector for Leishmania Entry into Macrophages. Journal of immunology (Baltimore, Md. : 1950) *173*, 6521-6525.

van Zee, K.J., Kohno, T., Fischer, E., Rock, C.S., Moldawer, L.L., and Lowry, S.F. (1992). Tumor necrosis factor soluble receptors circulate during experimental and clinical inflammation and can protect against excessive tumor necrosis factor alpha in vitro and in vivo. Proceedings of the National Academy of Sciences of the United States of America *89*, 4845-4849.

Varol, C., Mildner, A., and Jung, S. (2015). Macrophages. Development and tissue specialization. Annual review of immunology *33*, 643-675.

Verhoef, J.J.F., Carpenter, J.F., Anchordoquy, T.J., and Schellekens, H. (2014). Potential induction of anti-PEG antibodies and complement activation toward PEGylated therapeutics. Drug discovery today *19*, 1945-1952.

Vos, A.C.W., Wildenberg, M.E., Duijvestein, M., Verhaar, A.P., van den Brink, G.R., and Hommes, D.W. (2011). Anti-tumor necrosis factor-α antibodies induce regulatory macrophages in an Fc region-dependent manner. Gastroenterology *140*, 221-230.

Voskoboinik, I., Whisstock, J.C., and Trapani, J.A. (2015). Perforin and granzymes. Function, dysfunction and human pathology. Nature reviews. Immunology *15*, 388-400.

Wallis, R.S., and Ehlers, S. (2005). Tumor necrosis factor and granuloma biology. Explaining the differential infection risk of etanercept and infliximab. Seminars in arthritis and rheumatism *34*, 34-38.

Wanderley, J.L.M., Moreira, M.E.C., Benjamin, A., Bonomo, A.C., and Barcinski, M.A. (2006). Mimicry of Apoptotic Cells by Exposing Phosphatidylserine Participates in the Establishment of Amastigotes of Leishmania (L) amazonensis in Mammalian Hosts. Journal of immunology (Baltimore, Md. : 1950) *176*, 1834-1839.

Weissmuller, S., Semmler, L.Y., Kalinke, U., Christians, S., Muller-Berghaus, J., and Waibler, Z. (2012). ICOS-LICOS interaction is critically involved in TGN1412-mediated T-cell activation. Blood *119*, 6268-6277.

WHO (2017). Leishmaniasis. http://www.who.int/mediacentre/factsheets/fs375/en/.

Wilhelm, P., Ritter, U., Labbow, S., Donhauser, N., Rollinghoff, M., Bogdan, C., and Korner, H. (2001). Rapidly Fatal Leishmaniasis in Resistant C57BL/6 Mice Lacking TNF. The Journal of Immunology *166*, 4012-4019.

Wilhelm, P., Wiede, F., Meissner, A., Donhauser, N., Bogdan, C., and Korner, H. (2005). TNF but not Fas ligand provides protective anti-L. major immunity in C57BL/6 mice. Microbes and infection *7*, 1461-1468.

Zanger, P., Kötter, I., Kremsner, P.G., and Gabrysch, S. (2012). Tumor necrosis factor alpha antagonist drugs and leishmaniasis in Europe. Clinical microbiology and infection : the official publication of the European Society of Clinical Microbiology and Infectious Diseases *18*, 670-676.

Zaph, C., Uzonna, J., Beverley, S.M., and Scott, P. (2004). Central memory T cells mediate long-term immunity to Leishmania major in the absence of persistent parasites. Nature medicine *10*, 1104-1110.

Zaunders, J.J., Munier, M.L., Seddiki, N., Pett, S., Ip, S., Bailey, M., Xu, Y., Brown, K., Dyer, W.B., and Kim, M., et al. (2009). High levels of human antigen-specific CD4+ T cells in peripheral blood revealed by stimulated coexpression of CD25 and CD134 (OX40). Journal of immunology (Baltimore, Md. : 1950) *183*, 2827-2836.

Zhang, Y.-Z., and Li, Y.-Y. (2014). Inflammatory bowel disease. Pathogenesis. World journal of gastroenterology *20*, 91-99.

Zilberstein, D., and Shapira, M. (1994). The role of pH and temperature in the development of Leishmania parasites. Annual review of microbiology *48*, 449-470.

6 Abbreviations

°C	Degree Celsius
µl	Microliter
µM	Micromolar
µm	Micrometer
ADCC	Antibody-dependent cell-mediated cytotoxicity
AKT	Protein kinase B
APC	Antigen presenting cell
C3	Complement component 3
CD	Cluster of differentiation
CDC	Complement-dependent cytotoxicity
CDRs	Complementarity determining regions
CFSE	5(6)-Carboxyfluorescein diacetate N-succinimidyl ester
Ci	Cimzia®
CL	Cutaneous leishmaniasis
cm	Centimeter
CM	Complete-medium
CR	Complement receptor
d	Day/s
DAF	Decay acceleration factor
DC	Dendritic cell
DMSO	Dimethyl sulfoxide
EMA	European Medicines Agency
ELISA	Enzyme-linked Immunosorbent Assay
Fab	Fragment antigen-binding
Fc	Fragment crystallizable
FC	Flow cytometry
FcγR	Fcγ receptor
FCS	Fetal calf serum
FoxP3	Forkhead-Box-Protein P3
FSC	Forward scatter
g	Gram
g	Gravitational force
GL	Granulysin
GM-CSF	Granulocyte-macrophage colony-stimulating factor
GP63	Glycoprotein 63
GrA	Granzyme A
GrB	Granzyme B
h	Hour/s

HEPES	N-2-hydroxyethylpiperazine-N'-2-ethanesulfonic acid
hMDMs	Human monocyte-derived macrophages
Hu	Humira®
iC3b	Inactive complement component 3b
IF	Immunofluorescence
IFNγ	Interferon γ
IgG	Immunoglobulin G
IL	Interleukin
iNOS	Inducible nitric oxide synthase
kDa	Kilodalton
LAMP	Lysosomal-associated membrane protein
LCF	*Leishmania* chemotactic factor
Lm, *L. major*	*Leishmania major*
log phase	Logarithmic growth phase
LPG	Lipophosphoglycan
LSM	Leucocyte separation medium
mAbs	Monoclonal antibodies
MACS	Magnetic-activated cell sorting
MAPKs	Mitogen-activated protein kinases
MASPs	MBL-associated proteins
MBL	Mannose-binding lectin
MCP	Monocyte chemoattractant protein
MFI	Mean fluorescence intensity
MHC	Major histocompatibility complex
min	Minute/s
MIP	Macrophage inflammatory protein
ml	Milliliter
ML	Mucocutaneous leishmaniasis
MLA	Membrane-derived *Leishmania* antigen
MLKL	Mixed lineage kinase domain-like protein
mm	Millimeter
mM	Millimolar
MOI	Multiplicity of infection
mTNFα	Membrane TNFα
mTNFR	Membrane TNFα receptor
n	Number of donors
NADPH	Nicotinamide adenine dinucleotide phosphate
NFκB	Nuclear factor κB
ng	Nanogram
NK	Natural killer

NO	Nitric oxide
PBL	Peripheral blood lymphocyte
PBMC	Peripheral blood mononuclear cell
PBS	Phosphate buffered saline
PD-1	Programmed death-1
PEG	Polyethylene glycol
PF	Perforin
PFA	Paraformaldehyde
pg	Picogram
PI	Propidium iodide
Re	Remicade®
RFI	Relative fluorescence intensity
ROS	Reactive oxygen species
Rs	Remsima®
RT	Room temperature (22°C)
SD	Standard deviation
SLA	soluble *Leishmania* antigen
SSC	Side scatter
stat phase	Stationary growth phase
sTNFα	Soluble TNFα
TACE	TNFα-converting enzyme
Tbet	T-box transcription factor Tbx21
TCR	T-cell receptor
TGF-β	Transforming growth factor β
Th	T-helper
TIMP	Tissue inhibitor of metalloproteinases
TNFα	Tumor necrosis factor α
TRADD	TNFR1-associated death domain protein
TRAF2	TNFR-associated factor 2
Treg	Regulatory T-cell
v/v	Volume per volume
VL	Visceral leishmaniasis
vs	versus
w/v	Weight per volume
WHO	World Health Organization

7 List of figures

8 List of tables

9 Declaration of authorship

I hereby certify that I have written the present dissertation with the topic

Therapeutic anti-TNFα antibodies differentially affect *Leishmania* infection of primary human macrophages

independently, using no other aids then those I have cited. I have clearly mentioned the source of the passages that are taken word for word or paraphrased from other works.

The presented thesis has not been submitted in this or any other form to another faculty or examination institution.

Eidesstattliche Versicherung

Hiermit versichere ich, dass ich die vorgelegte Dissertation mit dem Titel

Therapeutic anti-TNFα antibodies differentially affect *Leishmania* infection of primary human macrophages

selbstständig verfasst habe und keine anderen als die angegebenen Quellen und Hilfsmittel verwendet habe. Die Stellen der Dissertation, die anderen Werken und Veröffentlichungen dem Wortlaut oder dem Sinn nach entnommen wurden, sind durch Quellenangaben gekennzeichnet.

Diese Dissertation wurde in der jetzigen oder in ähnlicher Form noch an keiner anderen Hochschule eingereicht und hat noch keinen sonstigen Prüfungszwecken gedient.

Langen, 26.02.2018

Katharina Arens

10 Acknowledgements

11 Curriculum Vitae

12 Publications